

**Novel Molecularly Imprinted Polymer Thin-Films as Micro-
Extraction Adsorbents Combined with Various Chromatographic
and Mass Spectrometry Systems for Selective Determination of Trace
Concentrations of Thiophene Compounds in Water**

by

© Hassan Yasin Hijazi

A Thesis submitted to the

School of Graduate Studies

in partial fulfillment of the requirements for the degree of

Doctor of Philosophy

Department of Chemistry

Memorial University of Newfoundland

November, 2017

St. John's, Newfoundland and Labrador

ABSTRACT

Thiophene compounds are polycyclic aromatic sulfur heterocycles (PASHs) present in petroleum in concentrations up to 7%, depending on the source. They are considered as the most relevant and problematic components in petroleum products due to their mutagenicity, carcinogenicity, and acute toxicity. These compounds can be used as organic markers for monitoring of oil pollution, which can come into marine waters through regulated oil discharges, accidental oil spills and shipping related inputs. Current analytical methods for thiophenes usually combine solid-phase extraction (SPE) with gas chromatography (GC) or high performance liquid chromatography (HPLC). However, matrix complexity, low analyte concentrations, and the low selectivity of SPE can limit the efficiency of separation and detection. To overcome these problems, selective sorbent materials, such as molecularly imprinted polymers (MIPs) can be used for analysis.

MIPs are synthetic polymers that contain artificial recognition sites formed by polymerization in the presence of a template molecule. The molecular recognition mechanism in MIPs is simple. They have a high mechanical and thermal stability, and can be prepared easily at low cost. In our work, MIPs are prepared as thin-films on glass substrates, simplifying fabrication and allowing for flexibility in deployment and use with a variety of detection systems. A pseudo-template is used in the imprinting process to avoid positive bias associated with template-bleeding, which can be problematic when working at low ($\mu\text{g L}^{-1}$) analyte concentrations. Ours is the first reported MIP for uptake of thiophene compounds from aqueous matrices. Binding affinity, heterogeneity, uptake behaviour of

thiophene compounds over a range of concentrations from 0.5-100 $\mu\text{g L}^{-1}$, and imprinting factors (*IFs*) for this MIP thin-film have been determined. Coupling of MIP thin-film with different detection systems such GC-MS, head-space GC with sulfur chemiluminescence detection (GC-SCD), and desorption electrospray ionization mass spectrometry (DESI-MS) has been accomplished. Linear calibration curves and reproducible results with low limit of detection values were achieved for the extraction of thiophene compounds from spiked seawater samples using these techniques. The results showed that the MIP films can be used effectively as a selective sorbent for thiophene compounds from water samples.

ACKNOWLEDGMENT

I would like first to thank my supervisor, Prof. Christina S. Bottaro, for her patient guidance, encouragement and advice which has provided me throughout my study. Her positive outlook and confidence in my research inspired me and gave me the confidence. I would also like to thank my supervisory committee members, Prof. Sunil V. Pansare and Dr. Peter L. Warburton for supervision and reviewing my thesis, our group members for sharing ideas and Centre for Chemical Analysis, Research and Training (C-CART) employees for training me on the research instruments and equipment. Thanks also go to my friends, Dr. Khaled Omari and Ahmad Q. Al Shra'ah for their help and advice. All thanks to the Canadian Society of Chemistry (CSC 2016), Analytical Division, for awarding me second place in the student poster competition.

This project would not be possible without the financial assistance of the following companies: Petroleum Research Newfoundland and Labrador (PRNL), Atlantic Innovation Fund (AIF), Natural Sciences and Engineering Research Council of Canada (NSERC). Finally, I extend my thanks to the Department of Chemistry, School of Graduate Studies (SGS), and the Memorial University of Newfoundland (MUN) for their services and financial support.

DEDICATION

First and foremost, I would like to thank ALLAH for mercy and blessings during my PhD program and let the dream become true. All thanks go to my lovely wife, Wafa, my lovely kids Jenan, Ahmad and Rama for their patience and support during my study. I would like to extend my gratitude to my lovely mother, my brothers, and my sisters for their support and encouragement.

This thesis is a gift to the soul of my lovely Father.

Table of Contents

ABSTRACT	ii
ACKNOWLEDGMENT.....	iv
DEDICATION	v
List of Tables	x
List of Figures	xi
List of Symbols, Nomenclature or Abbreviations	xv
Chapter 1: Introduction and literature survey	1
1.1. Introduction	2
1.2. Environmental and health impacts	5
1.3. Methods of analysis for thiophene compounds in the literature	7
1.4. Molecularly imprinted polymers (MIPs).....	10
1.4.1. Covalent versus non-covalent imprinting.....	11
1.4.2. Main components of MIPs	14
1.4.3. Optimization of MIP composition.....	17
1.4.4. Methods of MIPs preparation and formation.....	19
1.4.5. Characterization of MIPs.....	22
1.5. MIPs for thiophene compounds	28
1.6. Detection systems used with MIPs.....	29
1.6.1. Gas chromatography mass spectrometry (GC-MS).....	29
1.6.2. Headspace gas chromatography sulfur chemiluminescence detector (HS-GC-SCD)	31

1.6.3.	Desorption electrospray ionization mass spectrometry (DESI-MS)	34
1.7.	Thesis objectives	41
1.8.	Co-authorship statement.....	42
1.9.	References	43
Chapter 2: Novel molecularly imprinted polymer thin-film as micro-extraction adsorbent for selective determination of trace concentrations of thiophene compounds in water.....		
2.1.	Abstract	61
2.2.	Introduction.....	63
2.3.	Materials and methods	66
2.3.1.	Materials	66
2.3.2.	Pre-treatment and derivatization of glass slides	67
2.3.3.	Preparation of MIP thin-films.....	67
2.3.4.	Characterization of the thin-films.....	69
2.3.5.	Optimization and rebinding experiments.....	70
2.3.6.	Adsorption kinetics and binding isotherm experiments	71
2.3.7.	Analysis of real samples	73
2.4.	Results and discussion	74
2.4.1.	Optimization of MIP thin-film composition.....	74
2.4.2.	Morphology of the thin-films	86
2.4.3.	Optimization of the stirring speed of MIP analysis	88
2.4.4.	Adsorption kinetics of MIP thin-film	90
2.4.5.	Effect of sample volume on extracted amount by MIP thin-film.....	91
2.4.6.	Adsorption isotherms for thiophene compounds in seawater.....	95

2.4.7.	Analysis of real samples	98
2.4.8.	Selectivity of MIP thin-film	101
2.5.	Conclusions	104
2.6.	References	105
Chapter 3: Selective determination of semi-volatile thiophene compounds in water by		
molecularly imprinted polymer thin-film headspace gas chromatography sulfur		
chemiluminescence detector (MIP HS-GC-SCD)		
		111
3.1.	Abstract	112
3.2.	Introduction	113
3.3.	Materials and methods	115
3.3.1.	Materials	115
3.3.2.	Pre-treatment and derivatization of glass slides	116
3.3.3.	Preparation of MIP thin-film on a glass slide	116
3.3.4.	Instrumentations and conditions	117
3.3.5.	Analysis of water and seawater samples by MIP HS-GC-SCD	118
3.4.	Results and discussion	119
3.4.1.	Preparation of the MIP thin-films	119
3.4.2.	Optimization of HS oven temperature	121
3.4.3.	Optimization of HS equilibration time	123
3.4.4.	Analysis of thiophene compounds in seawater	124
3.5.	Conclusions	128
3.6.	References	129

Chapter 4: Indirect analysis of thiophene compounds in water: oxidation to sulfones followed by molecularly imprinted polymer thin-film desorption electrospray ionization mass spectrometry (MIP DESI-MS).....	132
4.1. Abstract	133
4.2. Introduction.....	134
4.3. Materials and methods	136
4.3.1. Materials	136
4.3.2. Pre-treatment and derivatization of glass slides	137
4.3.3. Preparation of MIP thin-films on a glass slides.....	137
4.3.4. Oxidation reaction of thiophene compounds in water	137
4.3.5. GC-MS analysis.....	138
4.3.6. DSEI-MS conditions.....	139
4.3.7. Analysis of water and seawater samples by MIP DESI-MS	140
4.4. Results and discussion	142
4.4.1. Preparation of MIP thin-films.....	142
4.4.2. Oxidation of thiophene compounds in water.....	143
4.4.3. DESI-MS analysis	147
4.4.4. Analysis of seawater	151
4.5. Conclusions.....	153
4.6. References.....	154
Chapter 5: Conclusions and future work.....	158
5.1. References	165

List of Tables

Table 1.1. Structures and aqueous solubility of some thiophene compounds.	4
Table 1.2. Examples of some analysis methods of PASHs in water samples and their figures of merit.....	8
Table 1.3. Binding isotherm models, adapted from [97].	24
Table 2.1. Composition of MIP pre-polymerization mixtures.....	77
Table 2.2. Imprinting factors (IF_s) for MIP compositions prepared with different monomers using 1:1 ratio of 1-octanol:methanol mixture as a porogen.	80
Table 2.3. Optimization of template to monomer to cross-linker ratio of 1-Vim-BPADMA MIP.	84
Table 2.4. Total binding capacity, average imprinting factors and relative standard deviations for 1-Vim- BPADMA MIP at different M:C ratios.....	85
Table 2.5. Freundlich fitting parameters to the adsorption isotherm for MIP and NIP.	98
Table 3.1. Percent recovery values of thiophene compounds at various sample volumes obtained from the MIP film HS-GC-SCD analysis of spiked DI water and seawater samples at the same concentration ($50 \mu\text{g L}^{-1}$).	127
Table 4.1. Optimal parameters and conditions for the DESI-MS analysis of dibenzothiophene sulfone compound.	147

List of Figures

Figure 1.1. Chromatograms obtained after microwave assisted extraction (MAE) of spiked soil (PAHs + OH-PAHs) (a) without clean-up of the extract (b) extract purified by MIPs (with a concentration factor of 4) and (c) extract percolated through non-imprinted polymers (NIPs), adapted with permission from [31].....	9
Figure 1.2. Schematic representation of a) non-covalent and b) covalent molecular imprinting processes.	13
Figure 1.3. Common functional monomers used in molecular imprinting procedures [33].	14
Figure 1.4. Chemical structures of common cross-linkers used in molecular imprinting [33].	15
Figure 1.5. Formation of radicals in DMPA and AIBN [59].....	16
Figure 1.6. Scatchard plot for PP _{Zn} M(TOAA), adapted with permission from [96].	24
Figure 1.7. Schematic diagram of a gas chromatography quadrupole mass spectrometer (GC/MS), taken with permission from [114].....	30
Figure 1.8. DESI source adapted with permission from [119].	34
Figure 1.9. A typical DESI mass spectrum of PAHs from (a) biomass burning aerosol (b) ambient aerosol. Acenaphthylene (Acy), acenaphthene (Ace), fluorene (Flo), anthracene (Ant), phenanthrene (Phe), fluoranthene (Flu) and pyrene (Pyr), benzo[a]anthracene (BaA), chrysene(Chry), benzofluoranthene (BbF), benzo[k], fluoranthene (BkF), benzo[a]pyrene (BaP), and dibenzo[a,h]anthracene(DbA). The inset shows the MS/MS of the m/z = 252 ion for BbF/BkF/BaP, adapted with permission from [129].....	37

Figure 1.10. DESI-MS spectra of the isomer pairs: (a) anthracene and phenanthrene, and (b) pyrene and fluoranthene. Adapted with permission from [130].	38
Figure 1.11. DESI-MS of a MIP (a) and a NIP (b) used for extraction from a 0.10 mg L ⁻¹ solution of 2,4-D and analogs in river water. The results for tap water are similar. The maximum absolute intensity of the base peak in (a) is 407, in (b) 195, taken with permission from [82].	39
Figure 2.1. Preparation process of MIP thin-film on a glass slide.	69
Figure 2.2. Chemical structure of targeted thiophene compounds and pseudo-template.	75
Figure 2.3. Selected monomers and cross-linkers.	76
Figure 2.4. MIP films prepared with a) chloroform, b) methanol, c) acetonitrile d) 1-octanol, and e) acetonitrile-PEG.	78
Figure 2.5. Comparison between six MIP films prepared as adsorbents for thiophene compounds from. Error bars represent standard deviation.	80
Figure 2.6. Comparison between the two MIP thin-films prepared with different cross-linkers (n=3). Error bars represent standard deviation.	83
Figure 2.7. Optimization of the template to monomer to cross-linker ratio (n=3). Error bars represent standard deviation.	85
Figure 2.8. SEM of a) the surface of MIP and b) NIP films and c) cross-section of MIP film.	86
Figure 2.9. The relationship between the polymerized volume of MIP and the peak area ratios of the adsorbed thiophene compounds in the MIP thin-film obtained from the GC-MS analysis.	88

Figure 2.10. Effect of stirring speeds on the binding capacities of thiophene compounds in the analysis by MIP after uploading for 2 h (n=3). Error bars represent standard deviation.	89
Figure 2.11. Adsorption kinetics of MIP thin-film for thiophene compounds in water (n=3). Error bars represent standard deviation.	91
Figure 2.12. a) Predicted effect of the seawater sample volume in the amount of analyte adsorbed (Initial concentration, C_0 , $50 \mu\text{g L}^{-1}$). b) Experimental effect of the seawater sample volume in the amount of analyte adsorbed (initial concentration, C_0 , $50 \mu\text{g L}^{-1}$). Error bars represent standard deviation (n = 3).	94
Figure 2.13. Adsorption isotherm of MIP and NIP for thiophene compounds fitted to Freundlich isotherm (equilibration time 15 h).	97
Figure 2.14. Calibration curves for thiophene compounds at various spiked concentrations in seawater samples. IS: Fluorene- d_{10} ($\text{RSD}_s \leq 6.0\%$, n = 3).	100
Figure 2.15. Selectivity of MIP thin-film for thiophene compounds versus p-cresol and indole (n=3). Error bars represent standard deviation.	102
Figure 2.16. GC-MS full-scan of 40 mL seawater sample spiked with thiophene compounds and interferents at the same concentrations ($100 \mu\text{g L}^{-1}$). IS: Fluorene- d_{10}	103
Figure 3.1. Chemical structure of targeted thiophene compounds and pseudo-template.	120
Figure 3.2. MIP thin-film HS-GC-SCD chromatogram of 50 mL seawater sample of thiophene compounds spiked at $50 \mu\text{g L}^{-1}$	121
Figure 3.3. Effect of the HS temperature on the analysis of thiophenes-MIP thin-film..	122

Figure 3.4. Effect of the HS equilibration time on the analysis of thiophenes-MIP thin-film.	124
Figure 3.5. Calibration curves of the analysis of thiophene compounds by MIP HS-GC-SCD in seawater samples at a range of 5-100 $\mu\text{g L}^{-1}$. ($\text{RSD}_s \leq 7.0\%$, $n = 3$).	125
Figure 4.1. DESI source with MIP slide.	140
Figure 4.2. Chemical structures of sulfone compounds produced from oxidation reactions of targeted thiophene compounds in water.	142
Figure 4.3. Graph of % conversion for the oxidation of total thiophene compounds as a function of time at 45°C and 65°C.....	144
Figure 4.4. GC-MS (SIM) chromatograms of targeted thiophene compounds for different oxidation reaction time at 65 °C. IS: Fluorene.	146
Figure 4.5. DESI-MS full scan of an MIP thin-film used for the extraction of the oxidation products of thiophene compounds in seawater sample. Protonated molecule and sodium adduct were detected.	149
Figure 4.6. DESI-MS/MS confirmation scan of dibenzothiophene sulfone (DBTO ₂) in MIP thin-film. Collision energy is 15 eV.....	151
Figure 4.7. Calibration curves of the oxidized form of DBT at various spiked concentrations in seawater samples.....	152
Figure 5.1. MIP HS-GC-SCD chromatogram obtained from the analysis of 50 mL seawater sample spiked with a mixture of thiophene compounds at a concentration of 50 $\mu\text{g L}^{-1}$.162	

List of Symbols, Nomenclature or Abbreviations

3-MBT – 3-methylbenzothiophene

4,6-DMDBT – 4,6-dimethyl-dibenzothiophene

4-MDBT – 4-methyldibenzothiophene

a – fitting parameter constant

ACN – acetonitrile

ACS – American Chemical Society

AIBN – azobisisobutyronitrile

APCI – atmospheric pressure chemical ionization

B – concentration of bound analyte

BET – Brunauer-Emmett-Teller

BPADMA – bisphenol A dimethacrylate

BT – benzothiophene

C – concentration of free analyte

CEAA – Canadian Environmental Assessment Agency

DBT – dibenzothiophene

DESI – desorption electrospray ionization

DI – desorption ionization

DMPA – 2,2-dimethoxy-2-phenylacetophenone

DVB – divinylbenzene

EGDMA – ethyleneglycol dimethacrylate

EI – electron ionization

ESI – electrospray ionization

FI – Freundlich isotherm

FID – flame ionization detector

FTICR – Fourier transform ion cyclotron resonance

FT-IR – Fourier-transform infrared

GC – gas chromatography

GC-MS – gas chromatography- mass spectrometry

h - hour

HD – sulfur mustard

HPLC – high-performance liquid chromatography

HS – headspace

IF – imprinting factor

IPN – interpenetrating polymers networks

IS – internal standard

K – partition coefficient

K – the adsorption constant

K_0 – the median binding affinity

LF – Langmuir-Freundlich

LOD – limit of detection

Log K_{ow} – octanol-water partition coefficient

m – heterogeneity index

m/z – mass to charge ratio

MALDI – matrix-assisted laser desorption/ionization

MeOH – methanol

MIP – molecularly imprinted polymers

MS – mass spectrometry

MSD – mass selective detector

M_w – molecular weight

n – amount of analyte adsorbed by the film

N – number of homogeneous site

NIP – non-imprinted polymer

NMR – nuclear magnetic resonance

N_t – the total number of binding sites

o-PD – o-phenylenediamine

PAHs – polycyclic aromatics hydrocarbons

PASHs – polycyclic aromatic sulfur heterocycles

PEG – polyethylene glycol

PPD – poly(o-phenylenediamine)

PTFE – polytetrafluoroethylene

Q – adsorption (binding) capacity

QCM – quartz crystal microbalance

QTOF – quadrupole-time-of flight

R^2 – the coefficient of determination for linear regression

rpm – rotation per minute

RSD – relative standard deviation

s – second

SAW – surface acoustic wave

SCD – sulfur chemiluminescence

SEM – scan electron microscopy

SERS – surface enhanced Raman spectroscopy or scattering

SIM – selected ion monitoring

SPE – solid-phase extraction

TOAA – tri-O-acetyladenosine

TQMS – triple quadrupole mass spectrometer

US-EPA – United States Environmental Protection Agency

UV – ultraviolet

v/v, % – volume percentage

w/w, % – weight percentage

Chapter 1: Introduction and literature survey

1.1. Introduction

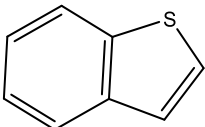
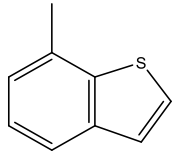
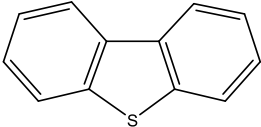
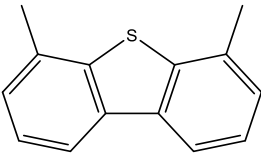
Keeping pollutants out of our oceans is a very difficult task. They are constantly affected by contaminants that come from natural and human sources [1]. Almost half of the oil pollution comes from natural oil seeps, although marine plants and animals have adapted to this source for hundreds or thousands of years. Other sources which come from transportation, extraction and consumption of oil are considered more problematic. Organic pollutants entering the ocean via these activities have many fates. The volatile pollutants escape to the atmosphere through evaporation and can be redeposited in colder climates, while other pollutants may undergo photodegradation reactions under sunlight to produce less or more toxic metabolites [2] or biodegradation by bacteria and fungi [3]. Degradation products could be more harmful to the environment than their precursor compounds. Non-degradable pollutants may persist for a long time before degradation, and can accumulate in marine life and transfer to humans through the food cycle.

Many studies have been undertaken to understand how these pollutants enter our oceans and their impacts on human and environment [4–6]. Environmental agencies, such as the United States Environmental Protection Agency (US-EPA) [7] and Canadian Environmental Assessment Agency (CEAA) [8], have issued regulations and decisions to determine the permissible concentration levels of pollutants in the environment. This can help in reducing the sources of pollution by forcing industry to find more effective strategies to treat them. For many reasons, developing new methods to track organic pollutants in marine water is a challenge. The complexity of the oil and the huge numbers of organic pollutants that seep into marine water makes their analysis difficult. Therefore, the environmental analysis

methods should be developed in a way that can separate and identify pollutants efficiently. To do this we should have a general idea about the oil composition.

The main oil components present in oil range from relatively simple hydrocarbons (alkanes, alkenes, etc.), monoaromatics, naphthenes, polycyclic aromatic hydrocarbons (PAHs), to a variety of sulfur and nitrogen containing compounds. Sulfur containing compounds are present in petroleum in concentrations of 0.05-10% depending on the source [9], and are usually removed by hydrodesulfurization process. The products of this process are hydrocarbons and hydrogen sulfide gas which is converted subsequently to sulfur or sulfuric acid [10]. Thiophene compounds are the major constituents of sulfur-containing compounds in crude oil. They are classified as polycyclic aromatic sulfur heterocycles (PASHs) compounds. Their aromaticity is less than benzene according to Hartree-Fock-Roothaan studies [11]. Electron pair on the thiophenic sulfur atom are delocalized in the aromatic π -electron system. As a consequence of that, the sulfur atom in thiophene ring resists the alkylation and oxidation reactions [12] making their removal by hydrodesulfurization difficult. Table 1.1 shows structures, aqueous solubility [13,14], melting points, vapour pressures, ionization potentials [15], and log K_{ow} [16,17] of the targeted thiophene compounds, where K_{ow} is the ratio of the concentration of a chemical in octanol phase and water phase at equilibrium at specified temperature. From Table 1.1, it can be observed that the aqueous solubility of thiophene compounds decreases as the number of aromatic and alkyl-substituents increases.

Table 1.1. Structures and aqueous solubility of some thiophene compounds.

Compound	Structure	Molecular weight (g/mol)	Aqueous solubility at 24°C (mg L ⁻¹)	Melting point (°C)	Vapour pressure at 25 °C (mmHg)	Ionization potential (eV)	Log K _{ow}
Benzothiophene (BT)		134.20	160	35.0	3.58 x 10 ⁻¹	8.1	3.12
3-Methylbenzothiophene (3-MBT)		148.22	49	33.1	1.32 x 10 ⁻¹	unavailable	3.71
Dibenzothiophene (DBT)		184.26	1.0	96.8	3.4 x 10 ⁻³	7.9	4.38
4,6-Dimethyl-dibenzothiophene (4,6-DMDBT)		212.31	unavailable	97.3	4.73 x 10 ⁻⁴	7.7	5.50

1.2. Environmental and health impacts

Thiophene compounds, such as benzothiophene and related methylated derivatives, are known to be persistent in the aquatic environments [17,18]. Their bioaccumulations and acute toxicity in marine organisms have been studied and assessed [13,19]. The PASHs are more stable than analogous polycyclic aromatic hydrocarbons (PAHs), and their stability increase with increasing of the alky-substituents on the aromatic rings. This stability in the environment and the fact that they are present in all crude oils make them useful as organic markers for oil pollution monitoring [18]. Biodegradation half-lives of these compounds are greater than six months in water and soil, and greater than one year in sediments [19]. Warner et al. [20] isolated some PASHs such as BT and DBT from marine samples and found that they bioaccumulate faster than PAHs. Miyake and Ogata [21] reported the presence of organo-sulfur compounds such as DBT in the soft body of the short-necked clam extract that was exposed to a suspension of crude oil in water. In another study, Eastmond et al. [22] compared the accumulation of some thiophene compounds with that of their analogous PAHs and found that BT was bioconcentrated in zooplankton *Daphnia magna* fifteen times more than naphthalene. Bates et al. [23] characterized quantitatively some organo-sulfur compounds in marine sediments and showed that DBT and its alkylated homologs are the predominant organic sulfur compounds in most of these sediment samples in his study. This study also revealed that DBT remained in the sediments contaminated with oil even after ten years, while other aromatics disappeared.

In a study of their impact on animals, BT produced adverse effects in male rats such as increasing the relative weights of liver and kidney, and increasing urine output [24].

Lethal concentration (LC_{50}) and lethal dose (LD_{50}) are usually used to measure the toxicity in the environment. The LC_{50} for animals refers to the concentration of a chemical that kills 50% of the test animals during the observation period, while the LD_{50} is the dose (usually oral or intravenous) of a chemical which causes the death of 50% of a group of tested animals; it is usually used to measure the short-term acute toxicity of a chemical [25]. In marine samples, the LC_{50} has been reported in *Daphnia magna* (water flea) after 48 h of exposure was 0.420 mg L^{-1} , while in fish (*poecilia reticulata*) it was 0.700 mg L^{-1} after 96 h of exposure. For animals, the reported value of LD_{50} in mice (given by mouth) was 470 mg kg^{-1} [26].

Unfortunately, there is only one study reported on the impact of thiophene compounds on human health. Amat et al. [27] carried out a study on the cytotoxicity and genotoxicity of six thiophene compounds (BT, DBT, benzo(*b*)naphtha(2,1-*d*)thiophene (BNT), 6-methylbenzo(*b*)naphtha(2,1-*d*)thiophene (6- CH_3BNT), dinaptho(2,1-*b*;1',2'-*d*)thiophene (DNT), and diphenanthro(9,10-*b*;9',10'-*d*)thiophene (DPT)) in liver human cell line (HepG2). The results showed that BT, DPT and DNT did not form DNA adducts (segments of DNA bound to a cancer-causing chemical) in HepG2 cell line, while DBT, BNT, and 6- CH_3BNT induced the DNA adduct formation. This study showed that some thiophene compounds are genotoxic for HepG2 cells.

1.3. Methods of analysis for thiophene compounds in the literature

There are few methods of analysis for thiophene compounds in the literature that specifically target them; most of the methods reported are for analysis of PASHs with PAHs. These methods usually involve the use of non-selective solid-phase extraction (SPE) with a range of detection methods [30-32]. Table 1.2 shows the figures of merit for some methods used for the analysis of PASHs. Although the values in the table show a very good analytical performance for most methods, the chromatograms of these methods sometimes include undefined and unresolved peaks because of the use of non-selective SPE methods, and thus could make identification and quantification more difficult.

Table 1.2. Examples of some analysis methods of PASHs in water samples and their figures of merit.

Analysis method	Analytes	Linearity Range ($\mu\text{g L}^{-1}$)	LOD ($\mu\text{g L}^{-1}$)	RSD (%)	%Recovery	Ref.
SPE-GC-FID GC-MS (SIM)	BT, DBT, Thianthrene, Thiophene-2-carboxylaldehyde)	0.1-1000	60 – 100	≤ 8.2	≥ 93.5	[28]
			40 - 80	≤ 7.8		
Stir bar SPE-HPLC-UV	3PAHs, BT, 3-MBT, DBT, 4,6-DMDBT	0.05-1000	0.007-0.103	6.3-12.9	≥ 93	[29]
SPE-HPLC-fluorescence HPLC-APCI-MS	6PAHs, BT, DBT, Benzo[b]naphthol-[2,3-d]thiophene, Benzo[b]naphthol-[2,1-d]thiophene)	0.06-100	0.02 (flu.)	2-15	≥ 70	[30]
			0.06 (MS)	3-8		

These limitations can be overcome by using more selective material such as molecularly imprinted polymers (MIPs). For instance, a MIP was used as a sorbent with GC-fluorescence for selective extraction of hydroxylated polycyclic aromatic hydrocarbons (OH-PAHs) from soil samples [31]. This method has low limit of detection values ($0.003\text{--}0.014 \mu\text{g g}^{-1}$) and low limits of quantification ($0.010\text{--}0.044 \mu\text{g g}^{-1}$). In addition, this method showed a high selectivity towards the OH-PAHs in the presence of some PAHs as interferences in the spiked soil sample because of the use of MIP as shown in Figure 1.1.

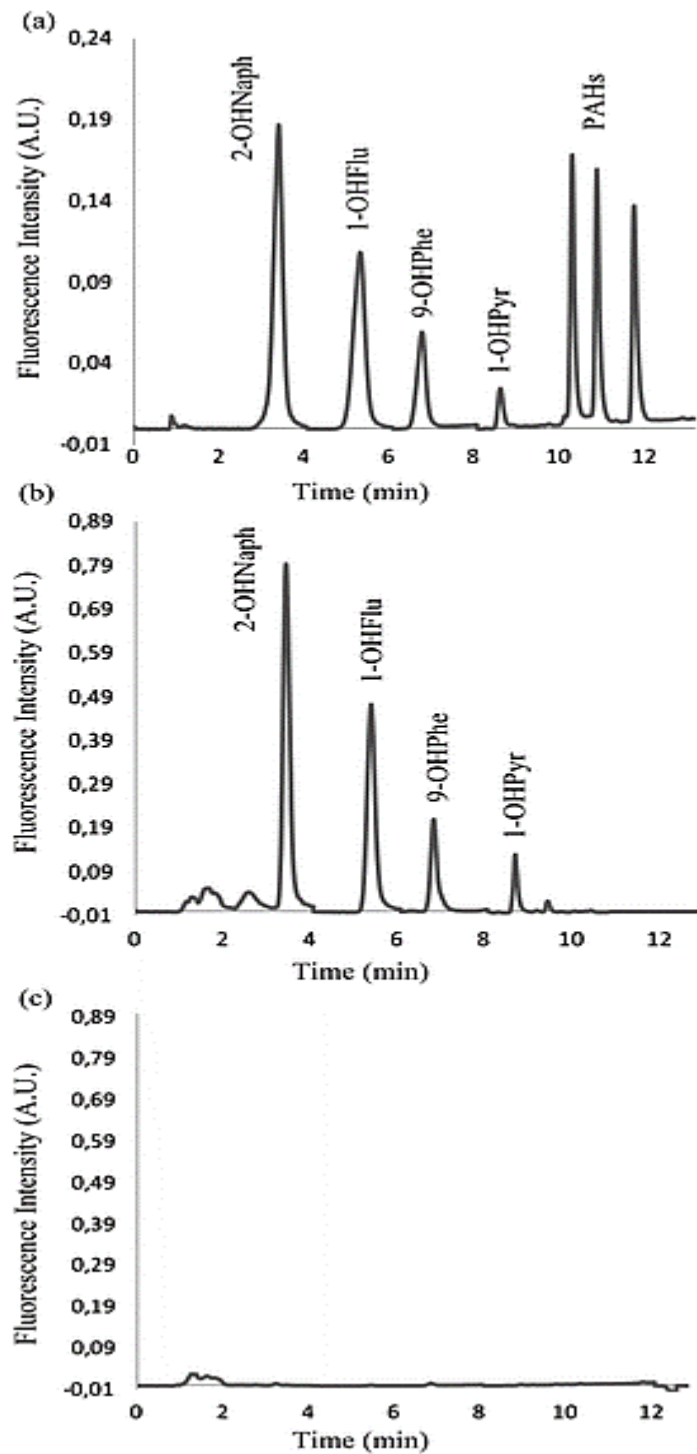


Figure 1.1. Chromatograms obtained after microwave assisted extraction (MAE) of spiked soil (PAHs + OH-PAHs) (a) without clean-up of the extract (b) extract purified by MIPs (with a concentration factor of 4) and (c) extract percolated through non-imprinted polymers (NIPs), adapted with permission from [31].

1.4. Molecularly imprinted polymers (MIPs)

MIPs are synthetic polymers with artificial recognition sites formed by polymerization of a material in the presence of a template molecule. Removal of the template creates an analyte selective robust material that can be easily used for a variety of applications. Molecular imprinting can be achieved through three approaches, covalent, non-covalent (self assembly), and semi-covalent imprinting [32–34].

The first work on non-covalent inorganic imprinting was started in early 1930s by Polyakov on imprinted silica gel [35]. A similar methodology was used later by Dickey [36] to prepare a selective adsorbent (silica gel) for methyl orange dye. In the early 1970s, the imprinting of organic polymers was reported for covalent imprinting of vinyl polymers [37]. Non-covalent organic imprinting was introduced later by Mosbach and Arshady [38].

The main advantage of using MIPs is the low cost of preparation in comparison with other materials that show similar selectivity over their biological counterparts [33]. Moreover, they have a good stability over a range of temperatures and pressures, and are relatively inert in acids, bases and organic solvents. Their structure should be rigid enough to maintain the structure of cavities after removing the template, while keeping some flexibility for releasing and up-taking of the template. Recent applications of MIPs include environmental pollutants [39–42], drug delivery [43,44], food analysis [45,46], chemical sensors [47,48], proteins [49] and receptor systems [50,51].

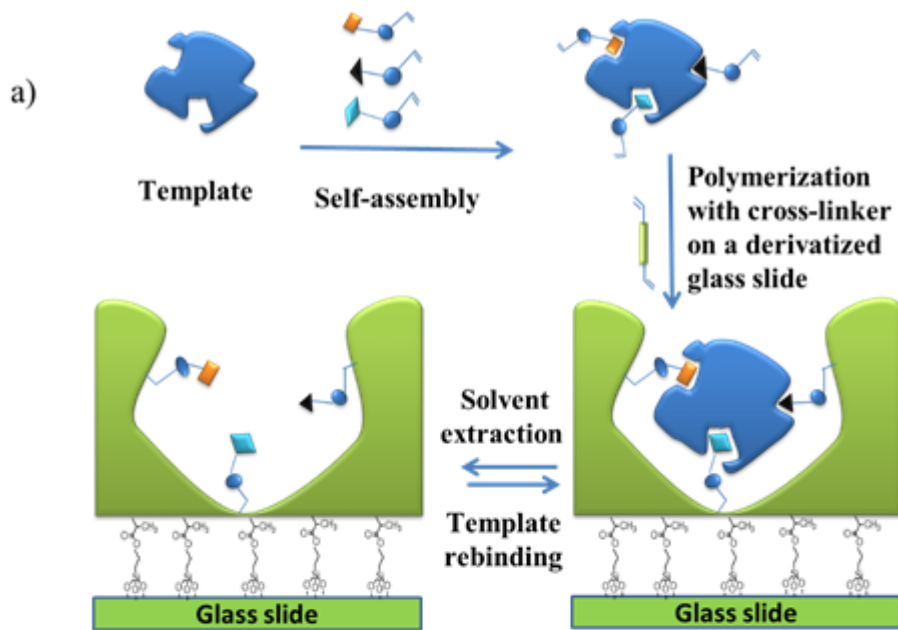
1.4.1. Covalent versus non-covalent imprinting

Non-covalent and covalent imprinting processes can be seen in Figure 1.2. Covalent imprinting is obtained by reacting the template with a functional monomer to form a covalent bond, which is intact through the polymerization process. The template is removed after polymerization by cleaving the bond, and this usually done by acid hydrolysis. Rebinding of analytes into the MIP is strong and very selective because there is a reformation of the bond. Although the binding sites in covalent MIPs are homogenous, the rebinding process is very slow and limited types of compounds such as alcohols, amines, ketones and carboxylic acids, can be imprinted [52]. Moreover, the derivatization of the template before the imprinting process sometimes is difficult and requires more experience in organic synthesis.

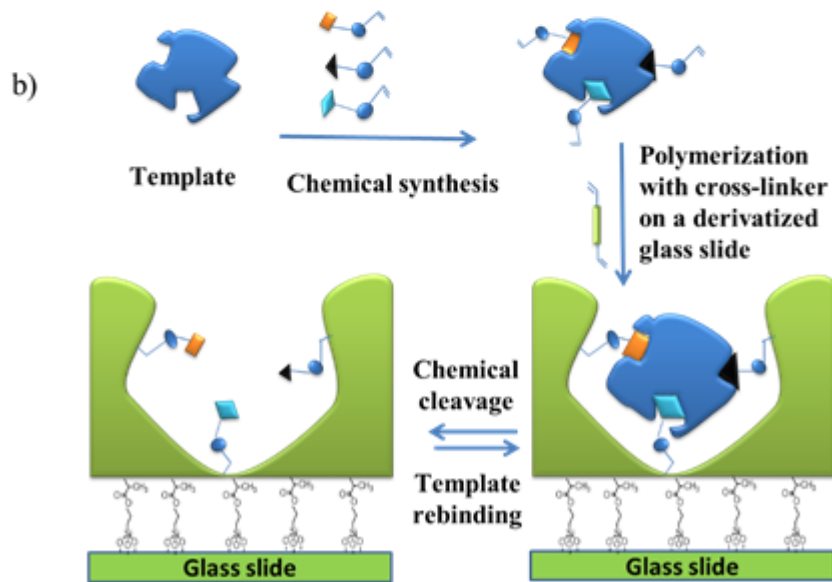
In non-covalent imprinting, the preparation is simpler and the template can rebind quickly. There is also a flexibility in choosing various templates and monomers. On the other hand, some drawbacks are present in this approach, for example, the template should be able to interact strongly with the functional monomer, e.g. through hydrogen bonding, dipole-dipole, ionic, hydrophobic and van der Waals interactions to form a stable complex [53]. Another limitation is coming from the fact that the stabilized interaction between the template and the functional monomer under hydrophobic imprinting conditions may be disrupted easily when the MIP is used for analysis in the polar environments [33].

An interesting approach called semi-covalent imprinting combines both covalent and non-covalent imprinting, where a covalent interaction is created for the imprinting process, while a non-covalent interaction takes place in the rebinding process [54]. The aim

of this approach is to produce a homogeneous MIP with higher binding capacities with high selectivities. It also allows the rebinding process with analytes occur more quickly than for a fully covalent MIP. However, the semi-covalent approach still suffers from the drawbacks of covalent imprinting such as the limitation in the number of compounds that can be imprinted and the necessity of template derivatization before imprinting in some cases.



Non-covalent imprinting



Covalent imprinting

Figure 1.2. Schematic representation of a) non-covalent and b) covalent molecular imprinting processes.

1.4.2. Main components of MIPs

The main components in any MIP system are the template, monomer, cross-linker, initiator, and solvent (porogen). The template is usually the analyte itself or can be an analogous compound to that analyte. Monomers (common examples are shown in Figure 1.3) are usually used in molar excess to the template in the imprinting process to enhance the formation of the template-monomer complex, which is governed by equilibrium between them. Methacrylic acid (MAA) is often used as a monomer due to its capability to form a hydrogen bonds with templates [55].

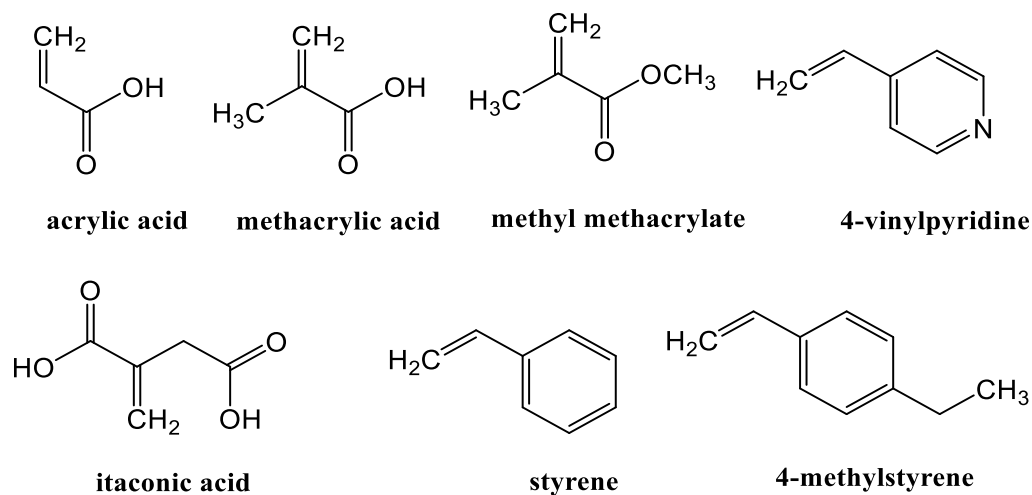
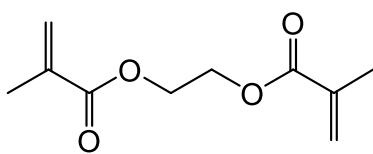
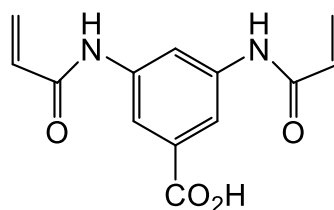


Figure 1.3. Common functional monomers used in molecular imprinting procedures [33].

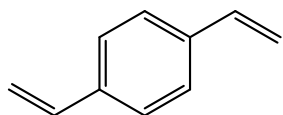
The cross-linker plays an important role in controlling of the morphology of polymer and in creating a material that possesses good mechanical properties [56]. Ethylene glycol dimethylacrylate (EGDMA) and divinylbenzene (DVB) are the most common crosslinking agents used [57] (Figure 1.4).



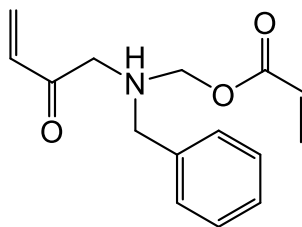
Ethylene glycol dimethacrylate



3,5-bis(acryloylamido)benzoic acid



1,4-divinylbenzene



N,O-bisacryloyl-phenylalaninol

Figure 1.4. Chemical structures of common cross-linkers used in molecular imprinting [33].

Initiators are used usually in small quantities compared to the monomer (1 wt.% or 1 mol %) with respect to the total number of moles of polymerizable double bonds [33]. Azobisisobutyronitrile (AIBN) is one of the most effective initiators in thermal polymerization, giving isobutyronitrile radicals after homolytic cleavage under heat or UV light [58] while 2,2-dimethoxy-2-phenylacetophenone (DMPA) is used as photoinitiator in photo-radical polymerization (Figure 1.5).

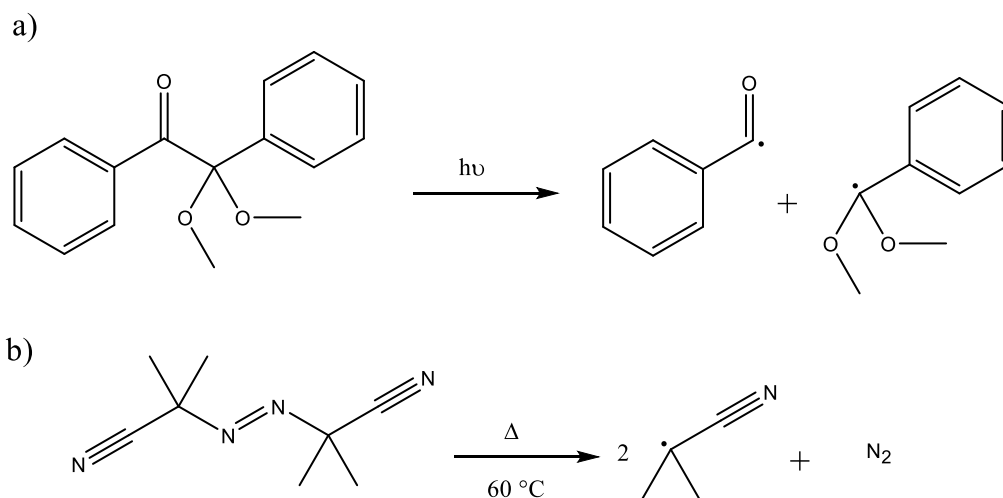


Figure 1.5. Formation of radicals in DMPA and AIBN [59].

The solvent used to bring all the MIP components together in one phase in the polymerization process is usually called the porogen (pore generator). A good solvent (solvating) typically produces microporous polymers, whereas a poor solvent (non-solvating) produces macroporous polymers [60,61]. MIPs should have good porosity to assure good accessibility of the analytes to the binding sites. This porosity can be promoted through selection of a proper porogen. Examples of some solvents used as porogens for MIPs preparation are toluene, chloroform, dichloromethane, methanol and acetonitrile [32]. Less polar porogens such as chloroform and dichloromethane are usually used to facilitate non-covalent interactions such as hydrogen bonding, while polar porogens such as methanol are used to enhance the hydrophobic interactions [55]. Water has been used previously as a porogen, for example, in the preparation of water-compatible polymers for the detection of 1-methyladenosine in human urine samples [62]. Unfortunately imprinting in water is difficult sometimes due to the limited range of water-soluble monomers and

cross-linkers [63]. The porosity of the MIP is also influenced by the porogen, for example, if the solubility of the formed polymer is low in the porogen, the phase separation will occur early and form large pores with lower surface area, and vice versa. MIP made without enough porogen has very poor selectivity because of the limited access of the analyte to the active binding sites [56].

1.4.3. Optimization of MIP composition

The optimization of the MIP composition must be made to obtain a material that has the desired analytical performance and morphological properties. The important factors in the MIP optimization are the initial selection of the monomer and the determination of the optimum mole ratio of the template to monomer. In covalent imprinting, the template to monomer ratio is dictated by the template monomer reaction stoichiometry, so optimization on this basis is uncommon [33]. On the other hand, optimization is very important in the fabrication of non-covalent MIPs due to the use of the non-stoichiometric molar ratio between the template and monomer which is used in the preparation of MIP. While generally, any template can be used in non-covalent imprinting, other factors such as unwanted interactions with cross-linker and sometimes self-association between the monomer molecules themselves cannot be avoided. Moreover, the monomer is usually added in excess, therefore it can be spread outside the receptor cavities which can lead to the formation of non-specific interactions. Another problem in non-covalent imprinting is the low number of high affinity receptor sites produced in comparison with the relative amount of template used. This may be due to the disruption of the weak bonds between the

template and monomer before polymerization, or due to the poor cross-linking, which produces less rigid cavities [63].

The targeted analyte which is usually selected as the template must be inert under the polymerization conditions, and this means that a template should be avoided if it has any functional group that could interfere or inhibit the free radical polymerization process. Moreover, the template should be stable during the polymerization so it will not decompose at elevated temperature or under UV irradiation [33]. In some cases, the template is replaced by another analogous compound called a pseudo-template [64–66]. This is made to overcome the problem which can occur due to the possibility of template bleeding from MIP during the analysis which leads to a significant increasing in the sample background and restriction of the application of MIP for detection at low levels of concentrations ($\mu\text{g L}^{-1}$). A pseudo-template must possess the same properties and share at least one characteristic functional groups with the original template.

Other factors such as optimization of the monomer to cross-linker ratio and the selection of porogen should be implemented to get the best composition. The mole ratio of the monomer to cross-linker is important because at high ratios, the binding sites in the polymer are very close and this may lead to inhibition in the binding between the neighbouring sites, while at low ratios the imprinting efficiency may be reduced due to the possibility of interactions between cross-linker and monomer or template. Some studies found that the influence of cross-linker on the physical properties of MIP is high with minor effect on the interaction between the template and monomer [67,68]. Since the stability of the template-monomer complex is crucial, the temperature of polymerization must be

controlled. The use of high temperature in the polymerization process may destabilize the interaction between the template and monomer, and taking into account that the free radical polymerization is an exothermic reaction, this may lead to the formation of a gel-like material with poor selectivity and stability [63].

The role of the porogen is significant and careful selection is necessary to produce an optimal MIP. In the non-covalent imprinting polymerization, the porogen enhances the template-monomer complex formation. Better rebinding capacity is obtained when uploading of analyte is carried in the same porogen used for the imprinting process. For example, the retention of 9-ethyladenine in an HPLC column packed with a polymer prepared with the same eluting solvent (acetonitrile) is almost three times greater than the retention in a column packed with the same polymer but prepared with a different solvent (chloroform) [56]. However, it is not always possible to prepare and analyze MIPs using the same solvent system, mainly because of limitations in solubility of the pre-polymerization components.

1.4.4. Methods of MIPs preparation and formation

MIPs can be prepared in various forms using different methods based on their applications. Bulk polymerization [69], suspension polymerization [70], precipitation polymerization, surface imprinting [71] and monolithic [72] polymerization are the common methods. The most common method is bulk polymerization, where the MIP is prepared by solution polymerization followed by a mechanical grinding to produce particulates. The powdered polymer is then sieved to obtain the desired particle size range

[73,74]. This method is simple, but time-consuming and the resulting particles usually have irregular sizes and shapes. Furthermore, a significant proportion of the active sites may be destroyed during the grinding process, which would reduce the binding capacity and selectivity of MIP.

To overcome these problems, MIPs can be prepared in other forms such as beads [75], membranes [76], and thin-films [77,78]. In this section, the discussion will be limited to the methods for preparation of thin-films, since the research presented here is aimed at preparation of MIPs in thin-films. Regardless of their applications, MIP thin-films can be prepared on substrates using methods such as surface coating [79,80], spin coating [81], sandwiching [82] and electrochemical polymerization [83,84] techniques. In surface coating, the polymer particles are prepared in advance by bulk or suspension polymerization, and then mixed with additives such as polyvinyl chloride (PVC) to help particles adhere to the surface of the substrate [80]. This method is simple, but suffers from poor control over the film thickness. Moreover, the use of additives may prevent the access of analytes to the binding sites. Spin coating is a more controllable technique and offers good control over the thickness and homogeneity of the thin-film [81].

In the spin coating method, a small amount of pre-polymerization mixture is applied on the center of a flat substrate. The substrate is then rotated with UV curing at a high speed (1600-6000 rpm) to spread the coating material by centrifugal force, leaving a thin-film polymer on the surface. The rotation is continued until the desired film thickness is achieved. The thickness of the film is affected by the viscosity and concentration of the pre-polymerization mixture; this leads to some limitations such as the necessity of having

a viscous pre-polymerization mixture and a limited selection of solvents [85]. Since most solvents used in the MIP preparation, such as chloroform, methanol, and acetonitrile, are relatively volatile, this method is very limited. Therefore, in situ polymerization using a sandwiching technique is an alternative to spin coating since any solvent can be used. For example, in our project, the pre-polymerization mixture is pipetted onto a derivatized glass slide and covered immediately with a cover glass and then photopolymerized under UV light. The cover slide is removed immediately after polymerization, leaving a polymeric thin-film with an average thickness of 15 μm . The thickness of the film can be varied over a range of a few microns by varying the pipetted amount of pre-polymerization mixture between the two surfaces. Another example of using this technique is thin-film fabrication for chemical sensors. Haupt et al. [86] prepared a chemical sensor for selective determination of the drug *S*-propranolol. This sensor was based on an MIP film as the recognition element and a quartz crystal microbalance (QCM) as the transducer. The film was prepared between a surface of a gold electrode and a quartz disk using the sandwiching technique. The polymerization was carried out under a UV irradiation at 350 nm for 10 min by placing the sandwich assembly on a flat window of a UV lamp with a cover quartz disk facing the lamp and then a weight of 0.5 kg was applied axially to the assembly. Jakusch et al. [87] also used the sandwiching technique to prepare a Fourier-transform infrared (FT-IR) sensor for selective detection of the herbicide 2,4-dichlorophenoxyacetic acid (2,4-D). The MIP film in this sensor is prepared on a surface of selenide attenuated total reflection elements.

If a thinner MIP film is required, the electrochemical polymerization technique can be used. For example, preparation of electrosynthesized poly(o-phenylenediamine) (PPD) on a QCM biomimetic sensor for glucose detection has been reported [83]. The electro-polymerization of o-phenylenediamine (o-PD) was achieved by cyclic voltammetry in the range 0.0-0.8 V from a solution of o-PD in an acetate buffer. They have found that, by controlling the amount of the circulated charge, the MIP film can be easily grown on the surface with a controlled thickness. The disadvantages of this technique are the requirement of conductive surfaces and the number of functional monomers suitable for this technique are limited.

1.4.5. Characterization of MIPs

Several techniques can be used to characterize the chemical and morphological properties of MIPs. For example, ^1H and ^{13}C nuclear magnetic resonance (NMR) can be used to confirm the formation of non-covalent template-monomer interactions [88]. FT-IR spectroscopy has been used to follow the changes in functional groups between the prepared polymer and the functional monomers that are used in the preparation of the polymer. Examples of these changes are the shift in or disappearance of the spectral peaks associated with the polymerizable groups of the functional monomers in the FTIR spectrum after polymerization [89,90]. Microscopic techniques, such as a scanning electron microscopy (SEM), are used to study the surface morphology of the polymer [91], and to measure the thickness of MIP films [92]. In SEM, a primary beam of electrons scans the

surface of the MIP; this process causes several kinds of interactions generating secondary electrons and back scattered electrons which can be used to create an SEM image [93].

Nitrogen sorption porosimetry by BET (Brunauer, Emmet and Teller) analysis is used to determine the surface area, pore volume, pore size distribution, and average pore diameter [94,95], while the mercury intrusion porosimetry method is used for the characterization of larger pores. In nitrogen sorption porosimetry experiments, a fixed amount of dry MIP is exposed to nitrogen gas at a series of fixed pressures. The amount of sorbed gas is calculated as a function of pressure, and then an adsorption isotherm is constructed from the application of BET theory and mathematical models. The mercury intrusion porosimetry technique is carried out in the same way, except that mercury is used instead of nitrogen gas. Unfortunately, the direct application of those techniques on MIP films is unfavorable due to necessity of removing the MIP films from the glass slide before measurement, which may lead to results that do not reflect the true morphological properties of these films.

Several binding isotherm models can be used to evaluate the binding equilibrium behaviour of MIPs (Table 1.3). Binding behaviour such as the binding capacity and association constants of MIPs in batch rebinding experiments are usually evaluated by the Scatchard analysis model [54,96].

Table 1.3. Binding isotherm models, adapted from [97].

Isotherm model	Linearized form	Plot	Parameters
Langmuir	$1/Q = (1/NK) + (1/C)$	(1/Q) vs. (1/C)	$K = \text{intercept/slope}$, $N = 1/\text{intercept}$
Scatchard	$Q/C = K_a N_t + K_a Q$	(Q/C) vs. Q	$K_a = \text{-slope}$, $N_t = \text{intercept/slope}$
Freundlich	$\log Q = m \log C + \log a$	$\log Q$ vs. $\log C$	$a = 10^{-\text{intercept}}$, $m = \text{slope}$
Langmuir–Freundlich	Solver function in Microsoft Excel	$\log Q$ vs. $\log C$	a, m, K and N_t

For example, Longo et al. [96] constructed a Scatchard plot between the ratio of the binding capacity of tri-O-acetyladenosine (TOAA) to the free concentration of TOAA ($Q/[TOAA]$) versus the binding capacity of TOAA (Q) at equilibrium (Figure 1.6). The total number of binding sites (N_t) and the association constant (K_a) were determined from the slope and the intercept of the curves.

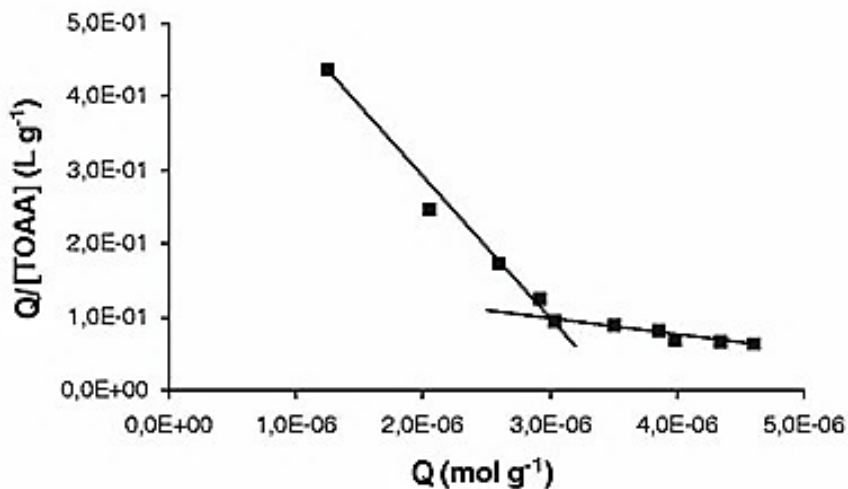


Figure 1.6. Scatchard plot for $PP_{ZnM}(TOAA)$, adapted with permission from [96].

Langmuir, Freundlich [98,99] and Langmuir-Freundlich (LF) isotherm models [100,101], which use data from batch rebinding experiments or chromatographic frontal-zone analysis, are also used to characterize and understand the binding behaviour of MIPs. From these plots, various parameters can be calculated such as, the total number of binding sites, heterogeneity indices (m), and fitting parameter constant (a) which is a measure of the capacity and average affinity of the polymer. These models measure the relationship between the equilibrium concentration of bound and free analyte over a certain concentration range.

The Langmuir isotherm is used based on the assumption that the adsorption of analyte takes place at specific homogeneous sites within the adsorbent. The concentration of the bound analyte (Q) can be calculated from the following equation:

$$Q = \frac{N K C}{1 + K C} \quad (1.1)$$

where N is the number of homogeneous sites, K is the binding affinity constant, and C is the concentration of free analyte in the solution. To obtain a Langmuir isotherm curve, the Equation (1.1) should be linearized as follows:

$$\frac{C}{Q} = \frac{1}{N K} + \frac{1}{N} C \quad (1.2)$$

The values of N and K can be determined by plotting C/Q versus C . Since MIPs are mainly classified as heterogenous material [102], this model is often not suitable for them.

The Freundlich isotherm model is used to describe the heterogeneity of the surface and multilayers within the adsorbent. It is a power function as follows:

$$Q = aC^m \quad (1.3)$$

where a is the Freundlich fitting parameter, related to the median binding affinity (K_0), and m is the heterogeneity index. The heterogeneity index describes the degree of adsorbent heterogeneity. Its values range between 0 and 1, and when m becomes closer to 1, the heterogeneity decreases and homogeneity increases. The Freundlich isotherm plot is obtained by rearranging of the Equation (1.3) to a linear form as:

$$\log Q = m \log C + \log a \quad (1.4)$$

By plotting $\log Q$ versus $\log C$, the values of a , and m can be calculated from the curve equation ($m = \text{slope}$ and $a = 10^{\text{intercept}}$).

A hybrid model called Langmuir-Freundlich (LF) isotherm was developed to model both homogenous and heterogeneous materials at low and high concentrations of sorbate [98,103]. This model is also known as the Sips equation [104,105]. In the case of MIPs, the Sips equation is used as a function to describe a specific relationship between the equilibrium concentration of bound analyte (Q) and the free analyte concentration (C) in solution as follows:

$$Q = \frac{N_t aC^m}{1 + aC^m} \quad (1.5)$$

where N_t is the total number of binding sites, a is the fitting parameter related to the median binding affinity (K_0) via $K_0 = a^{1/m}$. The heterogeneity index, m in Equation (1.5), is identical to that of the Freundlich isotherm. Since the LF isotherm has three fitting parameters (a , m and N_t), the linear analysis is not possible. Alternatively, the solver function in Microsoft Excel can be used by plotting $\log Q$ vs $\log C$ and adjusting the coefficient (R^2) to 1 by varying the fitting parameters. The advantage of the LF isotherm model over the Freundlich isotherm is the ability to measure the value of N_t directly from Equation (1.5) and does not require an independent measurement as in the case of Freundlich isotherm. However, the Freundlich isotherm is the best model to characterize the binding behaviour of MIPs compared to others because of its simplicity in describing the binding behaviour of non-covalent heterogeneous MIPs.

An important parameter in the imprinting process is called the imprinting factor (IF), which is used to evaluate the imprinting effect and to get an idea about the selectivity of MIPs. This parameter is calculated using the same data used for the study of equilibrium binding. In our work, the binding capacities (Q , $\mu\text{g g}^{-1}$) of MIP and NIP are calculated using the following equation:

$$Q = \frac{(C_0 - C) V}{m_{film}} \quad (1.6)$$

where C_0 ($\mu\text{g L}^{-1}$) is the initial concentration of the thiophene compound in the water sample, C ($\mu\text{g L}^{-1}$) is the concentration of the thiophene compound in the water sample at equilibrium, V (L) is the volume of the sample, and m_{film} (g) is the mass of the MIP film.

The IF represents the binding capacity of the MIP (Q_{MIP} , $\mu\text{g g}^{-1}$) over the binding capacity of the NIP (Q_{NIP} , $\mu\text{g g}^{-1}$) and is calculated as follows:

$$IF = \frac{Q_{MIP}}{Q_{NIP}} \quad (1.7)$$

1.5. MIPs for thiophene compounds

Most MIPs prepared for thiophene compounds are used to extract or remove these compounds from fuel or petroleum products. To our knowledge, there is no study or work on using MIPs for detecting these compounds in aqueous or environmental media. Tom et al. [106] prepared two MIPs by a bulk polymerization technique to remove 4,6-DMDBT from fuel. The first MIP was prepared with non-covalent imprinting using methacrylic acid as a monomer, EGDMA as a cross-linker, AIBN as an initiator, and chloroform as porogen. The polymer was packed into a stainless steel HPLC column and used as a solid HPLC phase in the analysis of thiophene compounds. The results showed that the imprinted polymer retained the 4,6-DMDBT slightly longer (selectivity factor, $\alpha = 1.1$) than the non-imprinted polymer. The second polymer was prepared using nickel (II) methacryloylhistidinedihydrate as a monomer with EGDMA and toluene as a porogen. This polymer gave a selectivity three times greater ($\alpha = 3.2$) than the non-imprinted polymer.

Xu et al. [107] prepared MIP as a sorbent for DBT from oil using a surface imprinting technique. The polymer composites (MIP/ $\text{K}_2\text{Ti}_4\text{O}_9$) are prepared using DBT as a template, 4-VP as a monomer, and potassium tetratitanate whiskers ($\text{K}_2\text{Ti}_4\text{O}_9$) as the

carrier; this crystalline material was chosen due to its mechanical and thermal stability. The $K_2Ti_4O_9$ was modified with 3-(methylacryloxy)propyltrimethoxy silane, and then 4-VP was grafted and polymerized on the surface of $K_2Ti_4O_9$ to produce P4VP/ $K_2Ti_4O_9$. The final step was imprinting the DBT over the P4VP/ $K_2Ti_4O_9$ using EGDMA as cross-linker and AIBN as an initiator. The prepared MIP showed selectivity for DBT of 2.5 times greater than that of other similar compounds such as BT, 4-MDBT, and 4,6-DMDBT. Xu et al. [108] also used the same approach by imprinting on a surface of TiO_2 particles.

1.6. Detection systems used with MIPs

MIPs can be coupled to various chromatographic and spectroscopic techniques for online and offline analysis. The discussion of detection systems used with MIPs will be limited only to those used in this research.

1.6.1. Gas chromatography mass spectrometry (GC-MS)

Identification and quantification of thiophene compounds in oil and marine water by gas chromatography (GC) coupled with a mass selective detector (MSD) is common to many methods including US EPA methods [9,21,28,109,110]. In GC, the compounds injected into the system are separated based on their boiling points and the partition between gaseous mobile phase and stationary liquid phase. The elution rate of each analytes in the column depends on the strength of adsorption, which in turn depends on the type of analyte and on the stationary phase of the column [111,112]. Usually, a mixture of standard targeted compounds is injected into the GC to obtain the peak retention times and to determine the response factors of these compounds for a selected detector. MS is

considered a universal detector and it is very selective compared to the more common flame ionization detector (FID) [113]. If the electron ionization (EI) source is used in the GC-MS, the analyte ionization and fragmentation will take place after elution from the GC column due to the interaction with the energetic electrons in the MS source. The molecular ions and fragment ions are then separated in the mass analyzer based on their mass-to-charge ratios (m/z) and a mass spectrum of each component is recorded. The most common mass analyzer coupled with GC is the quadrupole mass analyzer (Figure 1.7). This analyzer is compact, inexpensive, sensitive, and easy to operate. In addition to the full scan capability, it can be operated in selected ion mode (SIM) for higher sensitivity. In this mode, only ions with the requisite m/z typical for the targeted compound will be monitored to the exclusion of all others.

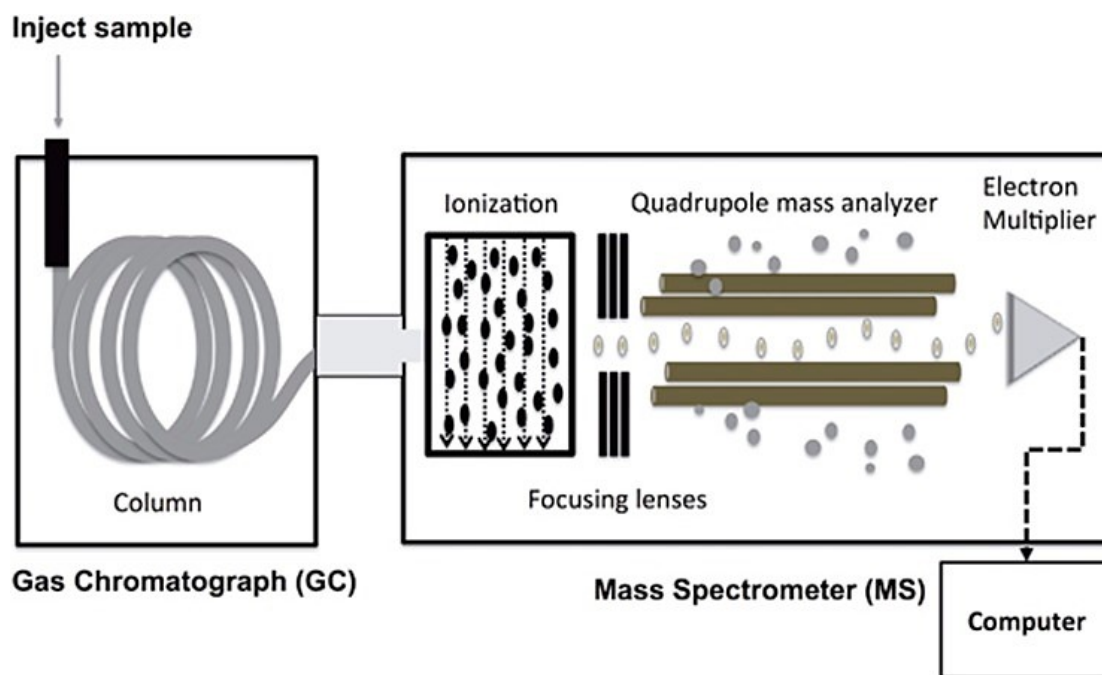


Figure 1.7. Schematic diagram of a gas chromatography quadrupole mass spectrometer (GC/MS), taken with permission from [114].

Although MS is very selective, it does not respond specifically to the sulfur atom present in sulfur-containing compounds as does the sulfur chemiluminescence detector (SCD). Therefore, with MS the degree of selectivity for thiophene compounds will depend on what other sample components give rise to the signal monitored (i.e. isobaric interferences). Using an MIP as a selective sorbent material for thiophene compounds prior to GC-MS analysis (see Chapter 2) greatly reduces the number of interferences that could be introduced with other components into the GC column. Moreover, the selectivity is further enhanced by using a highly selective detector such as SCD (see Chapter 3).

1.6.2. Headspace gas chromatography sulfur chemiluminescence detector (HS-GC-SCD)

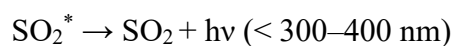
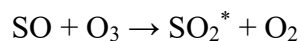
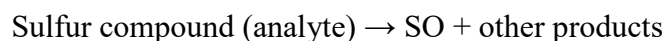
The thiophene compounds (BT, 3-MBT, DBT, 4-MDBT and 4,6-DMDBT) in this targeted research can be classified as semivolatile compounds [110,115]; this makes their analysis by a headspace technique (HS) accessible. HS refers to the gas phase components in contact and in equilibrium with another phase (liquid or solid), which sequesters most non-volatile or less volatile components. An aliquot from the gas phase can be transferred to an analyzer after equilibrium is achieved between phases without interference from non-volatile compounds in the sample. This method is called static-headspace, in which the two phases in the sample vial are under static conditions. Another type of headspace is called dynamic headspace in which a continuous flow of an inert gas is applied above a liquid or a solid sample or is bubbled through a liquid sample to strip out the volatile compounds, and then the volatile compounds are concentrated on a sorbent trap that is then rapidly

heated to desorb the analytes onto a GC for analysis (purge and trap). Since the method used in our work is a static-headspace, the detailed discussion will be limited to this type.

Headspace techniques can be coupled to various analytical systems such as GC-MS and GC-SCD, where the components in the gas phase (vapor) are separated first by GC and then detected by MS or SCD. HS-GC methods for the analysis of solid samples are widely used. For example, Chai et al. [116] reported a full evaporation HS-GC-FID method for the determination of a residual monomer in methyl methacrylate (MMA) polymer latex. The full evaporation was used in this method to overcome the problem of irreproducible results associated with the analysis of analytes in unpredictably changing sample matrices. Therefore, a very small amount (10-30 mg) of sample was used to ensure a near-complete transfer of analyte from the solid sample into a vapor phase. Equilibration was reached within 5 min at 110 °C. In another application, a determination of sulfur mustard (HD) and related compounds in soil samples was reported by Røen et al. [117] using a HS-GC-MS method. According to the author, a 2-mL saturated sodium chloride solution was added to the sample vial prior to HS analysis to increase the sensitivity by increasing of the partitioning of analytes into the headspace vial. A detection limit of 3 ng g⁻¹ was achieved for HD, while other compounds were detected at 0.2-0.7 ng g⁻¹. A shorter equilibration time in this method was applied in HD analysis compared to other sulfur compounds due to the rapid degradation of HD at a longer equilibration time.

In Chapter 3 of this thesis, a MIP thin-film was prepared on a glass slide and used as a sorbent to extract targeted thiophene compounds from seawater. The MIP film was treated as a solid sample and analyzed by HS-GC-SCD. The slide was placed in a headspace

vial at a constant temperature for a specific period. When the equilibrium was reached between the two phases, a small volume from the gas phase in the vial was injected into the GC column followed by a selective detection by SCD. This method is rapid and highly selective, since only volatile or semivolatile compounds are injected into the GC column. Because of this, the solvent extraction of the MIP film before GC-MS analysis as used in Chapter 2 is not necessary. Furthermore, the use of SCD for detection improves the selectivity [9,118]. The mechanism of sulfur detection by SCD can be summarized based on the following reactions [118]:



In this mechanism, the sulfur monoxide (SO) and other combustion products are transferred to the reaction cell. The reaction of SO with ozone (O₃), which is generated from the ozonator, produces an electronically excited sulfur dioxide (SO₂^{*}) and oxygen (O₂). The excited SO₂ returns to the ground state and emits a chemiluminescence light, which is measured by a photomultiplier tube. The intensity of emitted light from each analyte is proportional to the concentration of the analyte in the sample.

1.6.3. Desorption electrospray ionization mass spectrometry (DESI-MS)

DESI is an ambient ionization technique combining electrospray ionization (ESI) and desorption ionization (DI) methods [119]. The mechanism of ion formation in DESI was explained by a droplet pick-up mechanism [120]. Ionization is accomplished by directing an electrically charged spray to the sample surface under ambient conditions (Figure 1.8). The electrosprayed charged droplets and ions of solvent impact the surface of the sample with a specific velocity and form a thin layer on the surface, where extraction (or dissolution) of the analyte occurs. The impact of the charged droplets on the wetted surface generate gaseous ions of the analytes originally present on the surface. After solvent evaporation and ionization, the formed ions travel through the air to the interface and then to the mass spectrometer.

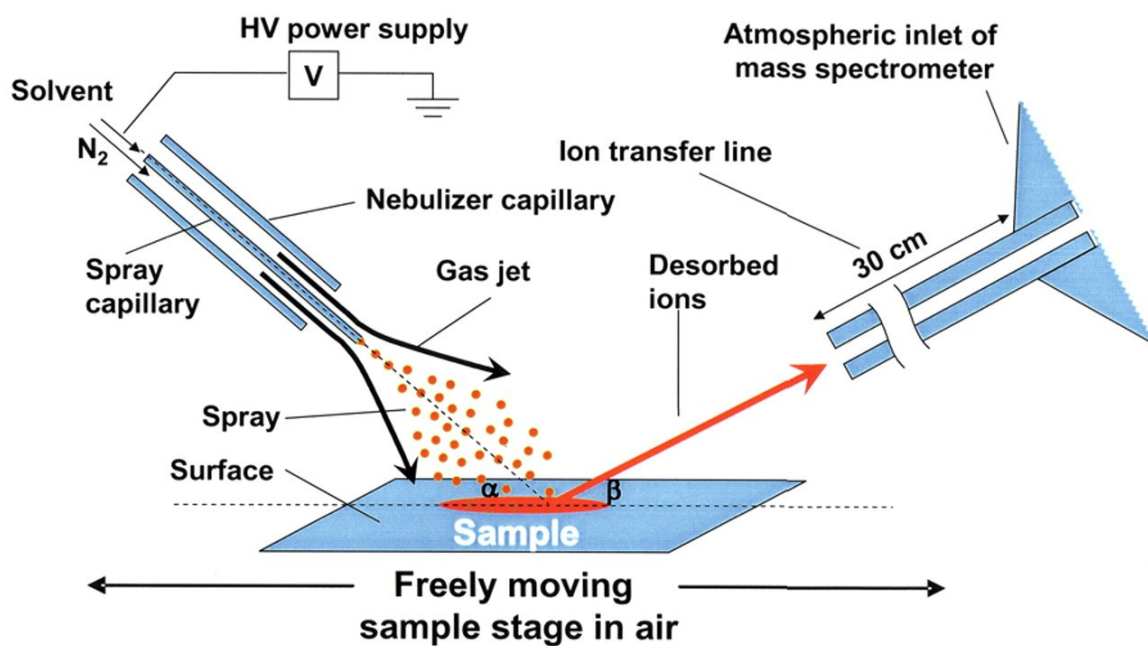


Figure 1.8. DESI source adapted with permission from [119].

In DESI analysis, no matrix is required as is the case for the matrix-assisted laser desorption/ionization (MALDI) technique [121], and usually an aqueous sample is deposited on an inert surface such as a polytetrafluoroethylene (PTFE) plate. The signal intensity in the mass spectrometer depends on many factors such as the type of analyte, the spray angle (α) and ions collection angle (β), the distance between the electrospray emitter and the surface, and the distance between the surface and the mass spectrometer inlet. These factors must be optimized to produce a higher signal intensity [119]. Several mass spectrometers have been used with DESI, such as triple quadrupole [122], quadrupole-time-of flight (QTOF) [123], linear ion trap [124], Orbitrap [125], and Fourier transform ion cyclotron resonance (FTICR) [126] mass spectrometers. The limits of detection in DESI is greater than those in the corresponding ESI experiments by an order of magnitude (femtomole). Standard deviations below 5% and accuracies of $\pm 7\%$ (relative error) have been reported [127]. DESI experiments can be applied to ionize polar and non-polar compounds, and it is applicable to small and large molecules [128]. Although DESI can be applicable to non-polar compounds, there is no reported work for the analysis of thiophene compounds by DESI, so it can be expected that the desorption ionization of thiophene compounds in DESI analysis will be very weak. This may be attributed to the high ionization energy of thiophene compounds which make their ionization by a soft ionization technique such as DESI unfavourable.

An example of the capability of DESI to ionize non-polar compounds is in the analysis of PAHs in biomass burning and ambient aerosols by Chen et al. [129]. The typical positive ion DESI spectrum of the analysis of PAHs in aerosols is shown in Figure 1.9.

They used methanol/acetic acid as the solvent spray to form molecular ions and protonated ions of PAHs. Although the method was used successfully to ionize targeted PAHs, the signal-to-noise ratio for some PAHs was poor and the sensitivity was low. This may be attributed to the high ionization energy of PAHs.

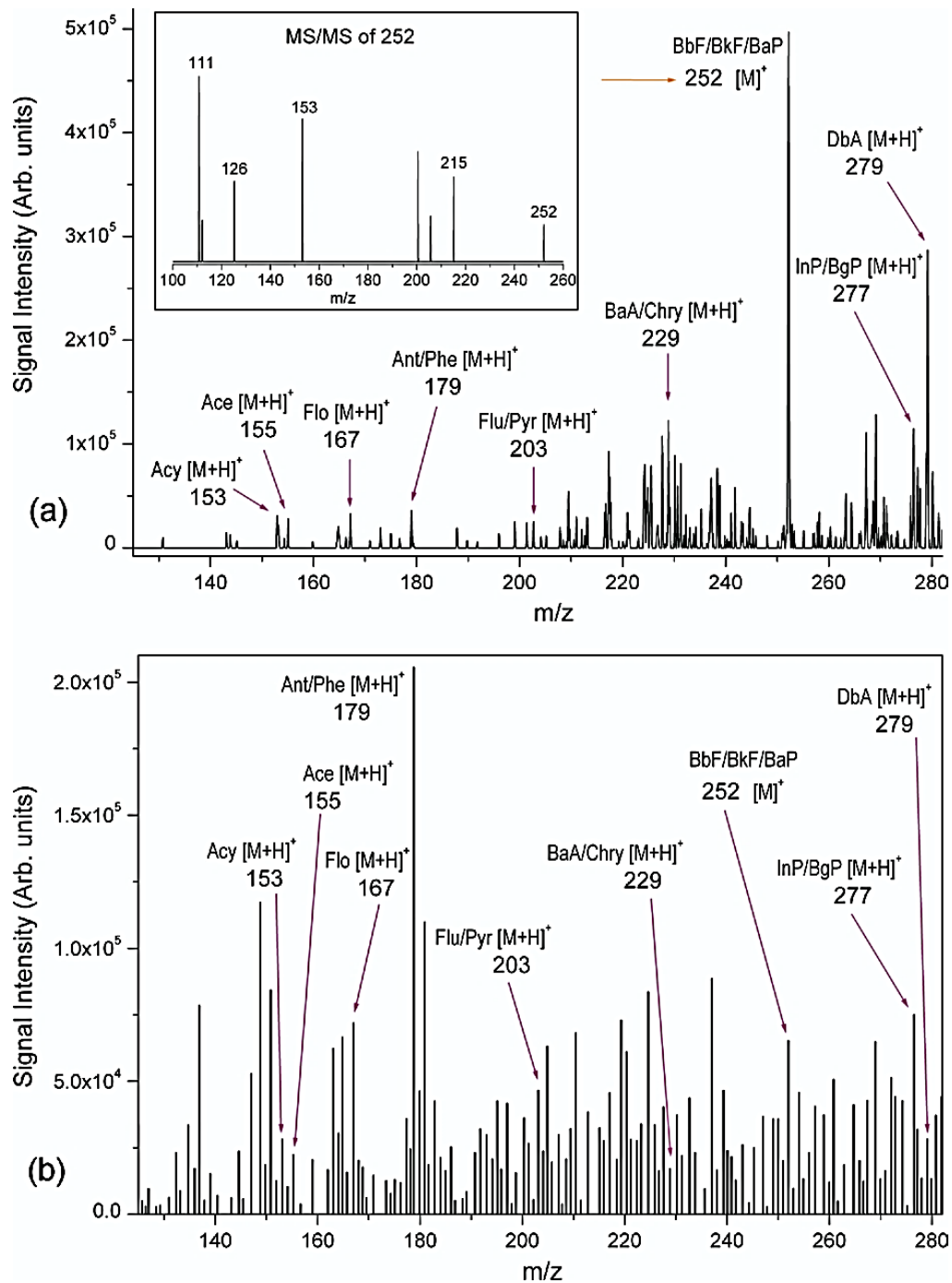


Figure 1.9. A typical DESI mass spectrum of PAHs from (a) biomass burning aerosol (b) ambient aerosol. Acenaphthylene (Acy), acenaphthene (Ace), fluorene (Flo), anthracene (Ant), phenanthrene (Phe), fluoranthene (Flu) and pyrene (Pyr), benzo[a]anthracene (BaA), chrysene(Chry), benzo[fluoranthene (BbF), benzo[k],fluoranthene (BkF), benzo[a]pyrene (BaP), and dibenzo[a,h]anthracene(DbA). The inset shows the MS/MS of the m/z = 252 ion for BbF/BkF/BaP, adapted with permission from [129].

To improve the peak intensity and sensitivity of PAHs, a reactive DESI experiment was used. Eftekhari et al. [130] developed a new detection method for PAHs based on cationization with silver ions. The addition of silver ions to the solvent spray (methanol) improved the sensitivity for PAHs and provided a good method to distinguish between the PAHs isomers. The interaction between the silver ion and the PAHs produced three main complexes $[\text{Ag}(\text{PAH})_n]^+$ ($n = 1, 2$), and $[\text{OH} + \text{Ag} + \text{PAH}]^+$ as seen in Figure 1.10. The ratios of the $[\text{PAH}]^+$ peak intensity to that of $[\text{Ag} + \text{PAH}]^+$, $[\text{Ag} + \text{OH} + \text{PAH}]^+$, $[\text{Ag}(\text{PAH})_2]^+$, and $[\text{PAH} + \text{O}_2]^+$ were used to differentiate the PAH isomers sharing the same molecular formula with different structures.

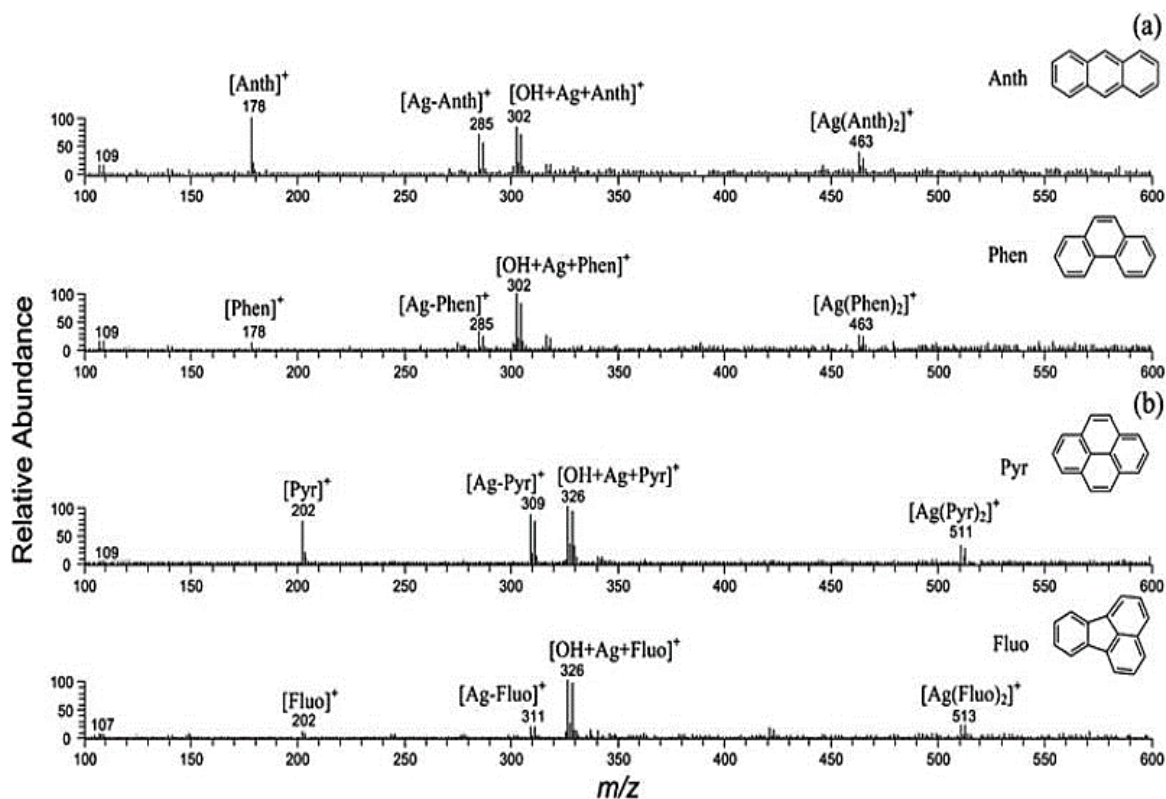


Figure 1.10. DESI-MS spectra of the isomer pairs: (a) anthracene and phenanthrene, and (b) pyrene and fluoranthene. Adapted with permission from [130].

Van Biesen et al. [82] reported the first use of MIP with DESI-MS for the detection of 2,4-dichlorophenoxyacetic acid (2,4-D) in water. The prepared MIP film was used to extract the analyte from a spiked tap water and river water. The selectivity of the MIP was compared to a non-imprinted polymer (NIP) using a sample river water spiked with 2,4-D and structurally related compounds phenoxyacetic acid (PAA), 4-chlorophenoxyacetic acid (4-CPA), 2,4,5-trichlorophenoxyacetic acid (2,4,5-T), and 2,4-dichlorophenylacetic acid (2,4-DCAA). The DESI-MS spectra of the MIP and NIP demonstrate the selectivity of MIP toward the analyte over the NIP (Figure 1.11). The MIP was shown to be much more selective toward the chlorinated analogs than the NIP.

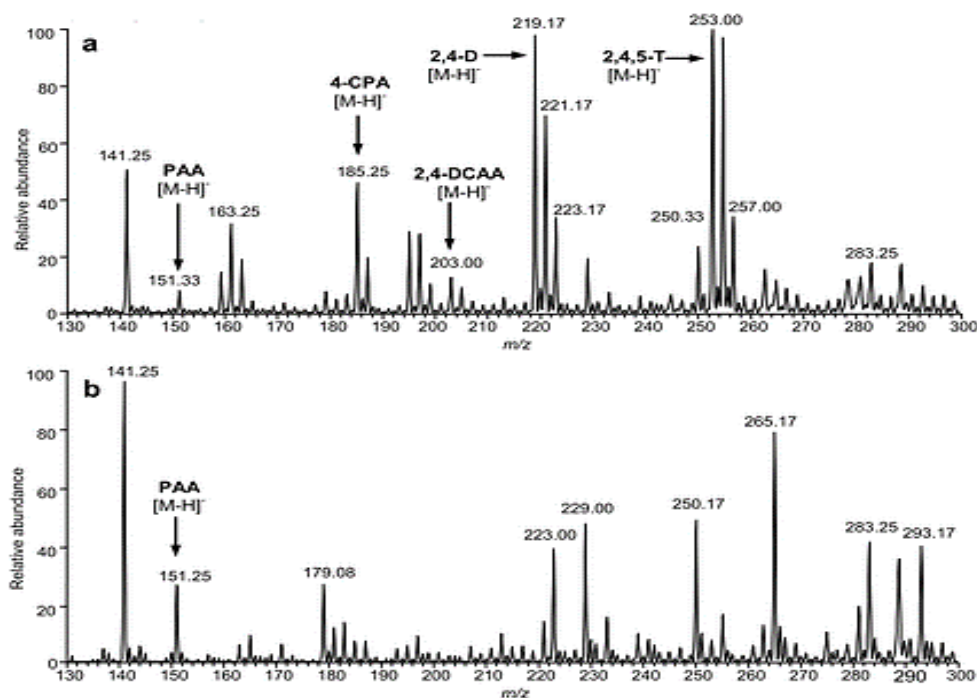


Figure 1.11. DESI-MS of a MIP (a) and a NIP (b) used for extraction from a 0.10 mg L⁻¹ solution of 2,4-D and analogs in river water. The results for tap water are similar. The maximum absolute intensity of the base peak in (a) is 407, in (b) 195, taken with permission from [82].

The previous example showed the applicability of DESI-MS to analyze the analytes bound to the MIP thin-films. This technique seems to be attractive since it is fast, sensitive and selective. Direct DESI analysis of the film, eliminates the extraction step needed after sample uploading as in the case of the analysis of thiophenes-MIP by GC-MS (see Chapter 2, Section 2.3.7). The sample exposed surface of the MIP film makes it suitable for high-throughput analysis, since many MIP films can be analyzed serially by DESI-MS.

1.7. Thesis objectives

The first objective of this thesis was to develop a new molecularly imprinted polymer thin-film (MIP thin-film) to extract thiophene compounds selectively from water samples. The second objective was to optimize the components of MIP to get the effective thin-film composition for the analysis of thiophene compounds in aqueous media. The third objective was to find a good methodology to produce a thin-film with acceptable shape and porosity to obtain a robust and reproducible film for the analysis. The final objective was to couple the developed thin-films with various chromatographic and mass spectroscopic analytical techniques, such as GC-MS, HS-GC-MS, and DESI-MS to establish more rapid and sensitive methods with desired reproducibility compared to the corresponding methods reported in the literature.

1.8. Co-authorship statement

The principal author (Hassan Y. Hijazi) declares that he contributed to all chapters of this thesis as the main researcher including: literature review, performing all experiments, collecting and analyzing the data, designing new experiments, presenting and discussing the data with the corresponding author, and writing the draft of all manuscripts. The corresponding author (Dr. Christina S. Bottaro) proposed the initial experiments and contributed to several aspects of the research chapters including supervision, data analysis, design of new experiments, and revision of all draft manuscripts. Chapter 3 was submitted for publication in peer reviewed journals with Hassan Y. Hijazi as first author and Dr. Christina S. Bottaro as the corresponding author. Chapter 2 and 4 will be prepared and submitted later with Hassan Y. Hijazi as first author and Dr. Christina S. Bottaro as corresponding author. There are no other co-authors were involved in the preparation of these manuscripts.

1.9. References

- [1] Farrington, B. J. W.; Medowell, J. E.; Scientists, S.; Hole, W. Mixing Oil and Water, Tracking the Sources and Impacts of Oil Pollution in the Marine Environment. *Oceanus* **2004**, *42* (3), 1–4.
- [2] Fathalla, E. M.; Andersson, J. T. Products of Polycyclic Aromatic Sulfur Heterocycles in Oil Spill Photodegradation. *Environ. Toxicol. Chem.* **2011**, *30* (9), 2004–2012.
- [3] Atlas, R. M.; Hazen, T. C. Oil Biodegradation and Bioremediation: A Tale of the Two Worst Spills in U.S. History. *Environ. Sci. Technol.* **2011**, *45* (16), 6709–6715.
- [4] Ivshina, I. B.; Kuyukina, M. S.; Krivoruchko, A. V.; Elkin, A. A.; Makarov, S. O.; Cunningham, C. J.; Peshkur, T. A.; Atlas, R. M.; Philp, J. C.; Fortney, J. L.; et al. Oil Spill Problems and Sustainable Response Strategies through New Technologies. *Environ. Sci. Process. Impacts* **2015**, *17* (7), 1201–1219.
- [5] Buskey, E. J.; White, H. K.; Esbaugh, A. J. Impact of Oil Spills on Marine Life in the Gulf of Mexico. *Oceanography* **2016**, *29* (3), 174–181.
- [6] Berthou, F.; Vignier, V. Analysis and Fate of Dibenzothiophene Derivatives in the Marine Environment. *Int. J. Environ. Anal. Chem.* **1986**, *27* (1–2), 81–96.
- [7] United States Environmental Protection Agency | US EPA <https://www.epa.gov/> (accessed Feb 27, **2017**).
- [8] Canadian Environmental Assessment Agency - Home <https://www.ceaa-acee.gc.ca/default.asp?lang=En> (accessed Feb 27, **2017**).
- [9] Hua, R.; Wang, J.; Kong, H.; Liu, J.; Lu, X.; Xu, G. Analysis of Sulfur-Containing

- Compounds in Crude Oil by Comprehensive Two-Dimensional Gas Chromatography with Sulfur Chemiluminescence Detection. *J. Sep. Sci.* **2004**, *27* (9), 691–698.
- [10] Speight, J. G. *The Desulfurization of Heavy Oils and Residua*; Dekker, **2000**.
- [11] Press, J. B.; Russell, R. K. Five-Membered Ring Systems. Part 1: Thiophenes & Se & Te Analogs. *Prog. Heterocycl. Chem.* **1994**, *6*, 82–105.
- [12] Gronowitz, S. *Thiophene and Its Derivatives*; Wiley, **1985**.
- [13] Seymour, D. T.; Verbeek, A. G.; Hruday, S. E.; Fedorak, P. M. Acute Toxicity and Aqueous Solubility of Some Condensed Thiophenes and Their Microbial Metabolites. *Environ. Toxicol. Chem.* **1997**, *16* (4), 658–665.
- [14] Pearlman, R. S.; Yalkowsky, S. H.; Banerjee, S. Water Solubilities of Polynuclear Aromatic and Heteroaromatic Compounds. *J. Phys. Chem. Ref. Data* **1984**, *13* (2), 555–562.
- [15] Lias, S. G.; Bartmess, J. E.; Liebman, J. F.; Holmes, J. L.; Levin, R. D.; Mallard, W. G. Gas-Phase Ion and Neutral Thermochemistry. *J. Phys. Chem. Ref. Data, Suppl. I.* **1988**, pp 1–861.
- [16] Durell, G.; Røe Utvik, T.; Johnsen, S.; Frost, T.; Neff, J. Oil Well Produced Water Discharges to the North Sea. Part I: Comparison of Deployed Mussels (*Mytilus Edulis*), Semi-Permeable Membrane Devices, and the DREAM Model Predictions to Estimate the Dispersion of Polycyclic Aromatic Hydrocarbons. *Mar. Environ. Res.* **2006**, *62* (3), 194–223.
- [17] Luellen, D. R.; Shea, D. Calibration and Field Verification of Semipermeable Membrane Devices for Measuring Polycyclic Aromatic Hydrocarbons in Water.

- Environ. Sci. Technol.* **2002**, *36* (8), 1791–1797.
- [18] Andersson, J. T. Polycyclic Aromatic Sulfur Heterocycles III. Photochemical Stability of the Potential Oil Pollution Markers Phenanthrenes and Dibenzothiophenes. *Chemosphere* **1993**, *27* (11), 2097–2102.
- [19] Environment and Climate Change Canada - Draft Screening Assessment - Petroleum Sector Stream Approach - Coal Tars and Their Distillates <http://www.ec.gc.ca/ese-ees/default.asp?lang=En&n=E34B0A52-1> (accessed Feb 28, 2017).
- [20] Warner, J. S. Determination of Sulfur-Containing Petroleum Components in Marine Samples. *Int. Oil Spill Conf. Proc.* **1975**, No. 1, 97–101.
- [21] Ogata, M.; Miyake, Y. Gas Chromatography Combined with Mass Spectrometry for the Identification of Organic Sulfur Compounds in Shellfish and Fish. *J. Chromatogr. Sci.* **1980**, *18* (11), 594–605.
- [22] Eastmond, D. A.; Booth, G. M.; Lee, M. L. Toxicity, Accumulation, and Elimination of Polycyclic Aromatic Sulfur Heterocycles in *Daphnia Magna*. *Arch. Environ. Contam. Toxicol.* **1984**, *13* (1), 105–111.
- [23] Bates, T. S.; Carpenter, R. Organo-Sulfur Compounds in Sediments of the Puget Sound Basin. *Geochim. Cosmochim. Acta* **1979**, *43* (8), 1209–1221.
- [24] Poon, R.; Davis, H. D.; Lecavalier, P.; Liteplo, R.; Yagminas, A.; Chu, I.; Bihun, C. Effects of Benzothiophene on Male Rats Following Short Term Oral Exposure. *J. Toxicol. Environ. Health* **1997**, *50* (1), 53–65.
- [25] Canadian Center for Occupational Health and Safety <https://www.ccohs.ca/oshanswers/chemicals/ld50.html> (accessed Jul 4, 2017).
- [26] Irwin, R. O. Y. J.; Service, N. P. Environmental Contaminants Encyclopedia

Dibenzothiophene Entry. *Natl. Park Serv.* **1997**.

- [27] Amat, A.; Pfohl-Leszkowicz, A.; Castegnaro, M. GENOTOXIC ACTIVITY OF THIOPHENES ON LIVER HUMAN CELL LINE (HepG2). *Polycycl. Aromat. Compd.* **2004**, 24 (4), 733–742.
- [28] Avino, P.; Notardonato, I.; Cinelli, G.; Russo, M. Aromatic Sulfur Compounds Enrichment from Seawater in Crude Oil Contamination by Solid Phase Extraction. *Curr. Anal. Chem.* **2009**, 5 (4), 339–346.
- [29] Yu, C.; Yao, Z.; Hu, B. Preparation of Polydimethylsiloxane/ β -Cyclodextrin/divinylbenzene Coated “dumbbell-Shaped” stir Bar and Its Application to the Analysis of Polycyclic Aromatic Hydrocarbons and Polycyclic Aromatic Sulfur Heterocycles Compounds in Lake Water and Soil by high performance liquid chromatography. *Anal. Chim. Acta* **2009**, 641 (1–2), 75–82.
- [30] Gimeno, R. .; Altelaar, a. F. .; Marcé, R. .; Borrull, F. Determination of Polycyclic Aromatic Hydrocarbons and Polycyclic Aromatic Sulfur Heterocycles by High-Performance Liquid Chromatography with Fluorescence and Atmospheric Pressure Chemical Ionization Mass Spectrometry Detection in Seawater and Sediment Samp. *J. Chromatogr. A* **2002**, 958 (1), 141–148.
- [31] Baltrons, O.; López-Mesas, M.; Palet, C.; Le Derf, F.; Portet-Koltalo, F. Molecularly Imprinted Polymer-Liquid Chromatography/fluorescence for the Selective Clean-up of Hydroxylated Polycyclic Aromatic Hydrocarbons in Soils. *Anal. Methods* **2013**, 5 (22), 6297.
- [32] Haupt, K.; Mosbach, K. Molecularly Imprinted Polymers and Their Use in Biomimetic Sensors. *Chem. Rev.* 2000, 100 (7), 2495–2504.

- [33] Yan, H.; Row, K. H. Characteristic and Synthetic Approach of Molecularly Imprinted Polymer. *Int. J. Mol. Sci.* **2006**, *7* (5), 155–178.
- [34] Shimizu, K. D.; Stephenson, C. J. Molecularly Imprinted Polymer Sensor Arrays. *Curr. Opin. Chem. Biol.* **2010**, *14* (6), 743–750.
- [35] Polyakov, M. V. Adsorption Properties and Structure of Silica Gel. *Zhurnal Fizieskoj Khimii 2 S* **1931**, *2*, 799–805.
- [36] Dickey, F. H. Specific Adsorption. *J. Phys. Chem.* **1955**, *59* (8), 695–707.
- [37] G. wulff, A. S. The Use of Polymers with Enzyme-Analogous Structures for the Resolution of Racemates. *Angew. Chemie Int. Ed.* **1972**, *11* (4), 334–342.
- [38] Arshady, R.; Mosbach, K. Synthesis of Substrate Selective Polymers by Host Guest Polymerization. *Macromol. Chem. Phys.* **1981**, *182* (2), 687–692.
- [39] Villar-Navarro, M.; Martín-Valero, M. J.; Fernández-Torres, R. M.; Callejón-Mochón, M.; Bello-López, M. Á. Easy, Fast and Environmental Friendly Method for the Simultaneous Extraction of the 16 EPA PAHs Using Magnetic Molecular Imprinted Polymers (Mag-MIPs). *J. Chromatogr. B* **2017**, *1044–1045*, 63–69.
- [40] Masqué, N.; Marcé, R. M.; Borrull, F.; Cormack, P. a; Sherrington, D. C. Synthesis and Evaluation of a Molecularly Imprinted Polymer for Selective on-Line Solid-Phase Extraction of 4-Nitrophenol from Environmental Water. *Anal. Chem.* **2000**, *72* (17), 4122–4126.
- [41] Jing, T.; Wang, J.; Liu, M.; Zhou, Y.; Zhou, Y.; Mei, S. Highly Effective Removal of 2,4-Dinitrophenolic from Surface Water and Wastewater Samples Using Hydrophilic Molecularly Imprinted Polymers. *Environ. Sci. Pollut. Res.* **2014**, *21* (2), 1153–1162.

- [42] Li, H.; Wei, X.; Xu, Y.; Lu, K.; Zhang, Y.; Yan, Y.; Li, C. A Thin Shell and “sunny Shape” Molecular Imprinted Fluorescence Sensor in Selective Detection of Trace Level Pesticides in River. *J. Alloys Compd.* **2017**, *705*, 524–532.
- [43] Hemmati, K.; Sahraei, R.; Ghaemy, M. Synthesis and Characterization of a Novel Magnetic Molecularly Imprinted Polymer with Incorporated Graphene Oxide for Drug Delivery. *Polymer (Guildf)*. **2016**, *101*, 257–268.
- [44] Puoci, F.; Iemma, F.; Picci, N. Stimuli-Responsive Molecularly Imprinted Polymers for Drug Delivery: A Review. *Curr. Drug Deliv.* **2008**, *5* (2), 85–96.
- [45] Anirudhan, T. S.; Christa, J.; Deepa, J. R. Extraction of Melamine from Milk Using a Magnetic Molecularly Imprinted Polymer. *Food Chem.* **2017**, *227*, 85–92.
- [46] Fan, D.; Jia, L.; Xiang, H.; Peng, M.; Li, H.; Shi, S. Synthesis and Characterization of Hollow Porous Molecular Imprinted Polymers for the Selective Extraction and Determination of Caffeic Acid in Fruit Samples. *Food Chem.* **2017**, *224*, 32–36.
- [47] Prasad, B. B.; Singh, K. Molecularly Imprinted Polymer-Based Core-Shells (Solid vs Hollow) @ Pencil Graphite Electrode for Electrochemical Sensing of Certain Anti-HIV Drugs. *Sensors Actuators B Chem.* **2017**, *244*, 167–174.
- [48] Yan, Y.-J.; He, X.-W.; Li, W.-Y.; Zhang, Y.-K. Nitrogen-Doped Graphene Quantum Dots-Labeled Epitope Imprinted Polymer with Double Templates via the Metal Chelation for Specific Recognition of Cytochrome *c*. *Biosens. Bioelectron.* **2017**, *91*, 253–261.
- [49] Tu, X.; Muhammad, P.; Liu, J.; Ma, Y.; Wang, S.; Yin, D.; Liu, Z. Molecularly Imprinted Polymer-Based Plasmonic Immunosandwich Assay for Fast and Ultrasensitive Determination of Trace Glycoproteins in Complex Samples. *Anal.*

- Chem.* **2016**, *88* (24), 12363–12370.
- [50] Chantada-Vázquez, M. P.; Sánchez-González, J.; Peña-Vázquez, E.; Taberner, M. J.; Bermejo, A. M.; Bermejo-Barrera, P.; Moreda-Piñeiro, A. Simple and Sensitive Molecularly Imprinted Polymer – Mn-Doped ZnS Quantum Dots Based Fluorescence Probe for Cocaine and Metabolites Determination in Urine. *Anal. Chem.* **2016**, *88* (5), 2734–2741.
- [51] Longo, L.; Vasapollo, G. Phthalocyanine-Based Molecularly Imprinted Polymers as Nucleoside Receptors. *Met. Based. Drugs* **2008**, *2008*, 281843.
- [52] Öpik, A.; Menaker, A.; Reut, J.; Syritski, V. Molecularly Imprinted Polymers: A New Approach to the Preparation of Functional Materials. *Proc. Est. Acad. Sci.* **2009**, *58* (1), 3–11.
- [53] Wulff, G. Molecular Imprinting in Cross-Linked Materials with the Aid of Molecular Templates— A Way towards Artificial Antibodies. *Angewandte Chemie International Edition in English*. Hüthig & Wepf Verlag September 15, **1995**, pp 1812–1832.
- [54] Whitcombe, M. J.; Rodriguez, M. E.; Villar, P.; Vulfson, E. N. A New Method for the Introduction of Recognition Site Functionality into Polymers Prepared by Molecular Imprinting: Synthesis and Characterization of Polymeric Receptors for Cholesterol. *J. Am. Chem. Soc.* **1995**, *117* (27), 7105–7111.
- [55] Vasapollo, G.; Sole, R. Del; Mergola, L.; Lazzoi, M. R.; Scardino, A.; Scorrano, S.; Mele, G. Molecularly Imprinted Polymers: Present and Future Prospective. *Int. J. Mol. Sci.* **2011**, *12* (9), 5908–5945.
- [56] Spivak, D. A. Optimization, Evaluation, and Characterization of Molecularly

- Imprinted Polymers. *Adv. Drug Deliv. Rev.* **2005**, *57* (12), 1779–1794.
- [57] Pichon, V.; Chapuis-Hugon, F. Role of Molecularly Imprinted Polymers for Selective Determination of Environmental Pollutants-A Review. *Anal. Chim. Acta* **2008**, *622* (1–2), 48–61.
- [58] Zhang, L. T.; Ito, K.; Vasudevan, V. K.; Yamaguchi, M. Molecularly Imprinted Polymers: New Tailor-Made Materials for Selective Solid-Phase Extraction. *TrAC - Trends Anal. Chem.* **2001**, *20* (9), 477–486.
- [59] Morrison, R. T.; Boyd, R. N. *Organic Chemistry*; Prentice Hall, **1992**.
- [60] Shivashankar, M.; Mandal, B. K. A Review on Interpenetrating Polymer Network. *International Journal of Pharmacy and Pharmaceutical Sciences.* **2012**, pp 1–7.
- [61] Mohamed, M. H.; Wilson, L. D. Porous Copolymer Resins: Tuning Pore Structure and Surface Area with Non Reactive Porogens. *Nanomaterials* **2012**, *2* (4), 163–186.
- [62] Scorrano, S.; Longo, L.; Vasapollo, G. Molecularly Imprinted Polymers for Solid-Phase Extraction of 1-Methyladenosine from Human Urine. *Anal. Chim. Acta* **2010**, *659* (1–2), 167–171.
- [63] Mayes, A. G.; Whitcombe, M. J. Synthetic Strategies for the Generation of Molecularly Imprinted Organic Polymers. *Advanced Drug Delivery Reviews.* 2005, pp 1742–1778.
- [64] Yin, J.; Meng, Z.; Du, M.; Liu, C.; Song, M.; Wang, H. Pseudo-Template Molecularly Imprinted Polymer for Selective Screening of Trace Beta-Lactam Antibiotics in River and Tap Water. *J. Chromatogr. A* **2010**, *1217* (33), 5420–5426.
- [65] Wang, X.; Fang, Q.; Liu, S.; Chen, L. The Application of Pseudo Template Molecularly Imprinted Polymer to the Solid-Phase Extraction of Cyromazine and Its

- Metabolic Melamine from Egg and Milk. *J. Sep. Sci.* **2012**, *35* (12), 1432–1438.
- [66] Kubo, T.; Koterawasa, K.; Naito, T.; Otsuka, K. Molecularly Imprinted Polymer with a Pseudo-Template for Thermo-Responsive Adsorption/desorption Based on Hydrogen Bonding. *Microporous Mesoporous Mater.* **2015**, *218*, 112–117.
- [67] Mollnelli, A.; O'Mahony, J.; Nolan, K.; Smyth, M. R.; Jakusch, M.; Mizaikoff, B. Analyzing the Mechanisms of Selectivity in Biomimetic Self-Assemblies via IR and NMR Spectroscopy of Prepolymerization Solutions and Molecular Dynamics Simulations. *Anal. Chem.* **2005**, *77* (16), 5196–5204.
- [68] Navarro-Villoslada, F.; San Vicente, B.; Moreno-Bondi, M. C. Application of Multivariate Analysis to the Screening of Molecularly Imprinted Polymers for Bisphenol a. *Anal. Chim. Acta* **2004**, *504* (1), 149–162.
- [69] Hwang, C. C.; Lee, W. C. Chromatographic Characteristics of Cholesterol-Imprinted Polymers Prepared by Covalent and Non-Covalent Imprinting Methods. *J. Chromatogr. A* **2002**, *962* (1–2), 69–78.
- [70] Flores, A.; Cunliffe, D.; Whitcombe, M. J.; Vulfson, E. N. Imprinted Polymers Prepared by Aqueous Suspension. *J. Appl. Polym. Sci.* **2000**, *77* (July), 1841–1850.
- [71] Nicholls, I. A.; Rosengren, J. P. Molecular Imprinting of Surfaces. *Bioseparation* **2002**, *10*, 301–305.
- [72] Yin, J.; Yang, G.; Chen, Y. Rapid and Efficient Chiral Separation of Nateglinide and Its L-Enantiomer on Monolithic Molecularly Imprinted Polymers. *J. Chromatogr. A* **2005**, *1090* (1–2), 68–75.
- [73] Mohajeri, S. A.; Karimi, G.; Aghamohammadian, J.; Khansari, M. R. Clozapine Recognition via Molecularly Imprinted Polymers; Bulk Polymerization versus

- Precipitation Method. *J. Appl. Polym. Sci.* **2011**, *121* (6), 3590–3595.
- [74] Baggiani, C.; Anfossi, L.; Baravalle, P.; Giovannoli, C.; Tozzi, C. Selectivity Features of Molecularly Imprinted Polymers Recognising the Carbamate Group. *Anal. Chim. Acta* **2005**, *531* (2), 199–207.
- [75] Mayes, a G.; Mosbach, K. Molecularly Imprinted Polymer Beads: Suspension Polymerization Using a Liquid Perfluorocarbon as the Dispersing Phase. *Anal. Chem.* **1996**, *68* (21), 3769–3774.
- [76] Krotz, J. M.; Shea, K. J. Imprinted Polymer Membranes for the Selective Transport of Targeted Neutral Molecules. *J. Am. Chem. Soc.* **1996**, *118* (95), 8154–8155.
- [77] Egli, S. N.; Butler, E. D.; Bottaro, C. S. Selective Extraction of Light Polycyclic Aromatic Hydrocarbons in Environmental Water Samples with Pseudo-Template Thin-Film Molecularly Imprinted Polymers. *Anal. Methods* **2015**, *7*, 2028–2035.
- [78] Chen, P.-Y.; Vittal, R.; Nien, P.-C.; Liou, G.-S.; Ho, K.-C. A Novel Molecularly Imprinted Polymer Thin Film as Biosensor for Uric Acid. *Talanta* **2010**, *80* (3), 1145–1151.
- [79] Kröger, S.; Turner, A. P. F.; Mosbach, K.; Haupt, K. Imprinted Polymer-Based Sensor System for Herbicides Using Differential- Pulse Voltammetry on Screen-Printed Electrodes. *Anal. Chem.* **1999**, *71* (17), 3698–3702.
- [80] Liang, C.; Peng, H.; Bao, X.; Nie, L.; Yao, S. Study of a Molecular Imprinting Polymer Coated BAW Bio-Mimic Sensor and Its Application to the Determination of Caffeine in Human Serum and Urine. *Analyst* **1999**, *124* (12), 1781–1785.
- [81] Hall, D. B.; Underhill, P.; Torkelson, J. M. Spin Coating of Thin and Ultrathin Polymer Films. *Polym. Eng. Sci.* **1998**, *38* (12), 2039–2045.

- [82] Van Biesen, G.; Wiseman, J. M.; Li, J.; Bottaro, C. S. Desorption Electrospray Ionization-Mass Spectrometry for the Detection of Analytes Extracted by Thin-Film Molecularly Imprinted Polymers. *Analyst* **2010**, *135* (9), 2237–2240.
- [83] Malitesta, C.; Losito, I.; Zambonin, P. G. Molecularly Imprinted Electrosynthesized Polymers: New Materials for Biomimetic Sensors. *Anal. Chem.* **1999**, *71* (7), 1366–1370.
- [84] Panasyuk, T. L.; Mirsky, V. M.; Piletsky, S. A.; Wolfbeis, O. S. Electropolymerized Molecularly Imprinted Polymers as Receptor Layers in Capacitive Chemical Sensors. *Anal. Chem.* **1999**, *71* (20), 4609–4613.
- [85] Schmidt, R. H.; Mosbach, K.; Haupt, K. A Simple Method for Spin-Coating Molecularly Imprinted Polymer Films of Controlled Thickness and Porosity. *Adv. Mater.* **2004**, *16* (8), 719–722.
- [86] Haupt, K.; Noworyta, K.; Kutner, W. Imprinted Polymer-Based Enantioselective Acoustic Sensor Using a Quartz Crystal Microbalance. *Anal. Commun.* **1999**, *36* (11–12), 391.
- [87] Jakusch, M.; Janotta, M.; Mizaikoff, B.; Mosbach, K.; Haupt, K. Molecularly Imprinted Polymers and Infrared Evanescent Wave Spectroscopy . A Chemical Sensors Approach. *Anal. Chem.* **1999**, *71* (1), 4786–4791.
- [88] Annamma, K. M.; Beena, M. Design of 2,4-Dichlorophenoxyacetic Acid Imprinted Polymer with High Specificity and Selectivity. *Mater. Sci. Appl.* **2011**, *2* (3), 131–140.
- [89] Sikiti, P.; Msagati, T. A.; Mamba, B. B.; Mishra, A. K. Synthesis and Characterization of Molecularly Imprinted Polymers for the Remediation of PCBs

- and Dioxins in Aqueous Environments. *J. Environ. Heal. Sci. Eng.* **2014**, *12* (1), 82.
- [90] Yusof, N. A.; Zakaria, N. D.; Maamor, N. A. M.; Abdullah, A. H.; Haron, M. J. Synthesis and Characterization of Molecularly Imprinted Polymer Membrane for the Removal of 2,4-Dinitrophenol. *Int. J. Mol. Sci.* **2013**, *14* (2), 3993–4004.
- [91] Li, X.; Li, M.; Li, J.; Lei, F.; Su, X.; Liu, M.; Li, P.; Tan, X. Synthesis and Characterization of Molecularly Imprinted Polymers with Modified Rosin as a Cross-Linker and Selective SPE-HPLC Detection of Basic Orange II in Foods. *Anal. Methods* **2014**, *6* (16), 6397.
- [92] Gryshchenko, A. O.; Bottaro, C. S. Development of Molecularly Imprinted Polymer in Porous Film Format for Binding of Phenol and Alkylphenols from Water. *Int. J. Mol. Sci.* **2014**, *15* (1), 1338–1357.
- [93] McMullan, D. Scanning Electron Microscopy 1928–1965. *Scanning* **1995**, *17* (3), 175–185.
- [94] Xia, Q.; Yun, Y.; Li, Q.; Huang, Z.; Liang, Z. Preparation and Characterization of Monodisperse Molecularly Imprinted Polymer Microspheres by Precipitation Polymerization for Kaempferol. *Des. Monomers Polym.* **2017**, *20* (1), 201–209.
- [95] Dai, C.; Zhang, J.; Zhang, Y.; Zhou, X.; Liu, S. Application of Molecularly Imprinted Polymers to Selective Removal of Clofibric Acid from Water. *PLoS One* **2013**, *8* (10), e78167.
- [96] Longo, L.; Scorrano, S.; Vasapollo, G. RNA Nucleoside Recognition by Phthalocyanine-Based Molecularly Imprinted Polymers. *J. Polym. Res.* **2010**, *17* (5), 683–687.
- [97] García-Calzón, J. A.; Díaz-García, M. E. Characterization of Binding Sites in

- Molecularly Imprinted Polymers. *Sensors Actuators B Chem.* **2007**, *123* (2), 1180–1194.
- [98] Umpleby, R. J.; Baxter, S. C.; Bode, M.; Berch, J. K.; Shah, R. N.; Shimizu, K. D. Application of the Freundlich Adsorption Isotherm in the Characterization of Molecularly Imprinted Polymers. *Anal. Chim. Acta* **2001**, *435* (1), 35–42.
- [99] Yang, G.; Wang, D.; Li, Z.; Zhou, S.; Chen, Y. Adsorption Isotherms on Aminoantipyrine Imprinted Polymer Stationary Phase. *Chromatographia* **2003**, *58* (1–2), 53–58.
- [100] Umpleby, R. J.; Baxter, S. C.; Chen, Y.; Shah, R. N.; Shimizu, K. D. Characterization of Molecularly Imprinted Polymers with the Langmuir - Freundlich Isotherm. *Anal. Chem.* **2001**, *73* (19), 4584–4591.
- [101] Turiel, E.; Perez-Conde, C.; Martin-Esteban, A. Assessment of the Cross-Reactivity and Binding Sites Characterisation of a Propazine-Imprinted Polymer Using the Langmuir-Freundlich Isotherm. *Analyst* **2003**, *128* (2), 137–141.
- [102] Rampey, A. M.; Umpleby, R. J.; Rushton, G. T.; Iseman, J. C.; Shah, R. N.; Shimizu, K. D. Characterization of the Imprint Effect and the Influence of Imprinting Conditions on Affinity, Capacity, and Heterogeneity in Molecularly Imprinted Polymers Using the Freundlich Isotherm-Affinity Distribution Analysis. *Anal. Chem.* **2004**, *76* (4), 1123–1133.
- [103] Umpleby, R. J.; Baxter, S. C.; Rampey, A. M.; Rushton, G. T.; Chen, Y.; Shimizu, K. D. Characterization of the Heterogeneous Binding Site Affinity Distributions in Molecularly Imprinted Polymers. *J. Chromatogr. B Anal. Technol. Biomed. Life Sci.* **2004**, *804* (1), 141–149.

- [104] Sips, R. On the Structure of a Catalyst Surface. *J. Chem. Phys.* **1948**, *16* (5), 490–495.
- [105] Sips, R. On the Structure of a Catalyst Surface. II. *J. Chem. Phys.* **1950**, *18* (8), 1024–1026.
- [106] Tom, L. A.; Gerard, C. L.; Hutchison, C. M.; Brooker, A. S. Development of a Novel Molecularly Imprinted Polymer for the Retention of 4,6-Dimethyldibenzothiophene. *Microchim. Acta* **2012**, *176* (3–4), 375–380.
- [107] Xu, W.-Z.; Zhou, W.; Bian, L.-H.; Huang, W.-H.; Wu, X.-Y. Preparation of Molecularly Imprinted Polymer by Surface Imprinting Technique and Its Performance for Adsorption of Dibenzothiophene. *J. Sep. Sci.* **2011**, *34* (14), 1746–1753.
- [108] Xu, P.; Xu, W.; Zhang, X.; Pan, J.; Yan, Y. Molecularly-Imprinted Material for Dibenzothiophene Recognition Prepared by Surface Imprinting Methods. *Adsorpt. Sci. Technol.* **2009**, *27* (10), 975–987.
- [109] US EPA 8275. Method 8275: Semivolatiles Organic Compounds (PAHs and PCBs) in Soils/sludges and Solid Wastes Using Thermal Extraction/gas Chromatography/mass Spectrometry (TE/GC/MS). *Method 8275A*. 1996, pp 1–23.
- [110] *Method 1625 , Revision B : Semivolatile Organic Compounds by Isotope Dilution GC / MS*; 1984.
- [111] Brenner, N. Gas Chromatography. Principles, Techniques and Applications. *J. Am. Chem. Soc.* **1963**, *85* (12), 1897–1898.
- [112] Hübschmann, H.-J. *Handbook of GC/MS : Fundamentals and Applications*, Third ed.; Weinheim, Germany : Wiley-VCH, **2015**.

- [113] McWilliam, I. G.; Dewar, R. A. Flame Ionization Detector for Gas Chromatography. *Nature*. 1958, pp 760–760.
- [114] Kim, I.; Suh, S.; Lee, I.; Wolfe, R. R. Applications of Stable, Nonradioactive Isotope Tracers in in Vivo Human Metabolic Research. *Exp. Mol. Med.* **2016**, *48* (12), e203.
- [115] Popp, P.; Möder, M.; McCann, I. Determination of Sulfur-Containing Compounds in Wastewater. **1999**, 227–237.
- [116] Chai, X. S.; Hou, Q. X.; Schork, F. J. Determination of Residual Monomer in Polymer Latex by Full Evaporation Headspace Gas Chromatography. *J. Chromatogr. A* **2004**, *1040* (2), 163–167.
- [117] Røen, B. T.; Unneberg, E.; Tørnes, J. A.; Lundanes, E. Headspace-Trap Gas Chromatography-Mass Spectrometry for Determination of Sulphur Mustard and Related Compounds in Soil. *J. Chromatogr. A* **2010**, *1217* (14), 2171–2178.
- [118] American Society for Testing and Materials Standard Method: ASTM D 5504-12, Determination of Sulfur Compounds in Natural Gas and Gaseous Fuels by Gas Chromatography and Chemiluminescence. **2013**, *5* (April), 1–12.
- [119] Takáts, Z.; Wiseman, J. M.; Gologan, B.; Cooks, R. G. Mass Spectrometry Sampling under Ambient Conditions with Desorption Electrospray Ionization. *Science* (80-.). **2004**, *306* (5695), 471–473.
- [120] Takáts, Z.; Wiseman, J. M.; Cooks, R. G. Ambient Mass Spectrometry Using Desorption Electrospray Ionization (DESI): Instrumentation, Mechanisms and Applications in Forensics, Chemistry, and Biology. *J. Mass Spectrom.* **2005**, *40* (10), 1261–1275.

- [121] Karas, M.; Krüger, R. Ion Formation in MALDI: The Cluster Ionization Mechanism. *Chemical Reviews*. American Chemical Society 2003, pp 427–439.
- [122] Shin, Y.; Drolet, B.; Mayer, R.; Dolence, K.; Basile, F. Desorption Electrospray Ionization Mass Spectrometry of Proteins. *Anal. Chem.* **2007**, *79* (9), 3514–3518.
- [123] Weston, D. J.; Bateman, R.; Wilson, I. D.; Wood, T. R.; Creaser, C. Direct Analysis of Pharmaceutical Drug Formulations Using Ion Mobility Spectrometry/quadrupole-Time-of-Flight Mass Spectrometry Combined with Desorption Electrospray Ionization. *Anal. Chem.* **2005**, *77* (23), 7572–7580.
- [124] Nyadong, L.; Green, M. D.; De Jesus, V. R.; Newton, P. N.; Fernández, F. M. Reactive Desorption Electrospray Ionization Linear Ion Trap Mass Spectrometry of Latest-Generation Counterfeit Antimalarials via Noncovalent Complex Formation. *Anal. Chem.* **2007**, *79* (5), 2150–2157.
- [125] Hu, Q.; Talaty, N.; Noll, R. J.; Cooks, R. G. Desorption Electrospray Ionization Using an Orbitrap Mass Spectrometer: Exact Mass Measurements on Drugs and Peptides. *Rapid Commun. Mass Spectrom.* **2006**, *20* (22), 3403–3408.
- [126] Bereman, M. S.; Nyadong, L.; Fernandez, F. M.; Muddiman, D. C. Direct High-Resolution Peptide and Protein Analysis by Desorption Electrospray Ionization Fourier Transform Ion Cyclotron Resonance Mass Spectrometry. *Rapid Commun. Mass Spectrom.* **2006**, *20* (22), 3409–3411.
- [127] Ifa, D. R.; Manicke, N. E.; Rusine, A. L.; Cooks, R. G. Quantitative Analysis of Small Molecules by Desorption Electrospray Ionization Mass Spectrometry from Polytetrafluoroethylene Surfaces. *Rapid Commun. Mass Spectrom.* **2008**, *22* (4), 503–510.

- [128] Cooks, R. G. Ambient Mass Spectrometry. *Science* (80-.). **2006**, *311* (5767), 1566–1570.
- [129] Chen, H.; Li, M.; Zhang, Y.-P.; Yang, X.; Lian, J.-J.; Chen, J.-M. Rapid Analysis of SVOC in Aerosols by Desorption Electrospray Ionization Mass Spectrometry. *J Am Soc Mass Spectrom* **2008**, *19* (3), 450–454.
- [130] Eftekhari, M.; Ismail, A. I.; Zare, R. N. Isomeric Differentiation of Polycyclic Aromatic Hydrocarbons Using Silver Nitrate Reactive Desorption Electrospray Ionization Mass Spectrometry. *Rapid Commun. Mass Spectrom.* **2012**, *26* (17), 2085–2092.

Chapter 2: Novel molecularly imprinted polymer thin-film as micro-extraction adsorbent for selective determination of trace concentrations of thiophene compounds in water

2.1. Abstract

A novel porous molecularly imprinted polymer thin-film (MIP thin-film) was prepared by in situ photo-radical polymerization on a glass slide and used as a micro-extraction adsorbent. Detection was carried out using gas chromatography-mass spectrometry (GC-MS) to afford a method suitable for the selective determination of trace concentrations of thiophene compounds in water. Thiophene compounds such as dibenzothiophene (DBT) are considered the most problematic aromatic organic pollutants, as they are more persistent and toxic compared to other analogous aromatic compounds in the environment. Various MIPs compositions were prepared and tested to obtain the best MIP thin-film for thiophene compounds analysis. The optimized thin-film consisted of 2-thiophenecarboxaldehyde as the template, 1-vinylimidazole (1-Vim) as the monomer, bisphenol A dimethacrylate (BPADMA) as the cross-linker, acetonitrile as the porogen, and PEG as additive. 2-Thiophenecarboxaldehyde was used as a pseudo-template to avoid the positive bias associated with template bleeding, which can be problematic in trace analysis. To improve the film porosity and wettability, the principle of interpenetrating polymer networks (IPN) was implemented by adding a linear polymer (polyethylene glycol, PEG, MW 20,000) to the pre-polymerization mixture. The adsorption behaviours of the thin-film, including stirring speed of analysis, adsorption kinetics, effect of sample volume, binding isotherms, and selectivity of MIP thin-film were investigated in detail. The highest adsorption capacity and imprinting factors (IF_s , 2.21-2.93) for all thiophene compounds were achieved at the template:monomer:cross-linker ratio of 1:4:8. The SEM images revealed that the optimized MIP thin-film exhibited a more porous structure compared to the non-imprinted one.

Excellent reproducibility was achieved for the extraction of thiophene compounds from spiked seawater samples ($RSD_s \leq 6.0\%$, $n = 3$). Calibration curves of spiked seawater were linear over a range of $0.5\text{-}100 \mu\text{g L}^{-1}$ and limit of detection values were in the range of $0.029\text{-}0.166 \mu\text{g L}^{-1}$. These results showed the suitability of MIP thin-film as a selective adsorbent for the selective extraction of thiophene compounds from water samples.

2.2. Introduction

Our environment is continuously impacted by oil through regulated discharges, accidental oil spills, shipping related inputs, run-off and intentional dumping. Every year, 380 million gallons of oil enter the world's oceans and coastal waterways from natural and human sources [1]. Thiophene compounds together with other sulfur containing compounds are present in petroleum in concentrations up to 10%, depending on the source [2]. They are usually removed by hydrodesulfurization process, in which hydrocarbons and hydrogen sulfide form [3]. Thiophene compounds such as DBT are considered the most problematic components in petroleum products due to their possible mutagenicity, carcinogenicity, and acute toxicity, particularly when compared to other analogous compounds in the environment [4–7].

There are few methods of analysis in the literature that selectively target thiophene compounds; most of these methods were developed for PASHs analysis with PAHs. The methods for PASHs usually involve the use of non-selective solid-phase extraction (SPE), which uses significant volumes of organic solvents for pre-conditioning and elution, and pre-concentration is achieved simultaneously with many other species [8–10]. Consequently, chromatograms often include undefined and unresolved peaks making identification and detection more complicated and difficult. The limitations of SPE can be overcome by using selective material such as MIPs.

MIPs are synthetic polymers with artificial molecular recognition sites formed by a polymerization process in the presence of a template molecule. Molecular imprinting can be achieved via covalent or non-covalent interactions between the template and functional

monomers during the polymerization process. The template removal after the polymerization process creates selective binding sites compatible with the size and shape of the analyte. Therefore, analytes with correct geometry and functionality will rebind selectively to these sites [11–13]. MIPs should be rigid enough to maintain the structure of the cavities after removing the template, while keeping some flexibility for the releasing and uptaking of the template [13].

The main advantage of using MIPs is the low cost of preparation compared with other materials that show high selectivity [12]. MIPs are also stable over a range of temperatures and pressures, and in acids, bases, and organic solvents [14].

Optimization of the MIP composition is very important when non-covalent imprinting is used. The key to success in this process is the initial selection of a suitable monomer that offers the best possible interaction with the template, followed by the optimization of the template to monomer and monomer to cross-linker ratios. Theoretically, any template can be used for imprinting but the template bleeding during analysis can artificially elevate the sample background and thus limits the application of MIP for trace analysis [15–17]. To overcome this problem, a pseudo-template which has an analogous structure with the original template, can be used. Traditional MIP preparation methods, such as bulk polymerization, usually produce selective polymers with high affinity, but sometimes features low capacity and poor ability for mass transfer of analytes to the selective sites. Moreover, the process of sieving can produce particles that have irregular shapes and sizes, while the grinding process can destroy some selective sites in the polymer. All these limitations could lead to an MIP with very poor analytical performance [18]. In

order to avoid these problems, MIPs can be prepared as thin-films; spin coating and “sandwiching” techniques are common methods of doing so [19–21]. Spin coating methods produce films with a controlled and uniform thicknesses, but problems such as low viscosity and high volatility of the pre-polymerization mixture frequently make this method unsuitable for MIP preparation [19,22]. “Sandwiching” and drop casting techniques are simple and effective alternative methods for thin-film preparation.

The role of the porogen (solvent) is significant and careful selection of a proper porogen is necessary to produce a porous polymer. Some experimental studies found that, the highest analyte rebinding to the polymer in the analysis can be obtained when carried in the same solvent used in the imprinting process [23,24]. Water has been used as a porogen; for example, a water-compatible polymer has been used for the detection of 1-methyladenosine in human urine samples [25], but unfortunately, imprinting in water can be difficult due to the limited range of water-soluble monomers and cross-linkers [26].

To our knowledge, there is no published work in the literature on the preparation or use of MIPs films for the analysis and detection of thiophene compounds in aqueous medium. Most MIPs prepared for these compounds are used to extract or remove these compounds from fuel or petroleum products [27–29]. In this research, a novel porous MIP thin-film was prepared on a glass substrate, and used for the selective extraction of thiophene compounds in water followed with detection by GC-MS in full scan and SIM mode. The morphology of thiophenes-MIP was assessed qualitatively using scanning electron microscopy (SEM). An improved porosity for the thin-film was achieved by adding the linear polymer polyethylene glycol (PEG) to the pre-polymerization solution to

exploit the advantages of polymers created with an interpenetrating polymer networks (IPN) principle [30]. The binding behaviour of MIP thin-films was assessed using the Freundlich isotherm model. This model was chosen due to its capability of evaluating the heterogeneity of MIPs. Adsorption behaviours and selectivity were investigated in detail. The prepared MIP thin-films were used successfully to extract thiophene compounds from water samples with no pre-treatment. Although there is a review in the literature which claims that, the films prepared by “sandwiching” technique cannot give reproducible results [31]. Our work revealed that it is possible to obtain a reproducible MIP films with satisfactory imprinting properties using this technique.

2.3. Materials and methods

2.3.1. Materials

Benzothiophene ($\geq 95\%$), 3-methylbenzothiophene (96%), dibenzothiophene ($\geq 99\%$), 4,6-dimethyldibenzothiophene (97%), 2-thiophenecarboxaldehyde (98%), p-cresol (99%) and indole (98%), fluorene-d10 (99%), methacrylic acid (99%), 4-vinylpyridine (95%), acrylamide ($\geq 99\%$), 1-vinylimidazol ($\geq 99\%$), acrylonitrile ($\geq 99\%$), allylamine ($\geq 99\%$), ethylene glycol dimethacrylate (98%), bisphenol A dimethacrylate ($> 98\%$), 2,2-dimethoxy-2-phenylacetophenone (99%), polyethylene glycol (average MW 20,000), 3-(trimethoxysilyl)propyl methacrylate (98%) were all purchased from Sigma Aldrich, Canada. Methanol, acetonitrile, chloroform, hexane, toluene, 1-octanol and hydrochloric acid (37% w/w) were ACS reagent grades and purchased from ACP chemicals. Glass slides ($25 \times 75 \text{ mm}^2$) and micro cover glasses ($18 \times 18 \text{ mm}^2$) were purchased from Fisher

Scientific, Canada. Deionized water (18 M Ω .cm) was produced by Barnstead Nanopure Diamond (18 M Ω) water purification system (Barnstead Nanopure Water Systems, Lake Balboa, CA, USA).

2.3.2. Pre-treatment and derivatization of glass slides

As stated previously, the MIPs were prepared on glass slides. To ensure a permanent adhesion, the slides were functionalized to allow the MIPs to be covalently grafted to the surface. In this process, the cut pieces of glass slides (25 x 25 mm²) were first soaked in a solution of methanol/hydrochloric acid (1:1) for 30 min, and then the slides were rinsed with tap water and deionized (DI) water and then dried at room temperature. The cleaned slides were placed in a silanization solution of 2% (v/v) of 3-(trimethoxysilyl) propyl methacrylate in toluene overnight (~12 h). The glass slides were finally washed with methanol and dried under nitrogen. The prepared glass slides were stored in a dark place until their use. The functionalized slides can be stored for several weeks without any noticeable loss in performance.

2.3.3. Preparation of MIP thin-films

Preparation of MIP thin-film was carried out via photoinitiated radical polymerization between a derivatized glass slide (25 x 25 mm²) and a quartz cover glass slide (18 x 18 mm²) (“sandwiching” technique) in four steps (Figure 2.1). In the first step, all ingredients (Table 2.1), including the template, monomer, cross-linker, porogen and additives (if applicable), were pipetted or weighed, and then vortexed until dissolution. The

mixture was degassed in a sonicator for 5 min to remove dissolved air. In the second step, 8 μL of the pre-polymerization complex was pipetted onto the center of a derivatized glass slide, and then covered immediately by a quartz cover slide. After the pipetted amount was left to spread evenly between the surface of the slide and the cover, the slide is exposed for 45 min to UV-light ($\lambda=254$ nm, 6W) produced from a hand-held UV lamp. In the third step, the cover slide was immediately removed using a sharp blade leaving the glass slide with the MIP film attached. To extract the template, the MIP coated slide was placed in methanol and was stirred for 3 h; this was then repeated for another 1 h with fresh methanol.

In the last step, the MIP slide was removed and rinsed with methanol and DI water and then dried at room temperature. The prepared slide can be stored and used after several weeks without any changes in analytical performance. The mass of the film (m_{film} , ~ 0.004 g) was obtained by subtracting the mass of the glass slide before polymerization from the mass of the slide with the attached film. An analytical balance (Mettler Toledo XS 105) with an accuracy of 0.01 mg was used for these measurements. The non-imprinted polymer was prepared in the same way, but in the absence of the template.

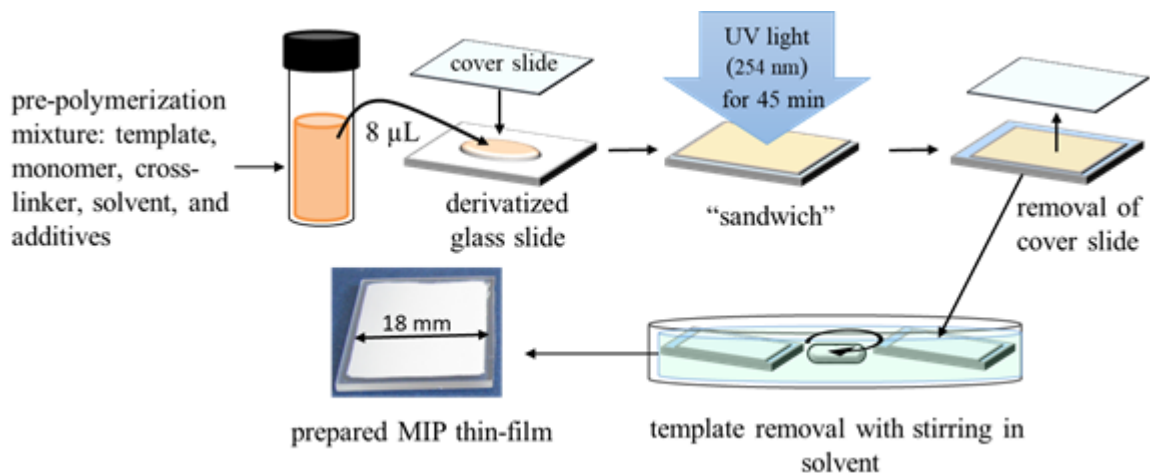


Figure 2.1. Preparation process of MIP thin-film on a glass slide.

2.3.4. Characterization of the thin-films

Scanning electron microscopy (SEM) images were taken using FEI Quanta MLA 650F SEM, acceleration voltage of 15 kV, and at a magnification of 50,000 times. The film thickness was determined using the instrument software from the cross-section images for the edges of MIP thin-film which taken with a 36° tilt angle at 10 kV accelerating voltage. All samples were sputtered with gold prior to analysis.

Analytical performance and optimization of the MIP thin-films were characterized by quantifying the bound analytes using an Agilent 6890 gas chromatograph (Mississauga, ON, Canada) equipped with an Agilent 7683 auto-sampler and coupled to an Agilent 5973 mass selective detector (MSD). Instrument control and data analysis were performed using Agilent ChemStation software version D.01.00 Build 75. A fused-silica capillary column (DB-5MS, 30 x 0.25 i.d.) with 0.25 μm stationary film thickness was used with helium (purity 99.999%) as the carrier gas with a flow rate of 1.2 mL min⁻¹. The initial oven

temperature was held at 50 °C for 1 min, and then increased to 280 °C at 20 °C min⁻¹, and was held at this temperature for 1 min. The total analysis run time was 13.5 min. The injector temperature was set at 280 °C and the injection was performed in the splitless mode.

2.3.5. Optimization and rebinding experiments

Various compositions of MIP films (Table 2.1) were prepared using 2-thiophene carboxaldehyde as a pseudo-template with different monomers, cross-linkers, and porogens, and then tested using binding experiment. The optimization experiments were performed first to select the best monomer. In the optimization experiment, the template:monomer:cross-linker (T:M:C) in a typical mole ratio of 1:4:20 was used to prepare MIP1-6. Several porogens including chloroform, methanol, acetonitrile, 1-octanol, and 1-octanol: methanol (1:1) were tested in the preparation of these polymers to determine the best porogen for the preparation. To improve the porosity of the thin-film, a PEG (MW 20,000) polymer was added to the pre-polymerization mixture in a concentration of 25% (w/w). This mixture was used to prepare MIP7-11 (Table 2.1 and 2.3). The adsorption capacity of the polymer was improved by using BPADMA as a cross-linker, instead of EDGMA, to prepare MIP8-11. The best T:M:C ratio was obtained by testing different ratios for the 1-Vim-BPADMA polymer (MIP9-11, Table 2.3). DMPA was used as photoinitiator in all MIP preparations. Acetonitrile was selected as the best porogen in the preparation of the final composition of MIP films.

In the rebinding experiments, each MIP slide was placed in a 100-mL beaker containing 40 mL of water spiked with a mixture of thiophene compounds at a

concentration of $100 \mu\text{g L}^{-1}$ each for uploading and was stirred for 2 h at room temperature. Stock spiking solutions of thiophene compounds were prepared in acetonitrile and stored in the refrigerator at $4 \text{ }^\circ\text{C}$ when not in use. Working solutions were prepared daily by appropriate dilution of the spiking solutions with distilled water. The amount of analyte adsorbed in the MIP on each slide Q_t ($\mu\text{g g}^{-1}$) at time t was calculated using the following equation:

$$Q_t = \frac{(C_0 - C_t) V}{m_{film}} \quad (2.1)$$

where C_0 ($\mu\text{g L}^{-1}$) is the initial concentration of thiophene compound in the water sample, C_t ($\mu\text{g L}^{-1}$) is the concentration of thiophene compound in the water sample at time t , V (L) is the volume of the sample and m_{film} (g) is the mass of the polymer film.

2.3.6. Adsorption kinetics and binding isotherm experiments

Binding experiments were performed to examine the adsorption kinetics and binding isotherms for the optimum composition of MIP thin-film in this work (MIP9, Table 2.4). In the adsorption kinetics experiments, each MIP slide was placed in a 250-mL beaker containing 200 mL of seawater spiked with thiophene compounds at a concentration of $50 \mu\text{g L}^{-1}$ with stirring. Uploading was studied for specific periods of time (1-24 h) at room temperature. The amount of adsorbed analyte in each slide Q_t ($\mu\text{g g}^{-1}$) at time t was calculated using the Equation (2.1) in Section 2.3.5 for each time.

The adsorption binding isotherm experiments were carried out by placing several MIP (or NIP) films in 100-mL beakers, each containing 40 mL of seawater sample spiked with thiophene compounds at initial concentrations of thiophene compounds ranging from 5 to 80 $\mu\text{g L}^{-1}$. The samples were left to upload for 15 h (equilibration time) at a stirring speed of 500 rpm. The binding capacity of analyte in each slide at equilibrium (Q , $\mu\text{g g}^{-1}$) was calculated using the following equation:

$$Q = \frac{(C_0 - C) V}{m_{film}} \quad (2.2)$$

The heterogeneity index (m) and fitting parameter constant (a , $\mu\text{g g}^{-1}$) were determined from the Freundlich isotherm curve, which was obtained from plotting of the following equation:

$$\log Q = m \log C + \log a \quad (2.3)$$

where C is the free concentration of the analyte in the sample ($\mu\text{g L}^{-1}$).

The imprinting factor (IF) values for all thiophene compounds were calculated using the Equation (1.6) and (1.7). Higher IF values indicate that the imprinting is successful and selective interactions exceed the non-selective sorption capacities intrinsic to the polymer components.

2.3.7. Analysis of real samples

Seawater samples were collected from St. John's harbour, (NL) in 4-L pre-cleaned amber glass bottles. No preservation method was used in the sampling process. The bottles were filled to the top to eliminate headspace, stoppered with screw caps, and sealed with Parafilm, and then labeled and stored in a cold place (~ 4 °C) until use.

For each sample, a single MIP slide was placed in a 100-mL beaker containing 40 mL of seawater spiked with known concentrations of thiophene compounds. The slide was left to upload with stirring for a specific period (usually 2 h). After uploading, the slide was removed from the solution and rinsed with a small amount of DI water, and then dried at room temperature for 5 min. The slide was then placed in a beaker containing 10 mL of hexane for extraction with stirring for 2 h. After the extraction finished, the slide was removed and the extract spiked with the internal standard (fluorene d-10), and then reduced to 1 mL under nitrogen. A 1- μ L portion of this solution was injected directly into the GC-MS for analysis. The mass spectra were recorded in a selected ion monitoring (SIM) mode, using 70 eV in the electron impact ionization source. The quantifier ions for the SIM were: $m/z = 134$ for BT; $m/z = 148$ for 3-MBT; $m/z = 184$ for DBT; $m/z = 212$ for 4,6-DMDBT; $m/z = 107$ for p-cresol and $m/z = 117$ for indole. The limit of detection (LOD) for each analyte was calculated as the concentration which is equal to 3 standard deviation of the lowest detectable concentration over the slope of the calibration curve. All MIP films analyses were conducted in triplicate. The binding capacity of each analyte adsorbed by MIP (Q_t) at a time t was calculated as previously indicated.

2.4. Results and discussion

2.4.1. Optimization of MIP thin-film composition

The noncovalent imprinting approach was adapted in this work to develop the thiophenes-MIP. Thiophene compounds such as DBT have a low number of functional groups (Figure 2.2), which makes their interactions with the selected monomer weak. Additionally, the use of the target analyte as the template in the imprinting of MIPs could lead to template bleeding during the analysis, which significantly elevates the sample background and restricts the application of the MIP. To overcome these problems, a pseudo-template with an analogous structure to the targeted analytes can be used in the imprinting process. In this work, 2-thiophenecarboxaldehyde was selected and used as pseudo-template in the preparation of MIP films (Figure 2.2). In addition to the possible π - π interaction between thiophenic ring of the template and the imidazole ring of 1-vinylimidazole monomer, this template also has an aldehyde group in its structure which could enhance the interaction with the selected monomer in the formation of the selective cavities. This has the potential to form a stronger template-monomer complex that is more likely to be conserved through the polymerization process. Consequently, more cavities with appropriate geometry would be formed. It is expected that the necessary interactions such as π - π interactions, hydrogen bonding, sulfur-nitrogen or sulfur-oxygen interactions between the target analyte and those monomers would be conserved with this template.

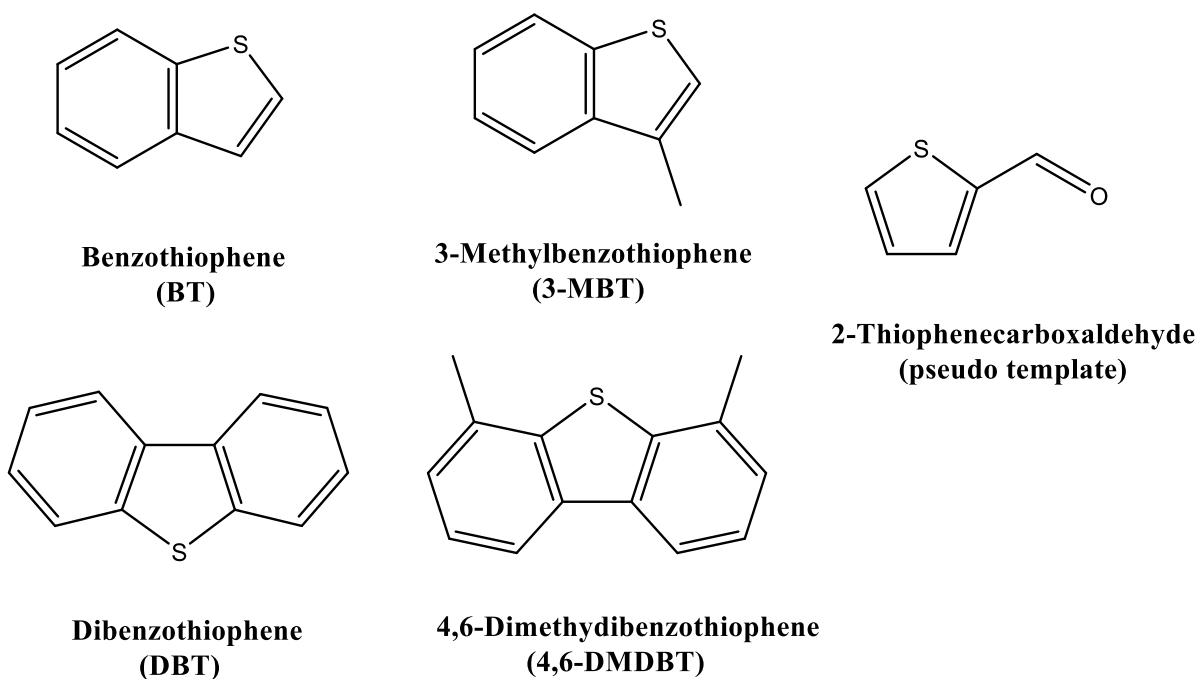
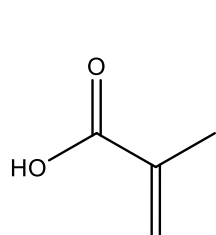
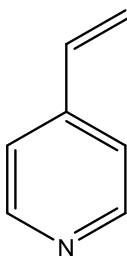


Figure 2.2. Chemical structure of targeted thiophene compounds and pseudo-template.

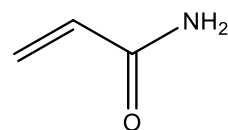
Six MIP film compositions (Table 2.1) were prepared using different monomers (Figure 2.3). The initial selection of these monomers was made based on the possibility of having strong interactions with the selected template. They were used in excess compared to the selected template to shift the equilibrium towards the formation of the template-monomer complex, which leads to the formation of more selective recognition cavities inside the MIPs.



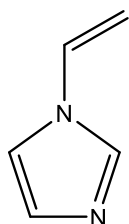
**Methacrylic acid
(MAA)**



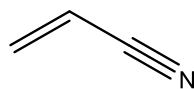
**4-Vinylpyridine
(4-VP)**



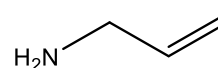
**Acrylamide
(AM)**



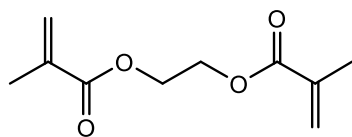
**1-Vinylimidazole
(1-Vim)**



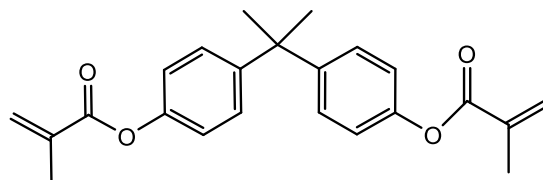
**Acrylonitrile
(Ac)**



**Allylamine
(AAM)**



**Ethylene glycol dimethacrylate
(EGDMA)**



**Bisphenol A dimethacrylate
(BPADMA)**

Figure 2.3. Selected monomers and cross-linkers.

Table 2.1. Composition of MIP pre-polymerization mixtures.

Polymer	Template	Monomer	Cross-linker	Photo-initiator	Solvent		PEG (25% w/w)
					1-octanol/MeOH 1:1	ACN	
MIP1	2-thiophene carboxaldehyde 0.18 mmol (20.0 μ L)	MAA 0.71 mmol (60.5 μ L)	EDGMA 3.57 mmol (673 μ L)	2,2-dimethoxy-2- phenylacetophenone (DMPA) 0.06 mmol (15.7 mg)	1000 μ L	-	-
MIP2		4-VP 0.71 mmol (77.1 μ L)			1020 μ L		
MIP3		AM 0.71 mmol (50.7 μ L)			984 μ L		
MIP4		1-Vim 0.71 mmol (64.6 μ L)			1006 μ L		
MIP5		Ac 0.71 mmol (46.7 μ L)			982 μ L		
MIP6		AAM 0.71 mmol (53.4 mg)			990 μ L		
MIP7		1-Vim 0.71 mmol (64.6 μ L)			-		
MIP8	2-thiophene- carboxaldehyde 0.11 mmol (10.3 μ L)	1-Vim 0.44 mmol (39.8 μ L)	BPADMA 2.20 mmol (800 mg)	0.04 mmol (9.6 mg)	-	675 μ L	210 mg

Several porogens were tested at the beginning of the work to find an appropriate porogen for the preparation of MIP films. Examples are chloroform, methanol, acetonitrile, and 1-octanol. Among all these porogens, only 1-octanol gave a stable and opaque film with a uniformly shaped surface. The films prepared with chloroform, methanol, and acetonitrile were brittle, flaky and weak with a glassy appearance (Figure 2.4 a), b) and c).

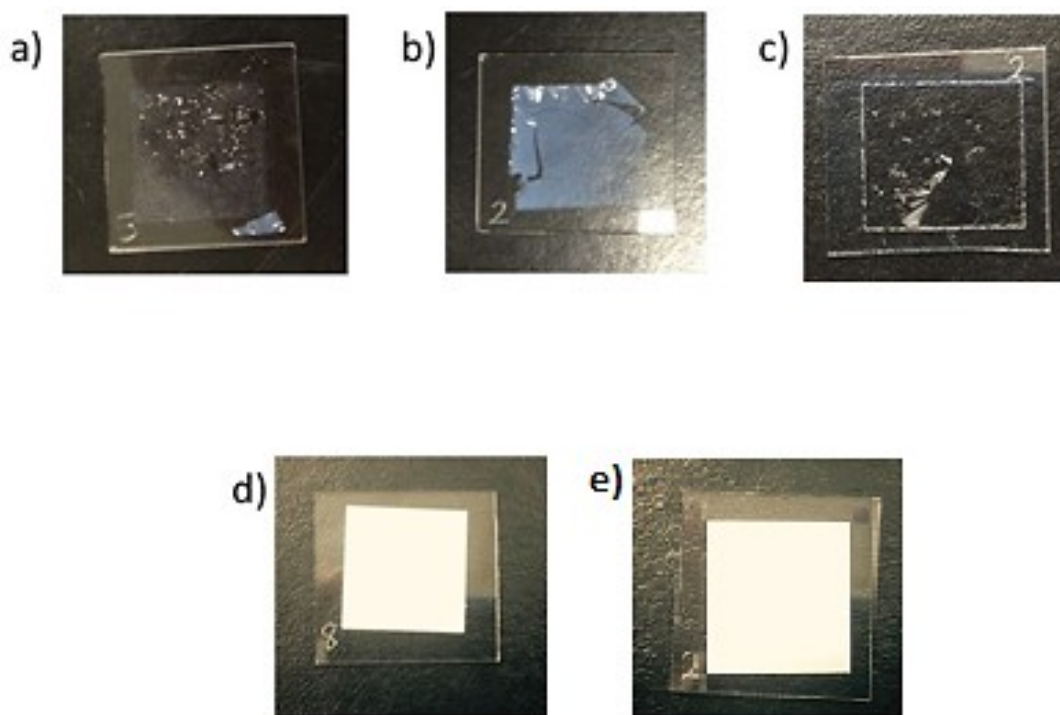


Figure 2.4. MIP films prepared with a) chloroform, b) methanol, c) acetonitrile d) 1-octanol, and e) acetonitrile-PEG.

The good results obtained for the MIP film using 1-octanol as a porogen can be attributed to the early phase separation that occurred during the photo-polymerization, which results in the formation of large pores in the polymer network, while in the case of

the other solvents, it is possible that the slow phase separation leads to much smaller pores and unstable “glassy” morphology [32,33]. Based on these results, 1-octanol was selected at the beginning of the work as the best porogen to prepare the six different MIP compositions. Unfortunately, the prepared thin-films showed poor imprinting factors ($IF \leq 1.13$) for all thiophene compounds. The low IF results for thiophene compounds may be ascribed to the poor accessibility of the analytes to the binding cavities of the MIP due to the use of cover slides in the preparation of the thin-films. It seems that the use of cover slide lead to the formation of a coherent non-porous layer on the surface of the polymer. Obtaining porous MIP thin-films with good porosity is very important because it enables a good access to the selective binding sites [34]. An attempt was made to make the upper layer of the thin-film more porous by using of a mixture of 1-octanol:methanol (1:1) as a porogen in the preparation of the six polymers. An improvement in the imprinting factors of the thiophene compounds was observed when a mixture of 1-octanol and methanol was used as a porogen. Therefore, this porogen is used the preparation of the six polymers (Table 2.1). From Figure 2.5 among the selected monomers, the MIP4 (1-vinylimidazole-MIP) showed the highest binding capacity and imprinting factors (Table 2.2) for all thiophene compounds. Thus, 1-vinylimidazole was selected as the best monomer for thiophenes-MIP.

Table 2.2. Imprinting factors (IF_s) for MIP compositions prepared with different monomers using 1:1 ratio of 1-octanol:methanol mixture as a porogen.

Polymer	Monomer	Cross-linker	Analyte			
			BT	3-MBT	DBT	4,6-DMDBT
MIP1	MAA	EDGMA	1.15	1.09	1.10	1.22
MIP2	4-VP		1.04	1.05	1.09	1.12
MIP3	AM		1.39	1.34	1.42	1.40
MIP4	1-Vim		1.22	1.49	1.64	1.66
MIP5	AC		1.06	1.07	1.14	1.26
MIP6	AAM		1.12	1.21	1.27	1.05

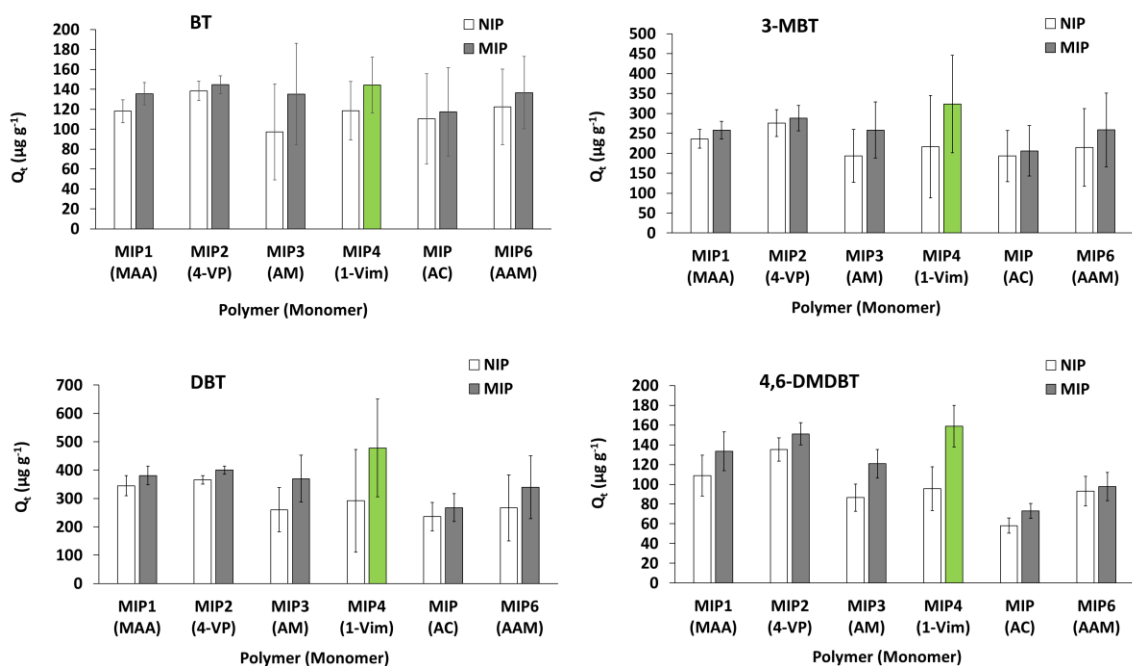


Figure 2.5. Comparison between six MIP films prepared as adsorbents for thiophene compounds from. Error bars represent standard deviation.

A small improvement in the imprinting factors of thiophene compounds with insufficient reproducibility (RSDs 5.0-18.0%) was observed when 1-octanol:methanol was used as a porogen. It was concluded from this study that perhaps this porogen was not enough to produce MIP films with higher imprinting factors and acceptable reproducibility as seen above.

Given that a range of solvent systems had been tried, a new approach was taken. The concept of interpenetrating polymer networks (IPN) was adapted in the preparation of the MIP films. A linear polymer-polyethylene glycol (PEG) with high molecular weight (MW 20,000) was added to the pre-polymerization mixture of MIP7 (Table 2.1). The percentage of PEG in the initial composition of the MIP film was 25% (w/w). Acetonitrile was found to be the best porogen for all components in the mixture. The resulting thin-film exhibited a shape similar to that obtained using 1-octanol as a porogen (Figure 2.4 e), but with improved properties as will be seen later.

To understand the role of PEG in producing films with good properties, we can refer to the films prepared using porogens such as chloroform, methanol and acetonitrile in the absence of PEG. During the polymerization process, the porogen determined the shape and pore structure of the polymer. An early phase separation forms a polymer with a porous structure while, a late phase separation could lead to the formation of a gel-like polymer. It seems that the presence of PEG enhances early phase separation and prevents the formation of the glassy film due to the low solubility of the newly forming crosslinked polymer.

One of the success keys of this work was the preparation of a viscous pre-polymerization mixture. When a small amount of the viscous mixture is placed on the slide, it will spread slowly and distribute evenly after being covered with the cover slide. The viscosity of the mixture can be modified by changing the percentage of components relative to the solvent (acetonitrile) until a mixture with acceptable viscosity is obtained. Although this may seem to be somewhat subjective, the viscosity is crucial in producing a thin-film with a uniform thickness and a regular surface shape in this preparation method. We found that the optimum percentage of all components in acetonitrile is 56.0 % (w/w).

The cross-linker has a major impact on the physical characteristics of the MIP as it controls the morphology of the polymer, stabilizes the imprinted sites, and improves the mechanical stability. However, some researchers found that the cross-linker has a less effect on the specific interactions between the template and the monomer [35–37]. The effect of its amount on the binding capacity and affinity of MIP was also studied. For example, Rampey et al. [38] studied this effect and observed a small change in the binding properties of the MIPs in his study. In an effort to further improve the adsorption properties of our thiophenes-MIP, another cross-linker, bisphenol A dimethacrylate (BPADMA), was used to prepare a new MIP thin-film (MIP8, Table 2.1). The binding capacities this polymer was compared with the binding capacity of the polymer prepared with EDGMA (MIP7), as seen in Figure 2.6.

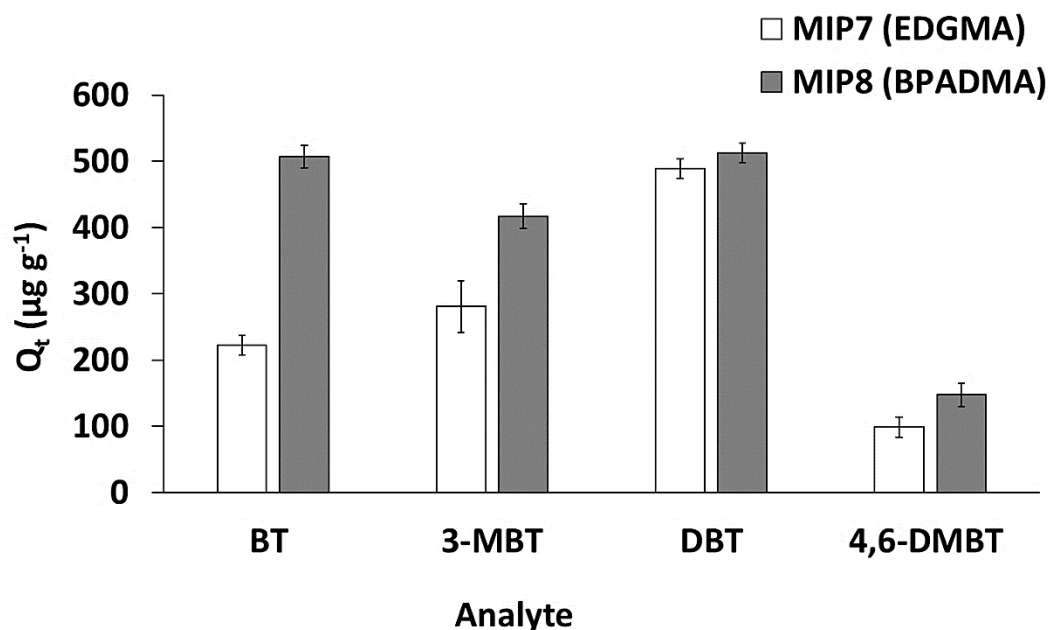


Figure 2.6. Comparison between the two MIP thin-films prepared with different cross-linkers (n=3). Error bars represent standard deviation.

The MIP8 showed a higher binding capacity compared to the MIP7, especially for BT and 3-MBT. This improvement may be attributed to the π - π interaction between the aromatic rings in BPADMA and the thiophenic group of targeted compounds. In our work, the greatest impact on the binding capacity and imprinting factors of the MIP was expected to be from the changes in the template and monomer concentrations, therefore, the concentration of the BPADMA was kept almost constant, while the concentration of the template and the monomer were varied (Table 2.3).

Table 2.3. Optimization of template to monomer to cross-linker ratio of 1-Vim-BPADMA MIP.

Polymer	M:C	2-thiophene-carboxaldehyde	1-Vim	BPADMA	DMPA	Acetonitrile/ (PEG, 25% w/w)
MIP9	1:2	0.27 mmol (25.6 μ L)	1.10 mmol (99.4 μ L)	2.20 mmol (800 mg)	0.05 mmol (12.1 mg)	930 μ L (300 mg)
MIP10	1:4	0.14 mmol (12.8 μ L)	0.55 mmol (49.7 μ L)		0.04 mmol (10.0 mg)	870 μ L (285 mg)
MIP11	1:8	0.07 mmol (6.4 μ L)	0.27 mmol (24.9 μ L)		0.04 mmol (9.0 mg)	838 μ L (275 mg)

From Figure 2.7 it can be observed that the 1:2 M:C mole ratio gave the highest total binding capacity (Total Q_t) and imprinting factors for thiophens (MIP9, Table 2.4). It seems that increasing of the concentration of the template and the monomer while keeping a constant mole ratio between them (1:4) produced more binding sites in the polymer. However, in this research, the MIP films prepared at monomer to cross-linker ratios less than 1:2 were weak and exhibited non-rigid structures and low reproducibility. The obtained imprinting factors were 2.93, 2.74, 2.86, and 2.21, for BT, 3-MBT, DBT, 4,6-DMDBT respectively.

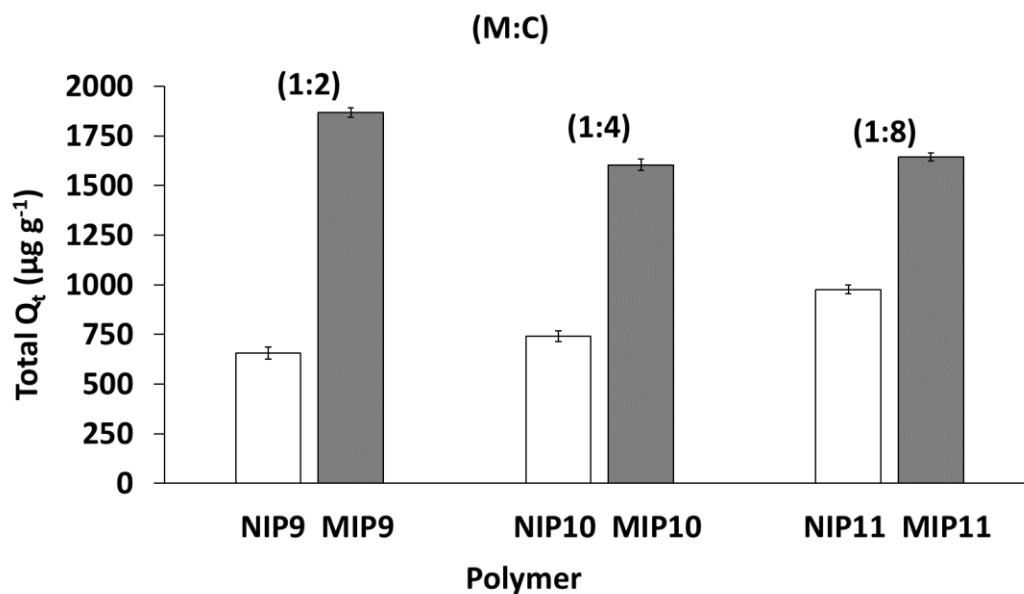


Figure 2.7. Optimization of the template to monomer to cross-linker ratio (n=3). Error bars represent standard deviation.

Table 2.4. Total binding capacity, average imprinting factors and relative standard deviations for 1-Vim- BPADMA MIP at different M:C ratios.

Polymer	M:C	Total Q _t (µg g ⁻¹)	RSD (%)	Average <i>IF</i>
NIP9	1:2	656.0	5.2	-
MIP9		1868.3	4.9	2.85
NIP10	1:4	741.1	3.7	-
MIP10		1603.9	2.9	2.16
NIP11	1:8	976.4	1.4	-
MIP11		1643.4	2.3	1.68

2.4.2. Morphology of the thin-films

SEM images were taken of the surface of the MIP9 and NIP9 thin-films (Figure 2.8 a) and b)). Both films exhibited porous surfaces, but the surface of the MIP showed significantly more porosity, with the appearance of more homogenous and more uniform pores on the surface.

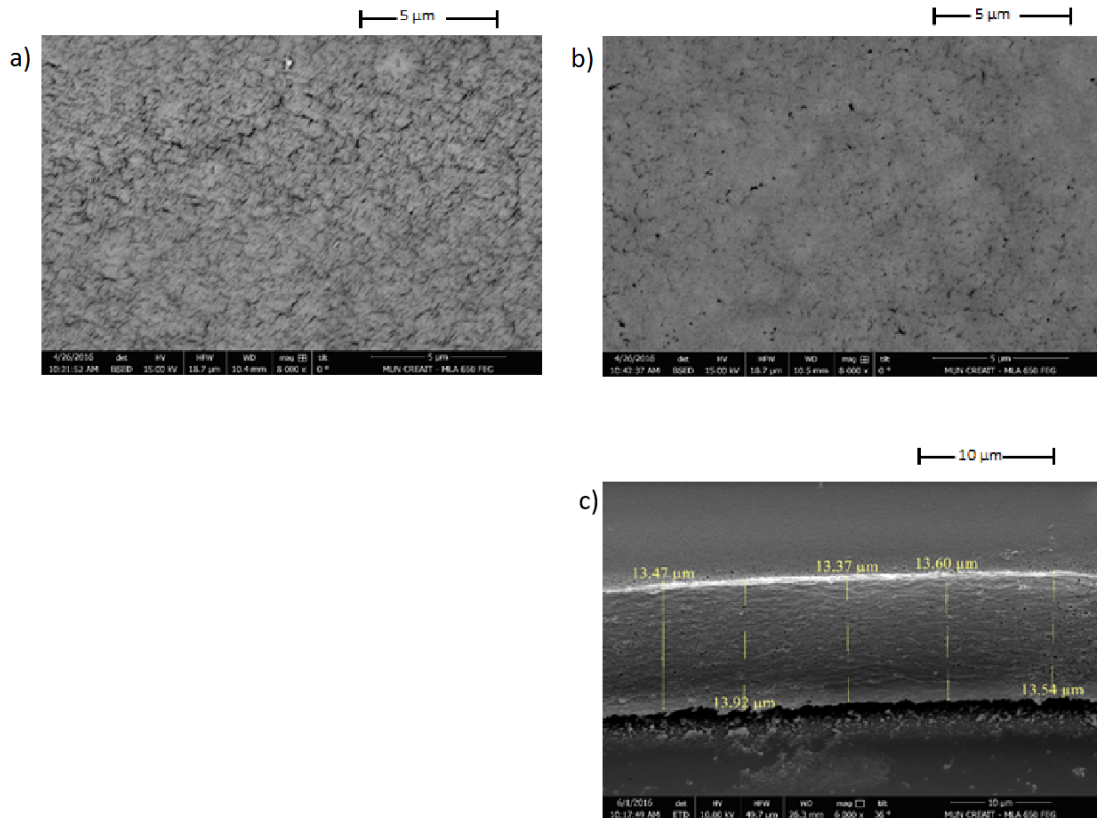


Figure 2.8. SEM of a) the surface of MIP and b) NIP films and c) cross-section of MIP film.

Although the addition of the linear polymer PEG was performed to improve the porosity of the thin-film, it is difficult to compare the porosity of the MIP film to that of the NIP film based on their SEM images, because the PEG was added to both. The improvement in the porosity can be ascribed to the removal of the template from the MIP film after washing the slide with methanol. This can be noticed also from the binding studies obtained in this research for the MIP and NIP films, which showed a better binding capacity for MIP compared to NIP. It seems that the presence of the template during the polymerization process not only aided in the formation of the selective binding sites in the polymer, but also caused some changes in the morphological properties of the polymer, such as the porosity. The thickness measurement for the edges of the MIP film (Figure 2.8 c) showed a uniform thickness of $\sim 13.5 \mu\text{m}$.

To investigate if the adsorption of analytes occurs at the surface or within the film, or both, the mass and thickness of MIP film can be varied while keeping its area constant ($18 \times 18 \text{ mm}^2$). To prepare these films, different volumes (6, 8, 10 μL) from the pre-polymerization mixture of MIP9 were pipetted onto the slides and polymerized using the procedure described in Section 2.3.3. It can be seen from Figure 2.9 that the peak area ratios of all thiophene compounds, which are relative to the internal standard (fluorene- d_{10}), increased linearly when the polymerized amount of MIP increased. These results demonstrate that the adsorption process for thiophene compounds occur within the porous structure of the film and not only at the surface.

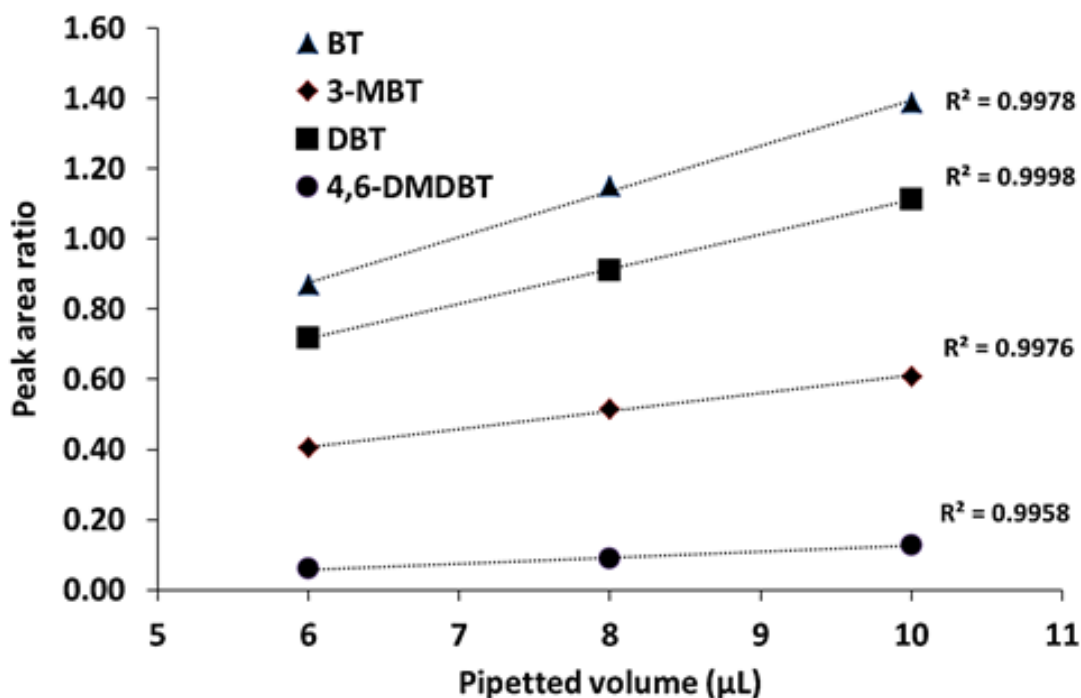


Figure 2.9. The relationship between the polymerized volume of MIP and the peak area ratios of the adsorbed thiophene compounds in the MIP thin-film obtained from the GC-MS analysis.

2.4.3. Optimization of the stirring speed of MIP analysis

Optimizing the stirring speed of the sample analysis by MIP is necessary to ensure maximum extraction of the analytes at the equilibrium time and to obtain the stirring speed that gives reproducible results. Also, higher stirring speed reduces the time required to reach the equilibrium by enhancing the diffusion of the analyte towards the MIP film and produces consistent mixing for the sample. Various speeds of stirring (125, 350, and 700 rpm) for 2 h uploading was tested using the optimized MIP film composition (MIP9, Table 2.2). Each MIP slide was placed in a beaker containing 40 mL of DI water spiked with thiophene compounds at a concentration of $100 \mu\text{g L}^{-1}$. Figure 2.10 showed that a stirring

speed of 400 rpm and above gave the highest binding capacities for all thiophene compounds. At stirring speeds higher than 700 rpm, irreproducible results were obtained; this may have happened because of the film damage caused by the extreme stirring. Thus, the 500-rpm stirring speed was selected for all further analysis.

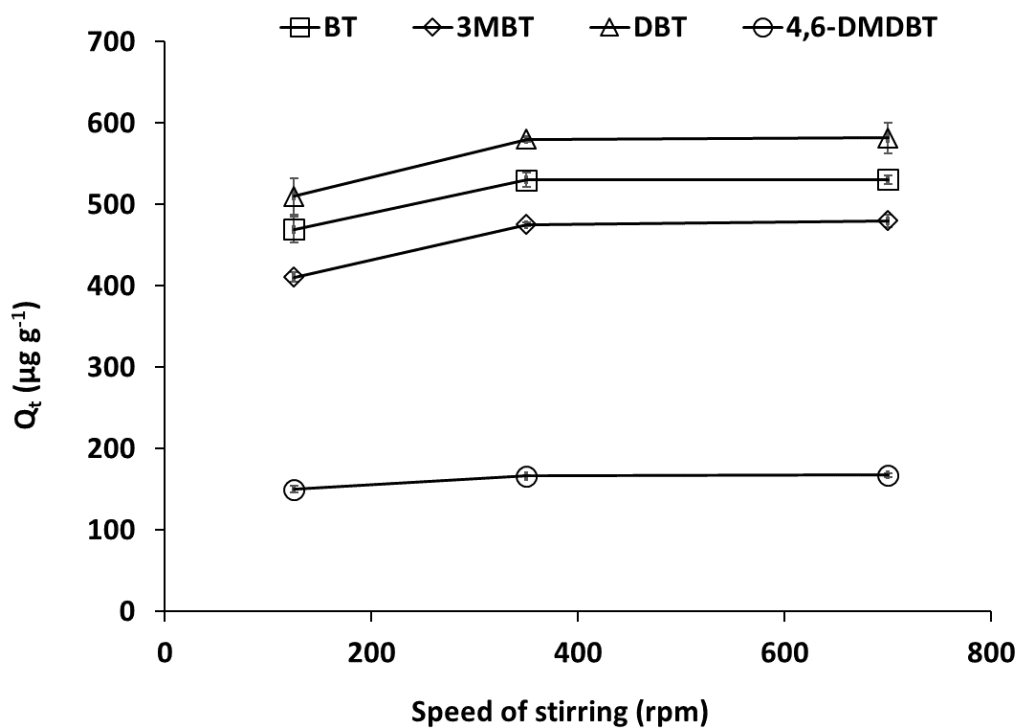


Figure 2.10. Effect of stirring speeds on the binding capacities of thiophene compounds in the analysis by MIP after uploading for 2 h ($n=3$). Error bars represent standard deviation.

2.4.4. Adsorption kinetics of MIP thin-film

The effect of the uploading time was investigated over a range of 1 to 24 h. Uploading of thiophene compounds to MIP films from 200 mL of DI water spiked with a mixture of spiked thiophene compounds at a concentration of $50 \mu\text{g L}^{-1}$ was evaluated. Figure 2.11 shows that the binding capacities of all thiophene compounds were increased rapidly within the first 8 h, and then slowly increased until the equilibriums reached at ~ 15 h with no change until 24 h. The rapid adsorption behaviour in the first 8 h can be ascribed to preferential adsorption of thiophene compounds onto the recognition sites. As these sites become more occupied with the time, it become difficult for thiophene compounds to bind rapidly into the MIP making the adsorption rate slower. These results showed that MIP thin-films can be suitable for short analyses with acceptable limit of detection values where rapid response is necessary and extended deployment analyses, where higher sensitivity with lower detection limits can be achieved. For simplicity, 2 h has been selected to be the uploading time for all analyses studies in our work. This time gave reliable responses for all thiophene compounds at a range of concentrations.

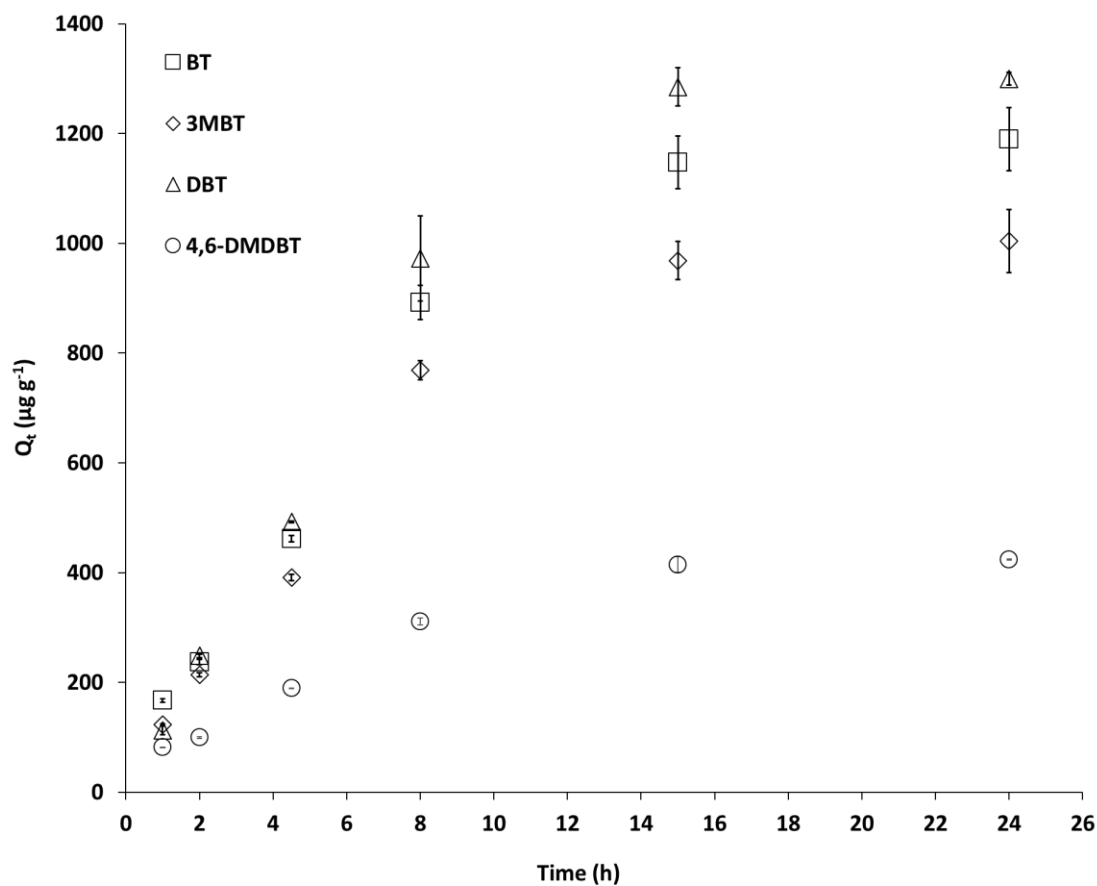


Figure 2.11. Adsorption kinetics of MIP thin-film for thiophene compounds in water (n=3). Error bars represent standard deviation.

2.4.5. Effect of sample volume on extracted amount by MIP thin-film

The effect of the sample volume on the amount of thiophene compounds extracted by MIP films from the seawater samples was studied. Sample volume is an important parameter because it affects the quantitative results. If the MIP film is treated like the fiber in solid-phase micro-extraction (SPME) then, the effect of the volume on the analysis can be negligible only when the volume is much larger than the capacity of the film [39]. To

understand how the volume of sample affects the analysis of MIP film, the relation between the amount of the analyte adsorbed by the film and the volume of sample can be predicted and compared with the experimental values. The amount of analyte adsorbed by the film (n) can be predicted using the following equation:

$$n = \frac{C_0 K V_{film} V_s}{V_s + K V_{film}} \quad (2.4)$$

where K is the partition coefficient between the sample and the film at equilibrium, V_{film} is the volume of the film, and V_s is the volume of the sample. The values of partition coefficients of thiophene compounds were calculated from the results obtained from the adsorption kinetics study (Figure 2.11) using the following equation:

$$K = \frac{C_{film}}{C_s} = \frac{(n/V_{film})}{C_0 - (n/V_s)} \quad (2.5)$$

where C_{film} is the concentration of the analyte in the film and C_s is the concentration of the analyte in the sample, and C_0 is the initial concentration of the analyte in the sample. The volume of the MIP film (V_{film}) was calculated using the volume of box formula as follows:

$$V_{film} = L \times W \times H \quad (2.6)$$

where L is the length of the box in mm, W is the width of the box in mm, and H is the height of the box in mm. Based on the dimensions ($18 \times 18 \text{ mm}^2$) and the measured thickness ($\sim 13.5 \text{ }\mu\text{m}$) of the MIP film, the volume of MIP film was found to be 4.37 mm^3 .

A series of uploading experiments using MIP films for a range of volumes between 10 and 800 mL at a $50 \text{ }\mu\text{g L}^{-1}$ of spiked seawater sample with thiophene compounds were

carried out. From the predicted effect (Figure 2.12 a), it can be observed that, the adsorbed amounts (n) of thiophene compounds increased sharply up to 200 mL, and then increased slightly up to 800 mL. Despite of the fact that our experiments are far from equilibrium, and despite of the effect of sample volume on the adsorption kinetics, the general behaviour in Figure 2.12 b appears to be similar to the one predicted from Figure 2.12 a. The amounts of thiophene compounds adsorbed by MIP films increased with the increasing of the sample volumes in the range studied, but unexpected results were obtained at a range of 50-200 mL where the adsorbed amount of thiophene compounds into the film mostly remain constant.

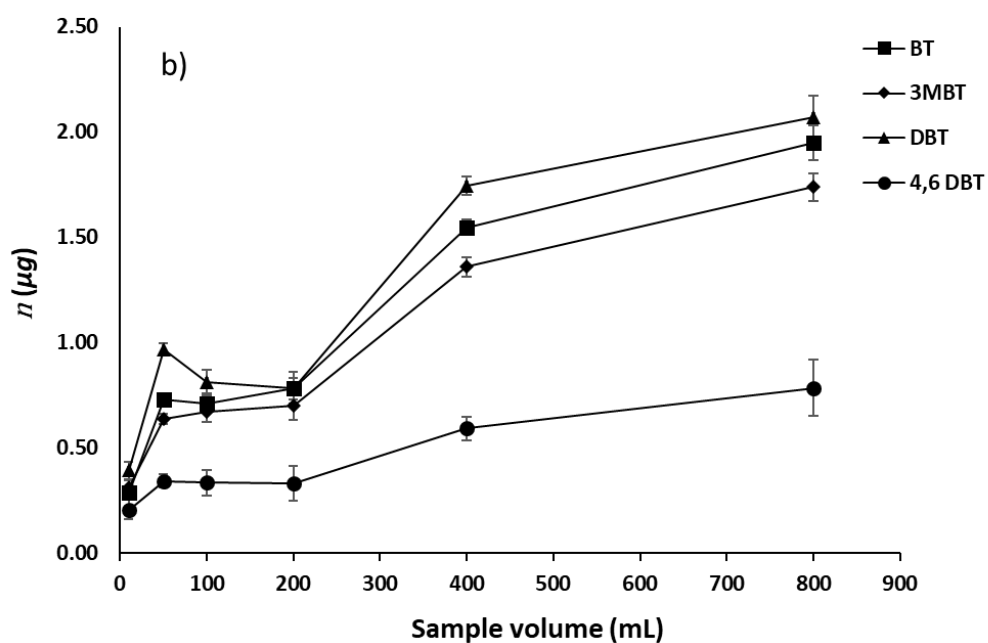
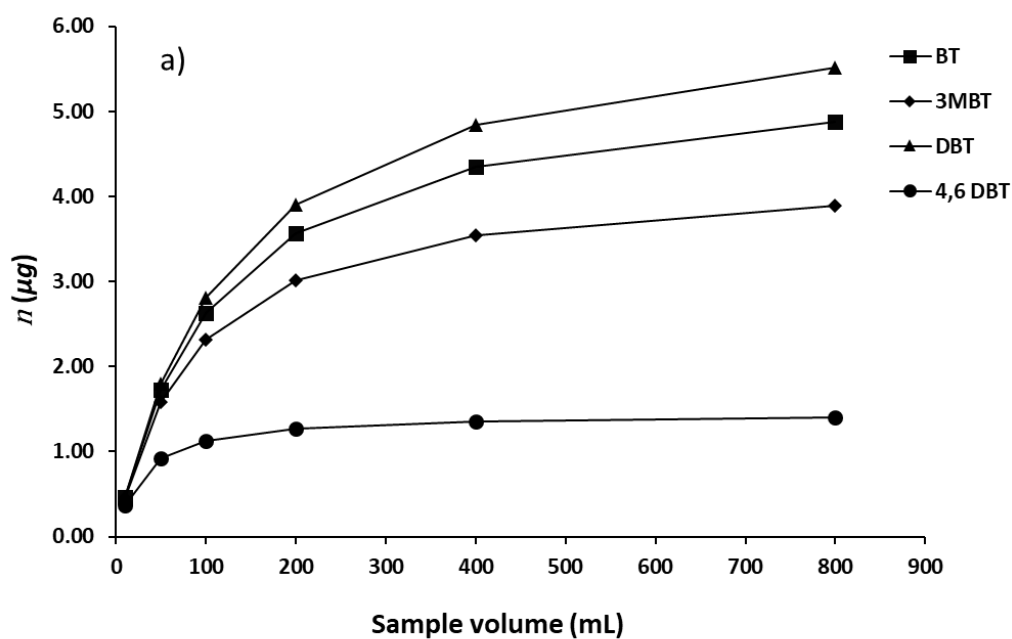


Figure 2.12. a) Predicted effect of the seawater sample volume in the amount of analyte adsorbed (Initial concentration, C_0 , $50 \mu\text{g L}^{-1}$). b) Experimental effect of the seawater sample volume in the amount of analyte adsorbed (initial concentration, C_0 , $50 \mu\text{g L}^{-1}$). Error bars represent standard deviation ($n = 3$).

In Figure 2.12 b), at lower volumes below 50 mL, a sharp increase in the adsorbed amounts of thiophene compounds into the film was observed. A slight decrease in the adsorbed amounts was noticed from 50 mL to 100 mL followed by a little increase up to 200 mL. After 200 mL, a rapid increase was observed up to 400 mL, and then slightly increased up to 800 mL. The results obtained for the range from 50-200 mL can be attributed to the decrease in the analytes diffusion into the binding sites of the film which occurred because of the increase in the sample volume. The influence of the sample volume was reduced after 200 mL due to the increasing of the amount of the analytes in the sample, which appeared as a rapid increase in the amount adsorbed up to 400 mL and then slightly increased up to 800 mL where the equilibrium was approached. These results revealed that the MIP films are suitable as an adsorbent at low and high sample volumes.

2.4.6. Adsorption isotherms for thiophene compounds in seawater

Several binding isotherm models can be used to evaluate the binding equilibrium behaviour of MIPs (Table 1.3, Chapter 1). Since the binding properties of the MIP was found to be negatively affected by heterogeneity [38], the best model to study these properties and measure the heterogeneity of MIP and NIP is the Freundlich isotherm model [38,40]. The Freundlich isotherm model was applied to both, and the curves were obtained by plotting Equation (2.3) in Section 2.3.6.

As shown in Figure 2.13, the MIP film exhibited higher adsorption capacities towards thiophene compounds than the NIP. The calculated fitting parameters for each

thiophene compound including heterogeneity index, m , and the Freundlich fitting parameter, a , which is related to the average binding affinity, K_0 ($K_0 = a^{1/m}$) are listed in Table 2.5. The heterogeneity index, m , describes the degree of adsorbent heterogeneity. Its values range between 0 and 1, and when m becomes closer to 1, the heterogeneity of material decreases and homogeneity increases. Heterogeneity usually limits the binding affinity and selectivity of the MIPs especially for non-covalent MIPs. These MIPs usually contain binding sites of varying affinity and selectivity because of non-stoichiometric or non-covalent imprinting mechanism [41].

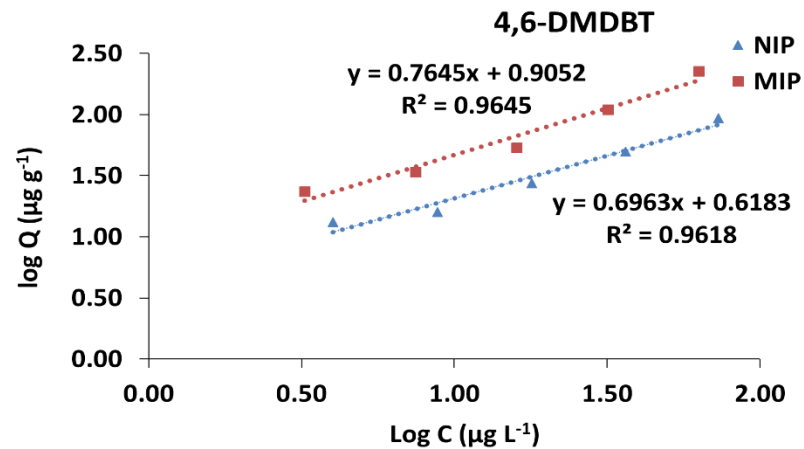
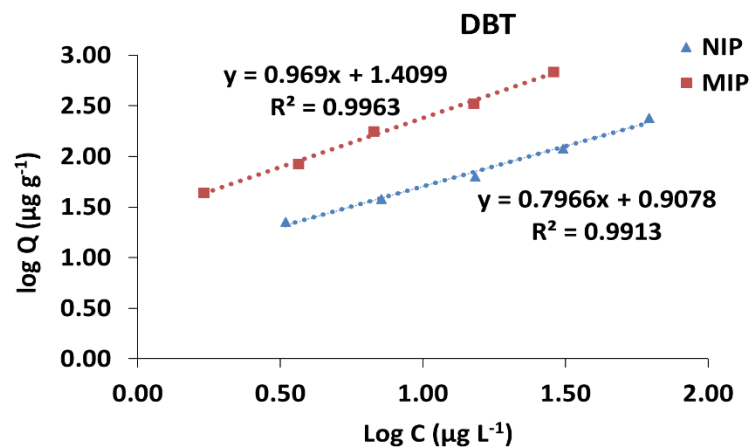
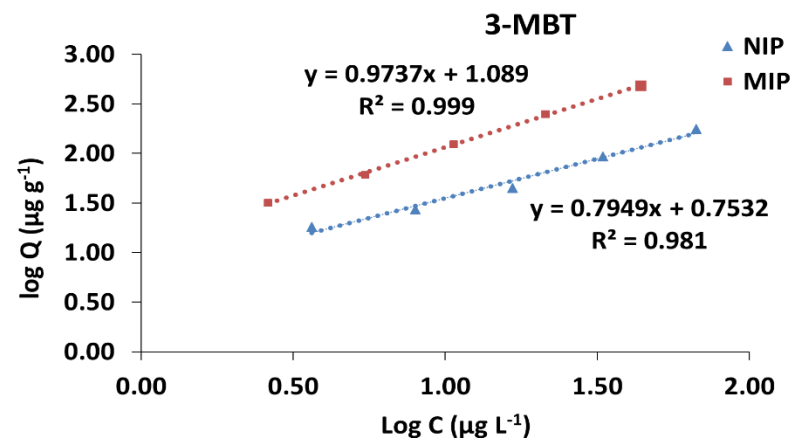
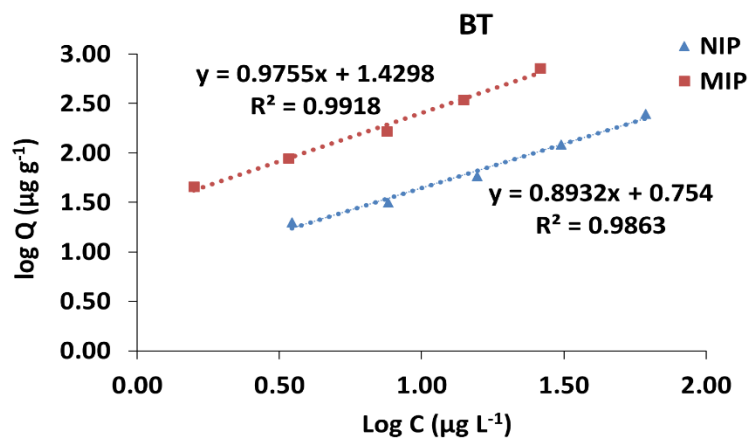


Figure 2.13. Adsorption isotherm of MIP and NIP for thiophene compounds fitted to Freundlich isotherm (equilibration time 15 h).

As shown in Table 2.5, the values of m and a demonstrated more binding sites homogeneity and binding affinity for the MIP compared to the NIP. However, MIP and NIP thin-films showed well-fitting to Freundlich isotherm parameters (R^2 , Table 2.5) with more fitting in the case of MIP thin-films.

Table 2.5. Freundlich fitting parameters to the adsorption isotherm for MIP and NIP.

Fitting parameter	m		a ($\mu\text{g g}^{-1}$)		K_0 ($\mu\text{g g}^{-1}$)		R^2	
	MIP	NIP	MIP	NIP	MIP	NIP	MIP	NIP
BT	0.976	0.893	26.903	5.675	29.222	6.985	0.9918	0.9863
3-MBT	0.974	0.795	12.274	5.665	13.135	8.862	0.9990	0.9810
DBT	0.969	0.797	25.698	8.087	28.511	13.791	0.9963	0.9913
4,6-DMDBT	0.765	0.696	8.039	4.152	15.277	7.726	0.9645	0.9618

2.4.7. Analysis of real samples

To evaluate the ability of the new MIP films for the extraction of thiophene compounds from real samples, seawater samples were collected and spiked with thiophene compounds at concentrations in the range of 0.5-40.0 $\mu\text{g L}^{-1}$. Analysis was carried out using thiophenes-MIPs without pre-treatment. A very good linearity (R^2) for each thiophene compound was obtained from the calibration curves (Figure 2.14). The limit of detection

values in seawater sample were 0.029, 0.040, 0.068, 0.166 $\mu\text{g L}^{-1}$ for BT, 3-MBT, DBT, and 4,6-DMDBT respectively. This method is reproducible with low relative standard deviations ($\text{RSD}_s \leq 6.0\%$).

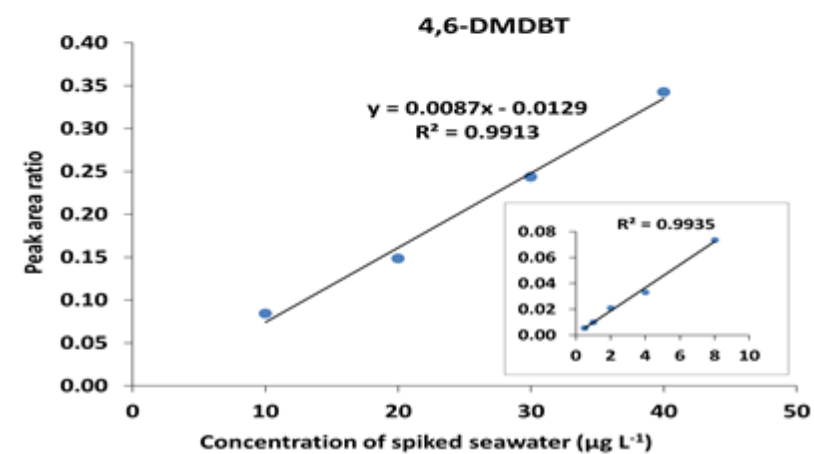
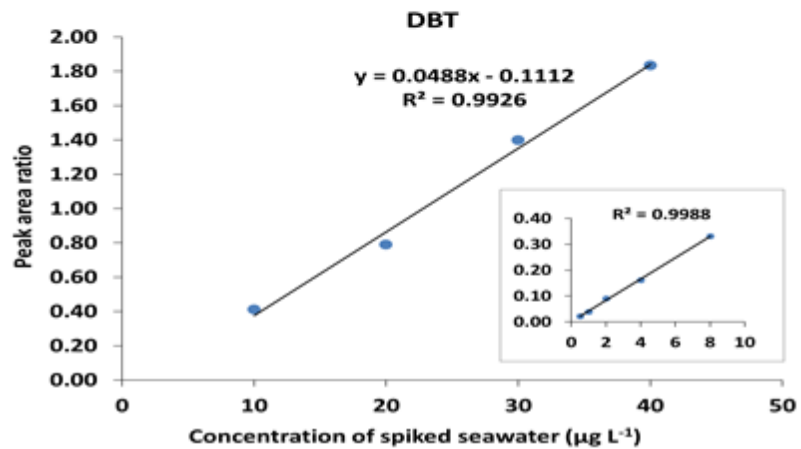
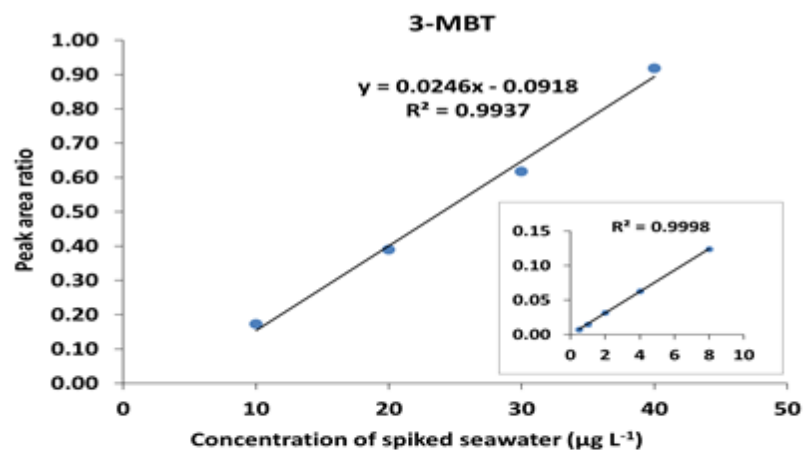
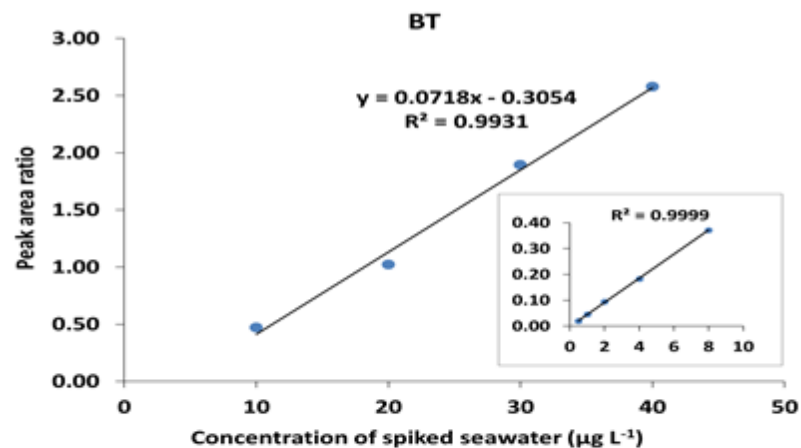


Figure 2.14. Calibration curves for thiophene compounds at various spiked concentrations in seawater samples. IS: Fluorene- d_{10} ($\text{RSD}_s \leq 6.0\%$, $n = 3$).

2.4.8. Selectivity of MIP thin-film

The possible interactions between the non-covalent MIPs and the analytes in the sample usually occur through hydrophobic, ionic, hydrogen bonding, and electrostatic interactions. If the hydrophobic is the dominant interaction type in our MIP and depending on the values of $\log K_{ow}$ of targeted thiophenes (Table 1.1, Chapter 1) then, the heavier thiophene compound will interact more. Among our analytes, the 4,6-DMDBT has the highest $\log K_{ow}$ value, so this analyte is expected to have the highest binding capacity among others. To verify that, the selectivity of MIP thin films was evaluated using p-cresol and indole compounds as interferents. The p-cresol represents polar aromatic compounds while the indole represents analogous compounds of thiophene compounds. A seawater sample was spiked with thiophene compounds and interferents at the same concentration ($100 \mu\text{g L}^{-1}$), and then analyzed by MIP GC-MS. The Figure 2.15 shows that the MIP film exhibited higher selectivity toward all thiophene compounds compared to other interferents except for 4,6-DMDBT, which showed equivalent adsorption selectivity compared to the indole. This may be attributed to the steric effect of the two methyl groups in 4,6-DMDBT (Figure 2.2), which restricts the access of this analyte to the cavities inside the MIP.

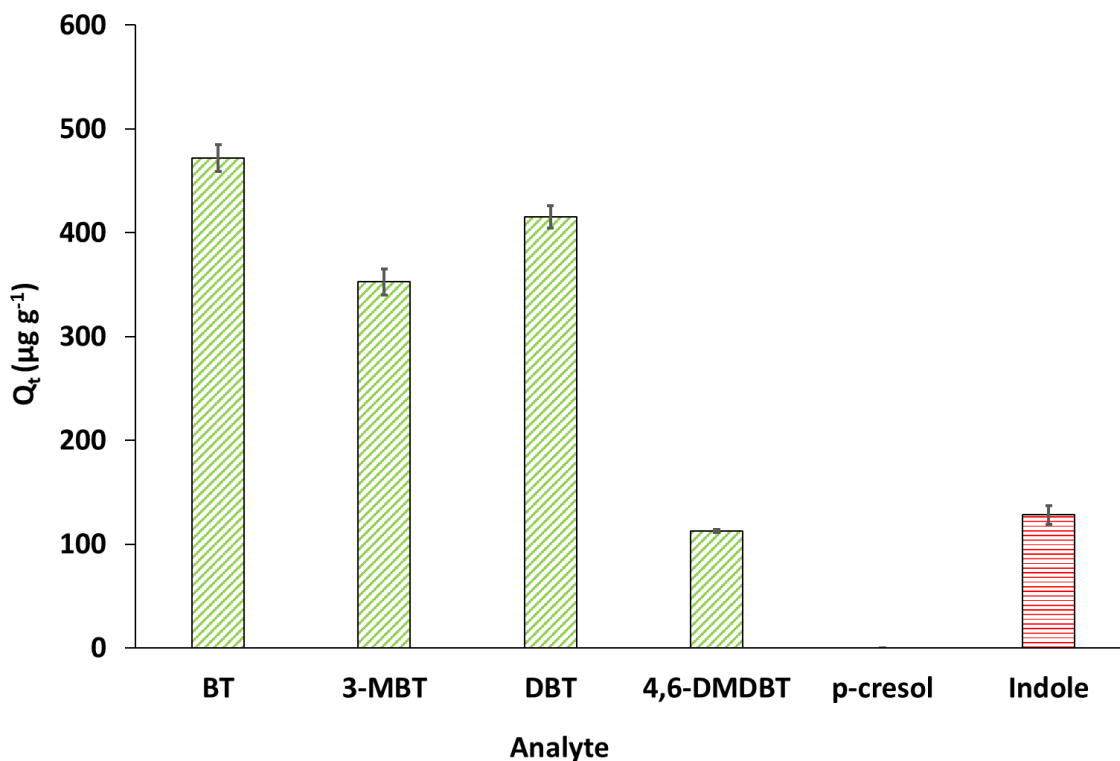


Figure 2.15. Selectivity of MIP thin-film for thiophene compounds versus p-cresol and indole (n=3). Error bars represent standard deviation.

From the previous results, it can be concluded that the interaction between our MIP and thiophene compounds is not only based on hydrophobic interaction since the highest binding capacity was observed for BT which has the lowest value of $\log K_{ow}$ compared to others. A typical full scan GC-MS chromatogram was shown in Figure 2.16; this chromatogram was obtained from the analysis of a spiked seawater sample (thiophene compounds and interferents are at the same concentration) by MIP GC-MS without pre-treatment. The chromatogram showed higher responses for thiophene compounds compared to the interferents and revealed that the MIP thin-film successfully extracted thiophene compounds selectively from the seawater sample.

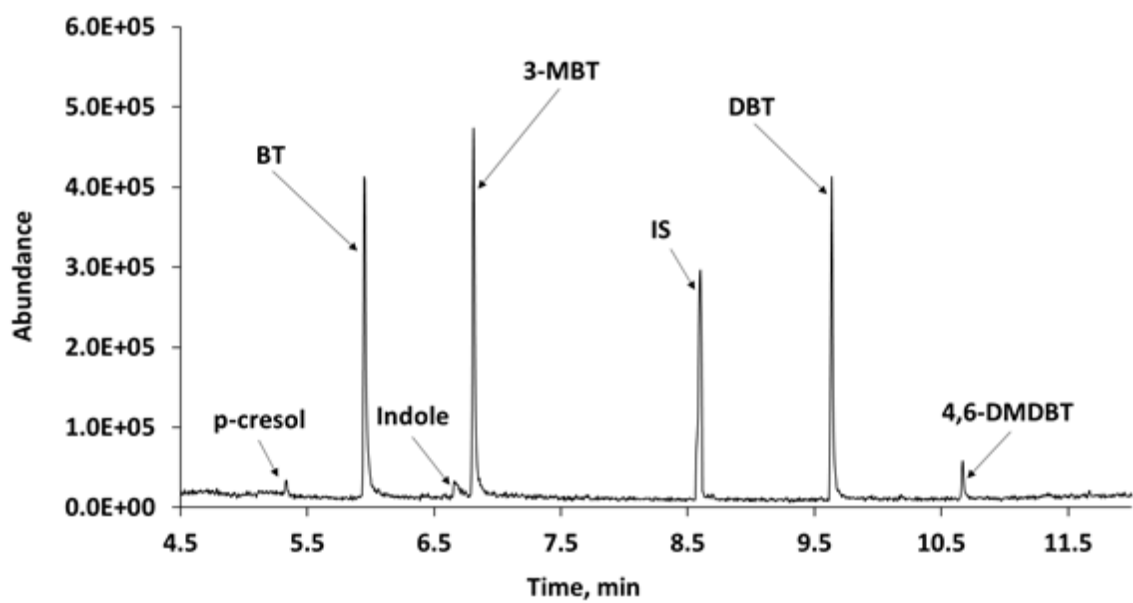


Figure 2.16. GC-MS full-scan of 40 mL seawater sample spiked with thiophene compounds and interferents at the same concentrations ($100 \mu\text{g L}^{-1}$). IS: Fluorene- d_{10} .

2.5. Conclusions

In this research, novel MIP thin-film on a glass slide was prepared as an adsorbent for the selective extraction of thiophene compounds in water. No sample preparation or pre-treatment was needed. The MIP thin-films displayed good binding behaviour, high selectivity, reproducibility, linearity, and low LOD values for thiophene compounds. The small size of MIP slides and the ease of preparation make them efficient for off-site and on-site environmental analysis, when combined with a suitable detection system. The preparation of thin-films in this work could be promising for the creation of reproducible thin-films for sensors and other applications.

2.6. References

- [1] Farrington, J. W.; Mcdowell, J. E. Mixing Oil and Water. *Science* (80-.). **2002**, *43* (June), 2156–2157.
- [2] Speight, J. G. *The Chemistry and Technology of Petroleum*; CRC Press, Taylor and Francis, **2014**.
- [3] Castro, B.; Whitcombe, M. J.; Vulfson, E. N.; Vazquez-Duhalt, R.; Bárzana, E. Molecular Imprinting for the Selective Adsorption of Organosulphur Compounds Present in Fuels. *Anal. Chim. Acta* **2001**, *435* (1), 83–90.
- [4] Gui-peng, Y. Photochemical Oxidation of Benzothiophene in Seawater. *Chinese J. Oceanol. Limnol.* **2000**, *18* (1), 85–91.
- [5] Kropp, K. G.; Fedorak, P. M. A Review of the Occurrence, Toxicity, and Biodegradation of Condensed Thiophenes Found in Petroleum. *Can. J. Microbiol.* **1998**, *44* (7), 605–622.
- [6] Berthou, F.; Vignier, V. Analysis and Fate of Dibenzothiophene Derivatives in the Marine Environment. *Int. J. Environ. Anal. Chem.* **1986**, *27* (1–2), 81–96.
- [7] Croisy, A.; Mispelter, J.; Lhoste, J.-M.; Zajdela, F.; Jacquignon, P. Thiophene Analogues of Carcinogenic Polycyclic Hydrocarbons. Elbs Pyrolysis of Various Aroylmethylbenzothiophenes. *J. Heterocycl. Chem.* **1984**, *21* (2), 353–359.
- [8] Avino, P.; Notardonato, I.; Cinelli, G.; Russo, M. Aromatic Sulfur Compounds Enrichment from Seawater in Crude Oil Contamination by Solid Phase Extraction. *Curr. Anal. Chem.* **2009**, *5* (4), 339–346.
- [9] Yu, C.; Yao, Z.; Hu, B. Preparation of Polydimethylsiloxane/ β -

- Cyclodextrin/divinylbenzene Coated “dumbbell-Shaped” stir Bar and Its Application to the Analysis of Polycyclic Aromatic Hydrocarbons and Polycyclic Aromatic Sulfur Heterocycles Compounds in Lake Water and Soil by Hig. *Anal. Chim. Acta* **2009**, *641* (1–2), 75–82.
- [10] Gimeno, R. .; Altelaar, a. F. .; Marcé, R. .; Borrull, F. Determination of Polycyclic Aromatic Hydrocarbons and Polycyclic Aromatic Sulfur Heterocycles by High-Performance Liquid Chromatography with Fluorescence and Atmospheric Pressure Chemical Ionization Mass Spectrometry Detection in Seawater and Sediment Samp. *J. Chromatogr. A* **2002**, *958* (1), 141–148.
- [11] Haupt, K.; Mosbach, K. Molecularly Imprinted Polymers and Their Use in Biomimetic Sensors. *Chem. Rev.* **2000**, *100* (7), 2495–2504.
- [12] Shimizu, K. D.; Stephenson, C. J. Molecularly Imprinted Polymer Sensor Arrays. *Curr. Opin. Chem. Biol.* **2010**, *14* (6), 743–750.
- [13] Yan, H.; Row, K. H. Characteristic and Synthetic Approach of Molecularly Imprinted Polymer. *Int. J. Mol. Sci.* **2006**, *7* (5), 155–178.
- [14] Vasapollo, G.; Sole, R. Del; Mergola, L.; Lazzoi, M. R.; Scardino, A.; Scorrano, S.; Mele, G. Molecularly Imprinted Polymers: Present and Future Prospective. *Int. J. Mol. Sci.* **2011**, *12* (9), 5908–5945.
- [15] Andersson, L. I.; Paprica, A.; Arvidsson, T. A Highly Selective Solid Phase Extraction Sorbent for Pre- Concentration of Sameridine Made by Molecular Imprinting. *Chromatographia* **1997**, *46* (1), 57–62.
- [16] Matsui, J.; Fujiwara, K.; Takeuchi, T. Atrazine-Selective Polymers Prepared by Molecular Imprinting of Trialkylmelamines as Dummy Template Species of

- Atrazine. *Anal. Chem.* **2000**, 72 (8), 1810–1813.
- [17] Liu, X.; Liu, J.; Huang, Y.; Zhao, R.; Liu, G.; Chen, Y. Determination of Methotrexate in Human Serum by High-Performance Liquid Chromatography Combined with Pseudo Template Molecularly Imprinted Polymer. *J. Chromatogr. A* **2009**, 1216, 7533–7538.
- [18] Yan, H.; Row, K. H. Characteristic and Synthetic Approach of Molecularly Imprinted Polymer. *Int. J. Mol. Sci.* **2006**, 7 (5), 155–178.
- [19] Schmidt, R. H.; Haupt, K. Molecularly Imprinted Polymer Films with Binding Properties Enhanced by the Reaction-Induced Phase Separation of a Sacrificial Polymeric Porogen. *Chem. Mater.* **2005**, 17 (5), 1007–1016.
- [20] Chou, P. C.; Rick, J.; Chou, T. C. C-Reactive Protein Thin-Film Molecularly Imprinted Polymers Formed Using a Micro-Contact Approach. *Anal. Chim. Acta* **2005**, 542 (1 SPEC. ISS.), 20–25.
- [21] Kryscio, D. R.; Peppas, N. A. Surface Imprinted Thin Polymer Film Systems with Selective Recognition for Bovine Serum Albumin. *Anal. Chim. Acta* **2012**, 718, 109–115.
- [22] Jakusch, M.; Janotta, M.; Mizaikoff, B.; Mosbach, K.; Haupt, K. Molecularly Imprinted Polymers and Infrared Evanescent Wave Spectroscopy . A Chemical Sensors Approach. *Anal. Chem.* **1999**, 71 (1), 4786–4791.
- [23] Spivak, D.; Gilmore, M. A.; Shea, K. J. Evaluation of Binding and Origins of Specificity of 9-Ethyladenine Imprinted Polymers. *J. Am. Chem. Soc.* **1997**, 119 (19), 4388–4393.
- [24] Kempe, M.; Mosbach, K. Binding Studies on Substrate- and Enantio-Selective

- Molecularly Imprinted Polymers. *Anal. Lett.* **1991**, *24* (7), 1137–1145.
- [25] Scorrano, S.; Longo, L.; Vasapollo, G. Molecularly Imprinted Polymers for Solid-Phase Extraction of 1-Methyladenosine from Human Urine. *Anal. Chim. Acta* **2010**, *659* (1–2), 167–171.
- [26] Mayes, A. G.; Whitcombe, M. J. Synthetic Strategies for the Generation of Molecularly Imprinted Organic Polymers. *Advanced Drug Delivery Reviews.* **2005**, pp 1742–1778.
- [27] Tom, L. A.; Gerard, C. L.; Hutchison, C. M.; Brooker, A. S. Development of a Novel Molecularly Imprinted Polymer for the Retention of 4,6-Dimethyldibenzothiophene. *Microchim. Acta* **2012**, *176* (3–4), 375–380.
- [28] Xu, P.; Xu, W.; Zhang, X.; Pan, J.; Yan, Y. Molecularly-Imprinted Material for Dibenzothiophene Recognition Prepared by Surface Imprinting Methods. *Adsorpt. Sci. Technol.* **2009**, *27* (10), 975–987.
- [29] Li, H.; Xu, W.; Wang, N.; Ma, X.; Niu, D.; Jiang, B.; Liu, L.; Huang, W.; Yang, W.; Zhou, Z. Synthesis of Magnetic Molecularly Imprinted Polymer Particles for Selective Adsorption and Separation of Dibenzothiophene. *Microchim. Acta* **2012**, *179* (1–2), 123–130.
- [30] Sperling, L. H.; Hu, R. Interpenetrating Polymer Networks. In *Polymer Blends Handbook*; Springer Netherlands: Dordrecht, **2003**; pp 417–447.
- [31] Sergey, P.; Anthony, T. Molecular Imprinting of Polymers; *Landes Bioscience*, **2006**.
- [32] Svec, F.; Frechet, J. M. J. Kinetic Control of Pore Formation in Macroporous Polymers. Formation of “Molded” Porous Materials with High Flow Characteristics

- for Separations or Catalysis. *Chem. Mater.* **1995**, 7 (6), 707–715.
- [33] Schmidt, R. H.; Belmont, A. S.; Haupt, K. Porogen Formulations for Obtaining Molecularly Imprinted Polymers with Optimized Binding Properties. In *Analytica Chimica Acta*; **2005**; Vol. 542, pp 118–124.
- [34] Alvarez-lorenzo, C.; Angel, C. Handbook of Molecularly Imprinted Polymers. **2013**, 402.
- [35] Mollnelli, A.; O'Mahony, J.; Nolan, K.; Smyth, M. R.; Jakusch, M.; Mizaikoff, B. Analyzing the Mechanisms of Selectivity in Biomimetic Self-Assemblies via IR and NMR Spectroscopy of Prepolymerization Solutions and Molecular Dynamics Simulations. *Anal. Chem.* **2005**, 77 (16), 5196–5204.
- [36] Navarro-Villoslada, F.; San Vicente, B.; Moreno-Bondi, M. C. Application of Multivariate Analysis to the Screening of Molecularly Imprinted Polymers for Bisphenol a. *Anal. Chim. Acta* **2004**, 504 (1), 149–162.
- [37] Shi, X.; Wu, A.; Qu, G.; Li, R.; Zhang, D. Development and Characterisation of Molecularly Imprinted Polymers Based on Methacrylic Acid for Selective Recognition of Drugs. *Biomaterials* **2007**, 28 (25), 3741–3749.
- [38] Rampey, A. M.; Umpleby, R. J.; Rushton, G. T.; Iseman, J. C.; Shah, R. N.; Shimizu, K. D. Characterization of the Imprint Effect and the Influence of Imprinting Conditions on Affinity, Capacity, and Heterogeneity in Molecularly Imprinted Polymers Using the Freundlich Isotherm-Affinity Distribution Analysis. *Anal. Chem.* **2004**, 76 (4), 1123–1133.
- [39] Gorecki, T.; Khaled, A.; Pawliszyn, J. The Effect of Sample Volume on Quantitative Analysis by Solid Phase Microextraction - Part 2. Experimental Verification. *Analyst*

1998, 123 (12), 2819–2824.

- [40] Umpleby, R. J.; Baxter, S. C.; Bode, M.; Berch, J. K.; Shah, R. N.; Shimizu, K. D. Application of the Freundlich Adsorption Isotherm in the Characterization of Molecularly Imprinted Polymers. *Anal. Chim. Acta* **2001**, 435 (1), 35–42.
- [41] Umpleby, R. J.; Baxter, S. C.; Rampey, A. M.; Rushton, G. T.; Chen, Y.; Shimizu, K. D. Characterization of the Heterogeneous Binding Site Affinity Distributions in Molecularly Imprinted Polymers. *J. Chromatogr. B Anal. Technol. Biomed. Life Sci.* **2004**, 804 (1), 141–149.

Chapter 3: Selective determination of semi-volatile thiophene compounds in water by molecularly imprinted polymer thin-film headspace gas chromatography sulfur chemiluminescence detector (MIP HS-GC-SCD)

3.1. Abstract

A novel method was developed by the coupling of MIP thin-film with HS-GC-SCD for selective determination of trace concentrations of thiophene compounds in water. Thiophene compounds are persistent organic pollutants of concern due to their mutagenicity, carcinogenicity, and acute toxicity in humans and the environment, and thus identifying and detecting them in water is a priority. The MIP thin-film was prepared on a glass substrate using a simple in-situ photo-polymerization method. Conditions for headspace (HS) analysis such as HS oven temperature and equilibration time were optimized. The highest peak area responses for thiophene compounds analysis were achieved at 260 °C headspace temperature with 10 min equilibration time. Acceptable reproducibility was obtained for selective analysis of thiophene compounds from the spiked seawater samples at RSDs \leq 7.0% (n = 3). Calibration curves of spiked seawater were linear over a range of 5-100 $\mu\text{g L}^{-1}$ and limit of detection (LOD) values were in the range of 0.193-0.513 $\mu\text{g L}^{-1}$. Low matrix effect was observed in the analysis of thiophene compounds in seawater samples.

3.2. Introduction

Thiophene compounds are PASHs present in oil and petroleum products in various concentrations depending on the source [1]. These compounds are usually classified with polycyclic aromatic hydrocarbons (PAHs) [2–4]. Removal of these compounds from petroleum is very difficult due to the resistivity of sulfur atom in thiophene compounds to alkylation or oxidation [5]. Thiophene compounds like dibenzothiophene and its alkylated derivatives are known for their persistence (e.g. mutagenicity, carcinogenicity, and acute toxicity) in marine environments [6–9]. They can be used as an organic marker for oil pollution [10,11], which can come in contact with marine water through oil spills or industrial activities. Few analysis methods are reported for thiophene compounds in the literature and most of these methods are for thiophene compounds analyzed with PAHs [12–14]. Those methods usually involve the use of non-selective solid-phase extraction (SPE) for pre-concentrations and usually require significant volumes of organic solvents. However, matrix complexity, low analyte concentrations and low selectivity of conventional SPE methods can limit the efficiency of separation and detection of targeted analytes. To overcome these problems, selective sorbent materials such as MIPs can be used for their analysis.

MIPs are synthetic polymers that contain artificial recognition sites formed by polymerization in the presence of a template molecule. MIPs provide a simple molecular recognition mechanism, high mechanical and thermal stability, and can be prepared easily at low cost. Common methods used to prepare MIPs include: bulk, suspension, precipitation and in-situ polymerizations. In this research, MIP thin-films were prepared on

glass substrates by in-situ polymerization. 2-Thiophenecarboxaldehyde was used as a pseudo-template in imprinting to solve the problem of positive bias associated with template-bleeding [15–17], which can be problematic when working at low analyte concentrations ($\mu\text{g L}^{-1}$). These thin-films were used as selective adsorbents for thiophene compounds in water and then coupled with HS-GC-SCD. The use of SCD enhances the selectivity of the method due to its unique sensitivity to sulfur compounds.

Preparation of MIPs as thin-films on a small glass slides makes their coupling and with by HS technique more applicable. The MIP slide is used to extract the analytes from water sample first, then the slide can be removed, dried, and inserted into the HS vial then analyzed. Headspace analysis is a powerful technique used to analyze trace levels of volatile and semi-volatile compounds in liquid or solid samples. When headspace is coupled with GC, only volatile compounds in the gas phase will be injected into the column; non-volatile components which could contaminate GC column are excluded. Moreover, this method is considered fast because the extraction step of analytes from MIP film using solvent after the uploading process in the conventional GC-MS method (see Chapter 2) is not necessary. This avoids much of the tedious sample handling and potential for sample losses associated with extraction and preconcentration prior to the GC analysis.

In our work, MIP thin-films were prepared on glass slides then used as a selective adsorbent for thiophene compounds in water. After the extraction accomplished, the MIP slides were transferred to HS vials. The vials were then sealed and subjected to the HS-GC-SCD analysis; partition of semi-volatile thiophene compounds between sample phase (thin-film) and gas phase (headspace) occurred. The HS parameters were optimized to maximize

the rate and extent of analyte desorption from the MIP into the HS; this was assessed by peak area responses. A small amount of pure acetonitrile was added to each HS vial prior to analysis to enhance the desorption process of thiophene compounds from thin-film to the gas phase (headspace) and to solve a reproducibility issue that hampered initial efforts.

3.3. Materials and methods

3.3.1. Materials

Benzothiophene ($\geq 95\%$), 3-methylbenzothiophene (96%), dibenzothiophene ($\geq 99\%$), 4-methyldibenzothiophene (96%), 4,6-dimethyldibenzothiophene (97%), 2-thiophenecarboxaldehyde (98%), 1-vinyl-imidazol ($\geq 99\%$), bisphenol A dimethacrylate ($>98\%$), 2,2-dimethoxy-2-phenylacetophenone (99%), polyethylene glycol (average MW 20,000), 3-(trimethoxysilyl)propyl methacrylate (98%) were all purchased from Sigma Aldrich, Canada. Methanol, acetonitrile, toluene and hydrochloric acid (37% w/w) were ACS reagent grade and purchased from ACP chemicals. Glass slides ($25 \times 75 \text{ mm}^2$) and quartz cover glasses ($18 \times 18 \text{ mm}^2$) were purchased from Fisher Scientific, Canada. Deionized water ($18 \text{ M}\Omega\cdot\text{cm}$) was produced by Barnstead Nanopure Diamond ($18 \text{ M}\Omega$) water purification system (Barnstead Nanopure Water Systems, Lake Balboa, CA, USA). 20-mL Agilent glass headspace vials, polytetrafluoroethylene (PTFE) lined septa with aluminium caps and ergonomic manual crimper were all purchased from Agilent Technologies, Canada.

3.3.2. Pre-treatment and derivatization of glass slides

The glass slides were cleaned first and then functionalized before coating with MIP films. The cut pieces of glass slides (25 x 22 mm²) were soaked in a solution of methanol/hydrochloric acid (1:1) for 30 min, and then rinsed with DI water, and dried at room temperature. The cleaned slides were placed in a silanization solution of 2% (v/v) of 3-(trimethoxysilyl) propyl methacrylate in toluene and left overnight. The derivatized slides were washed with methanol then dried under nitrogen. The prepared slides were stored in a dark place; these could be used for several weeks without reduction in performance.

3.3.3. Preparation of MIP thin-film on a glass slide

Preparation of the MIP thin-films was carried out via photo-radical polymerization of a thin layer of liquid pre-polymerization solution (“sandwiching” technique) between the derivatized glass slide (25 x 22 mm²) and the quartz cover glass slide (18 x 18 mm²) (Figure 2.1 in Chapter 2). The polymer components, 25.6 μL (0.27 mmol) of 2-thiophenecarboxaldehyde, 99.4 μL (1.10 mmol) of 1-vinylimidazole, 800 mg (2.20 mmol), of bisphenol A dimethacrylate, 12.1 mg (0.05 mmol) of 2,2-dimethoxy-2-phenylacetophenone, 300 mg (25% w/w) of polyethylene glycol and 930 μL of acetonitrile were all pipetted or weighed into a 4-mL glass vial. The vial was vortexed until a clear solution was obtained, then the mixture was degassed in a sonicator for 5 min to remove dissolved air.

An 8- μ L portion of this pre-polymerization complex was pipetted onto the surface of a derivatized glass slide and covered immediately by a quartz cover slide. The pipetted amount was left to spread evenly on the surface of the slide for a few seconds, then the glass slide was exposed to a UV-light ($\lambda=254$ nm, 6W) for 45 min. The cover slide was removed immediately after irradiation using a sharp blade. The glass slide with the coated MIP film was placed in a petri dish containing methanol and washed for 3 h to extract the template and unreacted components. This washing step was repeated for another 1 h with fresh methanol solvent.

The MIP slide was rinsed with methanol and DI water, and then dried at room temperature. The MIP slides can be stored and used for several weeks without observation of any changes in their analytical performance.

3.3.4. Instrumentations and conditions

Analysis and optimization experiments were performed using an Agilent 7697A headspace (HS) sampler with Agilent 7890A GC coupled to Agilent 355 SCD. The HS sampler was connected to the GC injector via the transfer line heated at 270 °C. 20-mL HS sample vials were used for analysis. Each vial with its content was moved to HS oven by auto-sampler, heated to 250 °C and then pressurized with N₂ gas to 15 psi by filling flow at 50 mL min⁻¹, and held for a 10-min equilibration time then injected into the GC inlet for 0.5 min injection time. A DB-sulfur SCD column (40 m x 0.32 mm, 0.75 μ m) was used for

separation. Nitrogen (purity >99.999%) is used as the carrier gas and vial pressurization gas. The flow rate of the carrier gas was 2 mL min⁻¹.

The initial GC oven temperature was held at 50 °C for 1 min, increased to 100 °C at 25 °C min⁻¹, and then increased to 170 °C at 15 °C min⁻¹, and finally increased to 260 °C at 15 °C min⁻¹ and held at this temperature for 2 min. The total run time of the GC analysis was 25 min. The injector temperature was set at 275 °C and the injection was performed at split ratio 1:1. The GC cycle was 40 min and the vial was shaken while in the oven at 71 shakes per min. The SCD Dual Plasma controller temperature was held at 800 °C. The flame reagent gases were air, 65 sccm; hydrogen, 45 sccm; and ozone, generated from ozone generator at 350 Torr. Analytes were identified by comparing their retention times with their corresponding pure reference compounds.

3.3.5. Analysis of water and seawater samples by MIP HS-GC-SCD

Seawater samples were collected from St. John's Harbour (NL) in 4-L pre-cleaned amber glass bottles. No preservation method was used in the sampling process. The bottles were filled to the top to eliminate headspace, stoppered with screw caps and sealed with parafilm then labeled and stored in a cold place (~4 °C) until use.

All water and seawater samples were analyzed using MIP slides without pre-treatment. Each MIP slide was placed in a beaker containing a known volume (mL) of spiked sample at a known concentration (µg L⁻¹) of thiophene compounds with stirring (500 rpm) for a specific period. Later, this slide was removed from the beaker and rinsed with

DI water for 1s and then dried at room temperature for 5 min. After drying the slide was cut with a diamond pen to two halves and inserted into a 20-mL HS vial, then 5 μ L of pure acetonitrile was pipetted inside. The slides cutting step can be avoided by fabricating the MIP slides in suitable dimensions which can be fit easily into the HS vial. The polytetrafluoroethylene (PTFE) lined septa with an aluminium cap was used to seal the vial and then the vial was placed on the HS auto-sampler tray for analysis. The peak area obtained from GC for each thiophene compound was directly proportional to its concentration in the water sample prior to analysis. The limit of detection (LOD) for each analyte was calculated as the concentration which is equal to 3 standard deviations of the lowest detectable concentration over the slope of the calibration curve. All MIP thin-films analyses were conducted in triplicate.

3.4. Results and discussion

3.4.1. Preparation of the MIP thin-films

Optimization and characterization of MIP thin-films were carried out in Chapter 2. In the preparation, 2-thiophenecarboxaldehyde was used as a pseudo-template instead of target analyte templates (Figure 3.1) to avoid the problem of template bleeding, which can significantly elevate the background analyte signal and restricts the application of MIP for trace analysis [15–17].

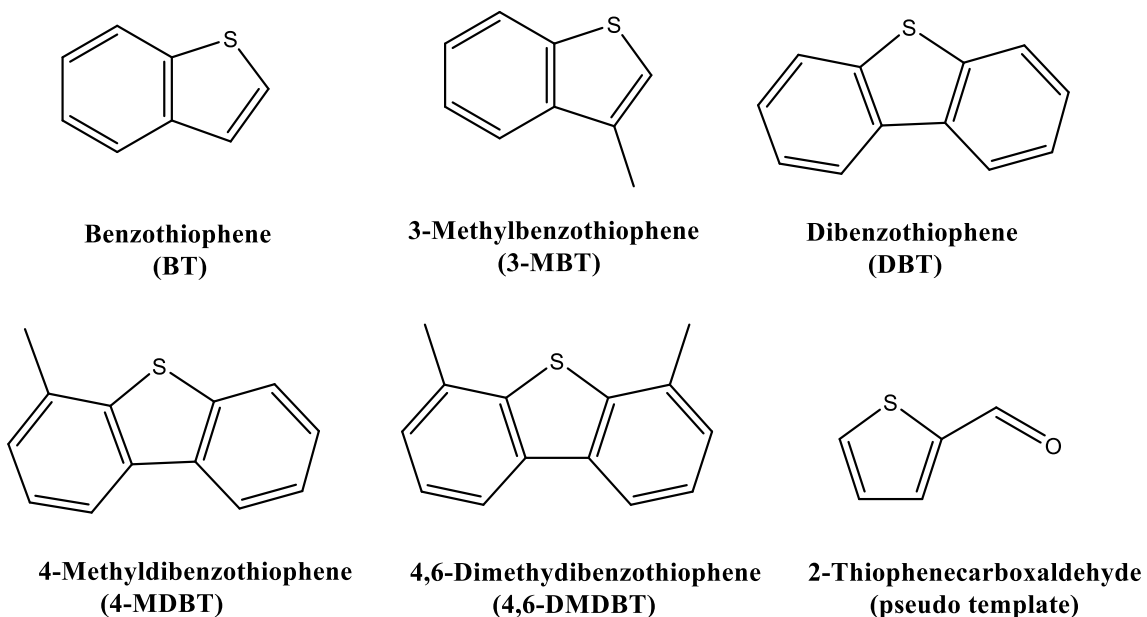


Figure 3.1. Chemical structure of targeted thiophene compounds and pseudo-template.

The peak obtained from the pseudo-template bleeding during the HS analysis can be seen in the chromatogram obtained from the analysis of seawater sample by MIP HS-GC-SCD (Figure 3.2). It is fortunate that this peak does not interfere the analysis of thiophene compounds. The thin-film itself does not contain any sulfur atoms in its structure except the unwashed trace amount of pseudo-template, so decomposition of film at a higher HS oven temperature did not produce any peaks which overlap with the peaks of thiophene compounds.

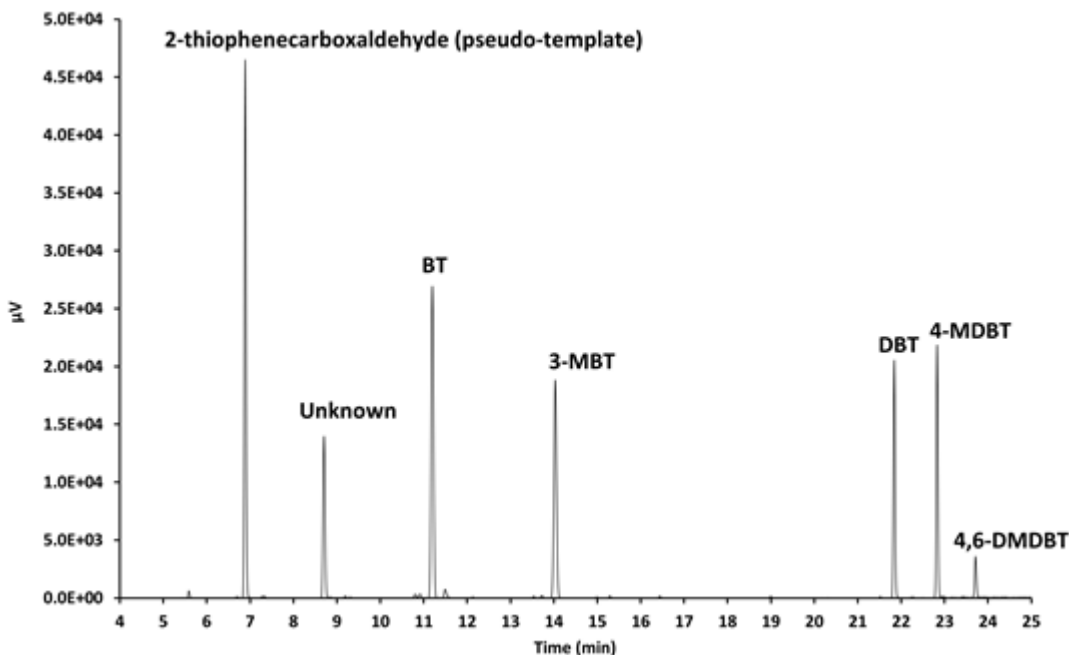


Figure 3.2. MIP thin-film HS-GC-SCD chromatogram of 50 mL seawater sample of thiophene compounds spiked at $50 \mu\text{g L}^{-1}$.

3.4.2. Optimization of HS oven temperature

The effect of the HS oven temperature on the peak area responses of the desorbed thiophene compounds in the MIP HS-GC-SCD analysis was studied over the range from 220°C to 280°C at 10 min equilibration time (Figure 3.3). HS oven temperature is an important parameter because it will affect the partition between the MIP thin-film and the gas phase (headspace) inside the vial. In this experiment, each thin-film was placed in a 100 mL of a standard aqueous solution spiked with a mixture of thiophene compounds at a concentration of $100 \mu\text{g L}^{-1}$. Each slide was left to upload for 2 h, and then removed, dried and analyzed by the HS-GC-SCD.

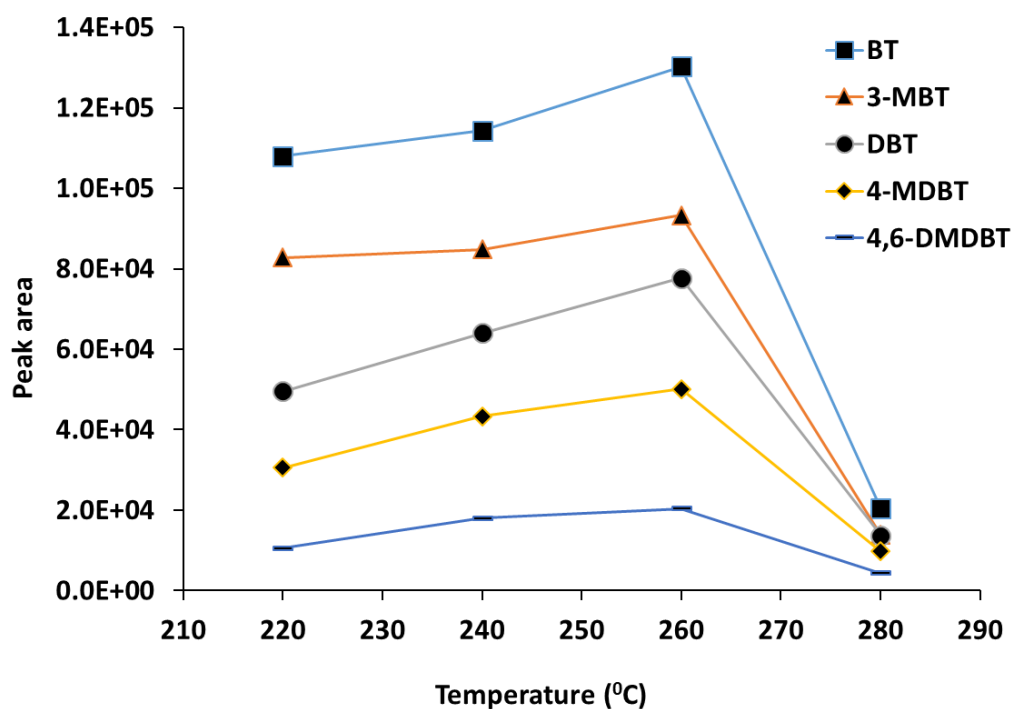


Figure 3.3. Effect of the HS temperature on the analysis of thiophenes-MIP thin-film.

As seen in Figure 3.3, the peak area responses of all thiophene compounds were increased from 220 °C to 260 °C, and then dropped abruptly at 280 °C. This may be due to the oxidation and decomposition of analytes at an elevated temperatures inside the vial or in the transfer line [18]. Decomposition of the film is also more likely to occur at higher HS temperatures [19] and the volatile products produced from this decomposition could be introduced into the GC column leading to a more complicated chromatogram with many unresolved peaks. This could make the detection of thiophene compounds a difficult task. In our work, this is not an issue since the SCD is selective to sulfur compounds and the MIP itself does not contain any sulfur compounds which can produce peaks in the chromatogram during HS analysis. Although the highest responses for thiophene

compounds were observed at a temperature of 260 °C, the temperature of 250 °C was selected as the optimum HS oven temperature in all experiments to avoid the risk of decomposition that may occur at this temperature at 260 °C.

3.4.3. Optimization of HS equilibration time

The effect of HS equilibration time on the peak area responses was investigated for different equilibration times at HS oven temperature of 250 °C (Figure 3.4). Equilibration time is critical when volatile molecules must undergo transfer between the solid-phase and headspace phase. The equilibration times of solid samples is usually longer than liquid samples [18] due to the slower diffusion of volatile components in the case of solid samples especially when the mass of solid samples is high and the porosity is low. In the case of our MIP thin-film, which analyzed as a solid sample, the mass is very low (~ 4 mg) and the material is porous, therefore the equilibration time is expected to be less.

In Figure 3.4, it can be observed that at 10 min equilibration time, the maximum responses for all thiophene compounds were achieved. The decrease in the peak area responses of all thiophene compounds after 10 min may be attributed to the thermal decomposition of thiophene compounds at longer equilibration times. Thus, the equilibration time for 10 min was used as the optimal value in all HS analyses.

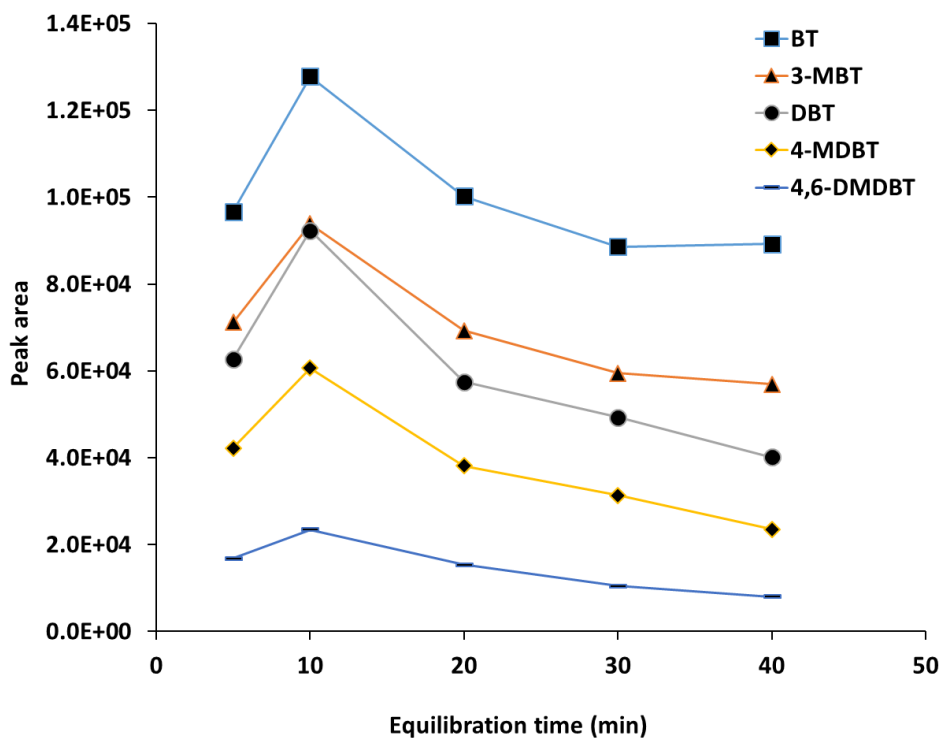


Figure 3.4. Effect of the HS equilibration time on the analysis of thiophenes-MIP thin-film.

3.4.4. Analysis of thiophene compounds in seawater

Detection and quantitation of semi-volatile thiophene compounds BT, 3-MBT, DBT, 4-MBDBT and 4,6-DMDBT in water by MIP HS-GC-SCD was evaluated. Seawater samples (100 mL each) were spiked with a mixture of thiophene compounds at concentration ranges of 5-100 $\mu\text{g L}^{-1}$ and then analyzed by MIP thin-films HS-GC-SCD without any pre-treatment. Five calibration curves were obtained for thiophene compounds (Figure 3.5). At the beginning of our work, the desorption of the analytes from the solid MIP coating showed variation in the peak area responses of the analytes resulting in a loss of the peak area precision. To solve this issue, 5 μL of acetonitrile was pipetted into the HS vial after the MIP slide was placed to aid in the desorption process of thiophene compounds

from thin-film, and thus improve the reproducibility of the results during the analysis. The use of internal standard in the analysis was not necessary since the method showed reproducible results.

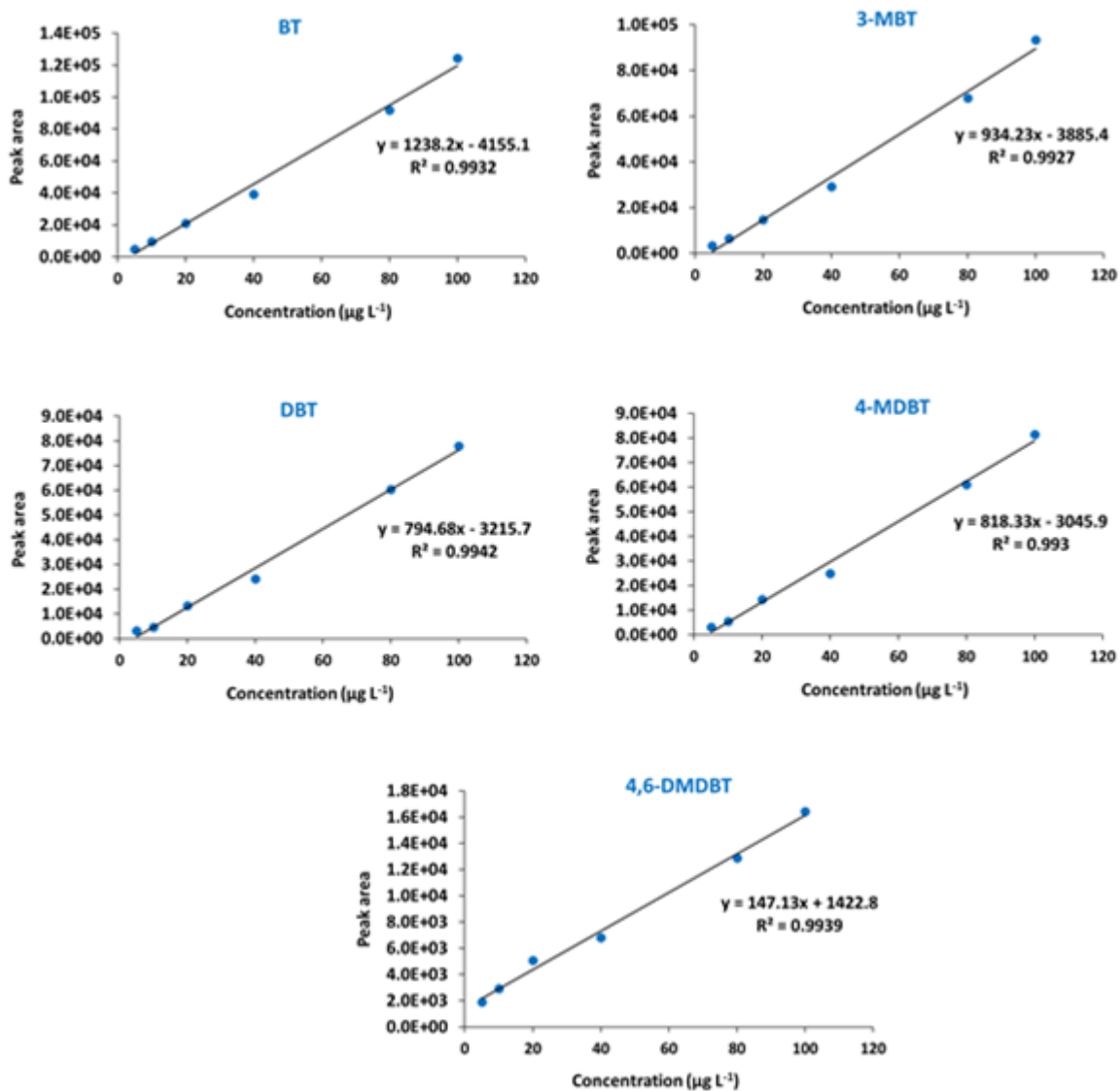


Figure 3.5. Calibration curves of the analysis of thiophene compounds by MIP HS-GC-SCD in seawater samples at a range of 5-100 $\mu\text{g L}^{-1}$. (RSDs \leq 7.0%, n = 3).

Very good linearity (R^2) was obtained for each thiophene compounds in seawater (Figure 3.5). The LOD values in seawater sample were 0.301, 0.206, 0.193, 0.416 and 0.513 $\mu\text{g L}^{-1}$ for BT, 3-MBT, DBT, 4-MDBT and 4,6-DMDBT respectively. This method showed a good reproducibility with low relative standard deviations ($\text{RSD}_s \leq 7.0\%$).

To investigate the matrix effect on the adsorption of thiophene compounds in seawater, a comparison between the percent recovery values of thiophene compounds in DI water and seawater (SW) was made. The effect is expected due to the presence of different organic and inorganic species in seawater, which could interfere and reduce their binding into the MIP. The influence of inorganic ions (Ca^{2+} , Mg^{2+} , and Fe^{2+}) and organic matter such as humic acid (HA) on the MIP percent recovery for 16 PAHs in seawater samples was studied [20]. The results showed that, the presence of NaCl did not have a significant effect on the adsorption of PAHs, giving 98.1% recovery, while the higher effect was observed from the presence of inorganic ions and HA, giving 93.2% recovery. In our study, various volumes (10, 50, 200, 400 and 800 mL) of DI water and seawater were spiked with a mixture thiophene compounds at the same concentration of 50 $\mu\text{g L}^{-1}$. After the samples were left to upload for 2 h, the MIP slides were analyzed by HS-GC-SCD. The sample volume was varied to see if the effect of matrix will change with the volume change.

As can be seen in Table 3.1, the higher recovery values of spiked thiophene compounds in DI water and seawater were observed at low sample volumes. These values of recovery decrease as the volumes of sample increase.

Table 3.1. Percent recovery values of thiophene compounds at various sample volumes obtained from the MIP film HS-GC-SCD analysis of spiked DI water and seawater samples at the same concentration ($50 \mu\text{g L}^{-1}$).

Sample volume (mL)	Analyte									
	BT		3-MBT		DBT		4-MDBT		4,6-DMDBT	
	DI	SW	DI	SW	DI	SW	DI	SW	DI	SW
10	40.2	38.8	33.6	29.9	50.5	49.1	42.2	41.5	22.9	21.5
50	26.2	24.4	20.6	18.0	29.5	28.9	20.6	19.9	12.2	9.6
100	12.2	11.8	10.9	9.7	12.1	11.9	10.0	9.4	5.8	4.6
200	6.8	6.6	5.9	5.1	6.1	5.7	4.8	4.2	3.1	2.3
400	7.2	6.9	6.3	5.6	7.4	6.8	5.3	5.0	3.3	2.4
800	4.7	4.4	4.0	3.7	4.6	4.1	3.7	3.2	2.5	1.7

The results indicated that the effect of matrices on the adsorption of thiophene compounds by MIP was not remarkable even at higher sample volumes, except in the case of 4,6-DMDBT, where the effect was more pronounced. The observed effect for 4,6-DMDBT could be explained based on the nature of the interactions between this analyte and the MIP in water. The 4,6-DMDBT has two methyl substituent on the benzene rings; these donating groups may weaken the π - π interactions [21] with the MIP, making the hydrophobic interaction more dominant. Thus, the matrices present in seawater could compete and disrupt the hydrophobic interaction, causing decrease in the percent recovery of the 4,6-DMDBT, as seen from the results in Table 3.1.

3.5. Conclusions

A new method for coupling of the MIP film with the HS-GC-SCD for selective determination of thiophene compounds in water samples was successfully achieved. No pre-treatment or pre-concentration steps other than using MIPs were necessary during the analysis. The advantages of the developed method include simplicity, rapid analysis and low limits of detection. Additional selectivity was achieved from using the SCD in the detection. The peak signal observed in the GC chromatogram, which was due to the bleeding of the pseudo-template from thiophenes-MIP, does not overlap with the detection of other analytes. The matrix effects on the adsorption of thiophene compounds by the MIP film in the seawater sample compared to the DI water are not significant at various sample volumes with more observable effect for 4,6-DMDBT. The results revealed that the developed method can be used for selective determination of thiophene compounds in environmental water sample at small and large sample volumes.

3.6. References

- [1] Speight, J. G. *The Chemistry and Technology of Petroleum*; CRC Press, Taylor and Francis, **2014**.
- [2] Sauer, T.; Boehm, P. The Use of Defensible Analytical Chemical Measurements for Oil Spill Natural Resource Damage Assessment. *Int. Oil Spill Conf. Proc.* **1991**, *1991* (1), 363–369.
- [3] Grung, M.; Holth, T. F.; Jacobsen, M. R.; Hylland, K. Polycyclic Aromatic Hydrocarbon (PAH) Metabolites in Atlantic Cod Exposed via Water or Diet to a Synthetic Produced Water. *J. Toxicol. Environ. Heal. Part A* **2009**, *72* (3–4), 254–265.
- [4] Chowdhury, K. H.; Husain, T.; Veitch, B.; Hawboldt, K. Probabilistic Risk Assessment of Polycyclic Aromatic Hydrocarbons (PAHs) in Produced Water. *Hum. Ecol. Risk Assess.* **2009**, *15* (5), 1049–1063.
- [5] Beens, J.; Tijssen, R. The Characterization and Quantitation of Sulfur-Containing Compounds in (Heavy) Middle Distillates by LC-GC-FID-SCD. *Hrc-Journal High Resolut. Chromatogr.* **1997**, *20* (3), 131–137.
- [6] Gui-peng, Y. Photochemical Oxidation of Benzothiophene in Seawater. *Chinese J. Oceanol. Limnol.* **2000**, *18* (1), 85–91.
- [7] Kropp, K. G.; Fedorak, P. M. A Review of the Occurrence, Toxicity, and Biodegradation of Condensed Thiophenes Found in Petroleum. *Can. J. Microbiol.* **1998**, *44* (7), 605–622.
- [8] Berthou, F.; Vignier, V. Analysis and Fate of Dibenzothiophene Derivatives in the

- Marine Environment. *Int. J. Environ. Anal. Chem.* **1986**, *27* (1–2), 81–96.
- [9] Croisy, A.; Mispelter, J.; Lhoste, J.-M.; Zajdela, F.; Jacquignon, P. Thiophene Analogues of Carcinogenic Polycyclic Hydrocarbons. Elbs Pyrolysis of Various Aroylmethylbenzothiophenes. *J. Heterocycl. Chem.* **1984**, *21* (2), 353–359.
- [10] Andersson, J. T. Polycyclic Aromatic Sulfur Heterocycles III. Photochemical Stability of the Potential Oil Pollution Markers Phenanthrenes and Dibenzothiophenes. *Chemosphere* **1993**, *27* (11), 2097–2102.
- [11] Andersson, J. T.; Hegazi, A. H.; Roberz, B. Polycyclic Aromatic Sulfur Heterocycles as Information Carriers in Environmental Studies. *Analytical and Bioanalytical Chemistry*. October 4, **2006**, pp 891–905.
- [12] Avino, P.; Notardonato, I.; Cinelli, G.; Russo, M. Aromatic Sulfur Compounds Enrichment from Seawater in Crude Oil Contamination by Solid Phase Extraction. *Curr. Anal. Chem.* **2009**, *5* (4), 339–346.
- [13] Yu, C.; Yao, Z.; Hu, B. Preparation of Polydimethylsiloxane/ β -Cyclodextrin/divinylbenzene Coated “dumbbell-Shaped” stir Bar and Its Application to the Analysis of Polycyclic Aromatic Hydrocarbons and Polycyclic Aromatic Sulfur Heterocycles Compounds in Lake Water and Soil by Hig. *Anal. Chim. Acta* **2009**, *641* (1–2), 75–82.
- [14] Gimeno, R. .; Altelaar, a. F. .; Marcé, R. .; Borrull, F. Determination of Polycyclic Aromatic Hydrocarbons and Polycyclic Aromatic Sulfur Heterocycles by High-Performance Liquid Chromatography with Fluorescence and Atmospheric Pressure Chemical Ionization Mass Spectrometry Detection in Seawater and Sediment Samp. *J. Chromatogr. A* **2002**, *958* (1), 141–148.

- [15] Andersson, L. I.; Paprica, A.; Arvidsson, T. A Highly Selective Solid Phase Extraction Sorbent for Pre- Concentration of Sameridine Made by Molecular Imprinting. *Chromatographia* **1997**, *46* (1), 57–62.
- [16] Matsui, J.; Fujiwara, K.; Takeuchi, T. Atrazine-Selective Polymers Prepared by Molecular Imprinting of Trialkylmelamines as Dummy Template Species of Atrazine.
- [17] Liu, X.; Liu, J.; Huang, Y.; Zhao, R.; Liu, G.; Chen, Y. Determination of Methotrexate in Human Serum by High-Performance Liquid Chromatography Combined with Pseudo Template Molecularly Imprinted Polymer. *J. Chromatogr. A* **2009**, *1216*, 7533–7538.
- [18] Kolb, B.; Ettre, L. S. *Static Headspace-Gas Chromatography : Theory and Practice*; Wiley, **2006**.
- [19] Beyler, C. L.; Hirschler, M. M. *SFPE Handbook of Fire Protection Engineering. CHAPTER 7. Thermal Decomposition of Polymers.*, 4. ed.; National Fire Protection Association: Quincy Mass., **1995**.
- [20] Song, X.; Li, J.; Xu, S.; Ying, R.; Ma, J.; Liao, C.; Liu, D.; Yu, J.; Chen, L. Determination of 16 Polycyclic Aromatic Hydrocarbons in Seawater Using Molecularly Imprinted Solid-Phase Extraction Coupled with Gas Chromatography-Mass Spectrometry. *Talanta* **2012**, *99*, 75–82.
- [21] Wheeler, S. E. Understanding Substituent Effects in Noncovalent Interactions Involving Aromatic Rings. *Acc. Chem. Res.* **2013**, *46* (4), 1029–1038.

Chapter 4: Indirect analysis of thiophene compounds in water: oxidation to sulfones followed by molecularly imprinted polymer thin-film desorption electrospray ionization mass spectrometry (MIP DESI-MS)

4.1. Abstract

A new method was developed by coupling MIP thin-film with DESI for indirect analysis of thiophene compounds in water. MIP thin-films were prepared on non-porous glass slides using a simple drop-casting method. The resulting films were used for indirect quantitative analysis of thiophene compounds in water by sorbing their oxidation products (sulfones) then interrogating the bound sulfones with DESI-MS. Thiophene compounds as a class of water-born pollutants were selected for their mutagenic, carcinogenetic and acute toxicity. Oxidation of thiophene compounds to sulfones in water was achieved by reaction with H₂O₂/formic acid mixture. Optimization of DESI source parameters such as capillary voltage, spray angle and ions collection angle, tip to surface distance, tip to inlet distance, surface to inlet distance and the MS inlet temperature were optimized. The optimal spray solvent composition was found to be MeOH/H₂O (95:5 v/v) containing 5 x 10⁻⁴ mol L⁻¹ NaCl. Among all sulfones, the protonated ion and sodium adduct signals were observed only for dibenzothiophene sulfone (DBTO₂) with remarkable intensities in the positive ion mode. The signal intensity of the [DBTO₂ + Na]⁺ adduct was used to construct a calibration curve for the determination of dibenzothiophene concentrations in seawater samples. The DESI-MS response was linear ($R^2 = 0.9756$) over the range 0.1-100 µg L⁻¹. The limit of detection for this method was 3 ng L⁻¹ and relative standard deviations (RSD_s ≤ 8.0%). These results showed that the developed method is ideal for indirect qualitative and quantitative analysis of dibenzothiophene compound in water samples.

4.2. Introduction

Rapid analysis methods for aqueous organic pollutants are of value for assessment of ubiquitous and often problematic contamination of aquatic environments. Thiophene compounds (Table 1.1, Chapter 1) are the major polycyclic aromatic sulfur heterocycles compounds found in petroleum [1]. These compounds enter the marine environment through oil spills and other industrial activities. Since thiophene compounds have an analogous structure to polycyclic aromatic hydrocarbons (PAHs), they could have the same characteristics of mutagenicity, carcinogenicity and acute toxicity [2]. Most methods of analysis used to detect thiophene compounds in water are based on solid-phase extraction (SPE) coupled to gas or liquid chromatography [3,4]. However, SPE methods mainly involve using non-selective C4 or C18 stationary phases, consequently other species in the sample may be preconcentrated with analytes giving chromatograms with poorly defined and unresolved peaks, which make the identification and detection of targeted analytes more complicated. A selective material such as a molecularly imprinted polymer (MIP) can be used to overcome these problems.

MIPs are synthetic polymers containing artificial recognition sites formed by the polymerization of a material in the presence of a template molecule [5,6]. MIPs are attractive due to the simplicity of the preparation and low cost. Development of MIPs require careful selection of its components, which usually include the monomers, cross-linker, and initiator. Optimizing the ratio of each component to the other with simultaneous attention to the solvent (porogen) is crucial, since getting an MIP with a good analytical performance is very important. The stability of MIPs over a range of temperatures and

pressures and relative inertness in acidic and basic solutions [7] make MIPs ideal for environmental water analysis. MIPs can be prepared in different forms including beads, films, and nanoparticles [8]. When MIP is prepared as thin-films on a non-porous substrate and coupled to the DESI-MS, it becomes a powerful technique for the analysis of many organic pollutants in water. For example, MIP thin-film was prepared and coupled with DESI-MS for the detection of 2,4-dichlorophenoxyacetic acid (2,4-D) and four analogs in water previously [9]. The DESI is an ambient ionization technique in which ionization is accomplished by directing an electrospray charged droplets beam onto the sample surface under ambient conditions [10]. The beam of charged ions forms a thin liquid layer on the surface, where extraction, dissolution and ionization of compounds occur; the continuous impact of the charged droplets leads to the emission of secondary charged droplets containing analytes, which are then drawn into the mass spectrometer through mass inlet (droplet pick-up mechanism). Lower limits of detection in sub-ng L⁻¹ range were successfully achieved [11,12]. RSD values below 5% and accuracies of ± 7% (relative error) have been also reported for DESI-MS [11]. The observed ions of the DESI spectra in the positive ion mode usually include protonated ions, [M + H]⁺, sodium adducts [M + Na]⁺, ammoniated adducts [M + NH₄]⁺ while in the negative ion mode, deprotonated ions [M - H]⁻, and chloride adducts [M + Cl]⁻ are observed. To compensate for the low detectability of thiophene compounds in the DESI analysis, thiophene compounds can be converted to more detectable compounds such as sulfones. This can be carried out through the oxidation reaction with hydrogen peroxide (H₂O₂) and formic acid. Oxidation of thiophene compounds to sulfoxides and sulfones by hydrogen peroxide and formic acid in a non-aqueous media such as petroleum products was reported by other researchers [13–

15]. The purpose of these researches was to reduce the percentage of sulfur-containing compounds in these products by converting them to ones that can be readily removed. Dehkordi et al. [13] observed that increasing the temperature has a positive effect on the percent conversion of thiophene compounds; they found that the oxidation reaction at 30 and 40 °C was not completed even after 3 h, while at 50 °C, the conversion was 100% in less than 90 min.

In our work, MIP thin-films were prepared on glass slides and used to extract sulfone compounds from water. These compounds are produced from the oxidation of thiophene compounds in water by H₂O₂ and formic acid at 65 °C. After completion of extraction, the slides were removed, dried, and then analyzed by DESI-MS in the positive ion mode.

4.3. Materials and methods

4.3.1. Materials

Benzothiophene (≥95%), 3-methylbenzothiophene (96%), dibenzothiophene (≥99%), 4,6-dimethyldibenzothiophene (97%), 2-thiophenecarboxaldehyde (98%), fluorene (98%), 1-vinylimidazol (≥99%), bisphenol A dimethacrylate (>98%), 2,2-dimethoxy-2-phenylacetophenone (99%), polyethylene glycol (average Mw 20,000), 3-(trimethoxysilyl) propyl methacrylate (98%), hydrogen peroxide (30% w/w), formic acid (≥98%), sodium hydroxide (≥97%), and sodium chloride (≥99%) were all purchased from Sigma Aldrich, Canada. Methanol (Optima grade), acetonitrile (Optima grade), and water

(Optima LC/MS grade) were all purchased from Thermo Fisher Scientific (Ottawa, ON, Canada). Methanol, acetonitrile, toluene and hydrochloric acid (37% w/w) were ACS reagent grades and purchased from ACP chemicals. Glass slides (25 × 75) mm², cover glasses (18 × 18 mm²) and 20-mL disposable scintillation vials were purchased from Fisher Scientific, Ottawa, ON, Canada. Deionized water (18 MΩ.cm) was produced by Barnstead Nanopure Diamond (18 MΩ) water purification system (Barnstead Nanopure Water Systems, Lake Balboa, CA, USA).

4.3.2. Pre-treatment and derivatization of glass slides

The pre-treatment and derivatization of glass slides (25 x 25 mm²) were carried out using the procedure in Chapter 2, Section 2.3.2. The prepared glass slides were stored in a dark place until use.

4.3.3. Preparation of MIP thin-films on a glass slides

Preparation of MIP thin-films was carried out via photo-radical polymerization by simple drop casting between a derivatized glass slide (25 x 25 mm²) and quartz cover glass slide (18 x 18 mm²) using the procedure in Chapter 3, Section 3.3.3.

4.3.4. Oxidation reaction of thiophene compounds in water

The experimental procedure for the oxidation of thiophene compounds to sulfones in water was developed by modifying published procedures [13–15]. Further optimization for the oxidation procedure of thiophene compounds in water was required since the previous oxidation work was performed in petroleum products and not in aqueous medium. Oxidation reactions in water were studied at two different temperatures (40 and 65 °C) for

various periods (0, 0.5, 1, 2 and 3 h). Two sets of 20-mL vials were used, each vial contains 10 mL of DI water spiked with a mixture thiophene compounds at a concentration of 400 $\mu\text{g L}^{-1}$. A 0.4-mL aliquot of H_2O_2 and 0.2 mL of formic acid were added to each vial. Each set was placed in a separate oil bath at a temperature of 40 °C and 65 °C with magnetic stirring. The final pH in each vial was 1.5. Two vials from each set were removed from the oil bath after a specific period, cooled in an ice bath, and then extracted with dichloromethane (3 x 3 mL); the organic phase was collected and preconcentrated under a stream of nitrogen to 1 mL. The extract was spiked with fluorene (internal standard) before final injection in the GC. A 1- μL portion of this solution was injected directly into the GC-MS for analysis at selected ion monitoring (SIM) mode. The percent conversion of each thiophene compounds in this work was calculated based on the disappearance of thiophene compounds during the oxidation reaction. All experiments are conducted in duplicate. Percent conversions of thiophene compounds were calculated using their initial concentrations in reaction at 0 min (C_0) and after t min reaction (C_t). The % conversion were expressed as,

$$\% \text{ Conversion} = \frac{(C_0 - C_t)}{C_0} \times 100 \quad (4.1)$$

4.3.5. GC-MS analysis

Analysis of thiophene compounds before and after the oxidation reactions was performed using an Agilent 6890 GC equipped with an Agilent 7683 auto-sampler and coupled to an Agilent 5973 mass selective detector (MSD). Instrument control and data

analysis were performed using Agilent ChemStation software version D.01.00 Build 75. A fused-silica capillary column (DB-5MS, 30 m x 0.25 mm i.d.) with 0.25 μm stationary film thickness was used with helium (purity 99.999%) as the carrier gas, flow rate of 1.2 mL min^{-1} . The initial oven temperature was held at 50 $^{\circ}\text{C}$ for 1 min, increased to 280 $^{\circ}\text{C}$ at 20 $^{\circ}\text{C min}^{-1}$, and held at this temperature for 1 min. The total analysis run time was 13.5 min. The injector temperature was set at 280 $^{\circ}\text{C}$, and the injection was performed in splitless mode. The mass spectra were recorded in SIM mode, using 70 eV in the electron impact ionization source.

4.3.6. DSEI-MS conditions

DESI-MS analyses were carried out in the positive mode using commercial DESI source (Omni SprayTM source, Prosolia Inc., Indianapolis, IN, USA) coupled to a triple quadrupole mass spectrometer (Waters XevoTM TQ-S, Milford, USA). The DESI source (see Figure 4.1) consists of a spray head mounted on an automated 2D stage. The spray solvent was introduced to the sample surface through a fused silica capillary tube (0.05 mm i.d., 0.15 mm o.d.) from a controlled syringe pump. The ions formed in the DESI source were transferred through the capillary inlet to the mass spectrometer. Parameters including capillary voltage, solvent flow rate, nitrogen gas pressure, spray angle, ions collection angle, tip to surface distance, tip to inlet distance, surface to inlet distance and the MS inlet temperature were all optimized. Different spray solvents systems were examined including methanol, methanol/water (95:5 v/v) and methanol/water (95:5 v/v) containing $5 \times 10^{-4} \text{ mol L}^{-1}$ sodium chloride. The optimization experiments for DESI-MS were performed using MIP

slides uploaded for 10 min in solutions obtained from the oxidation of 10 mL samples spiked with a mixture of thiophene compounds at a concentration of $10 \mu\text{g L}^{-1}$.

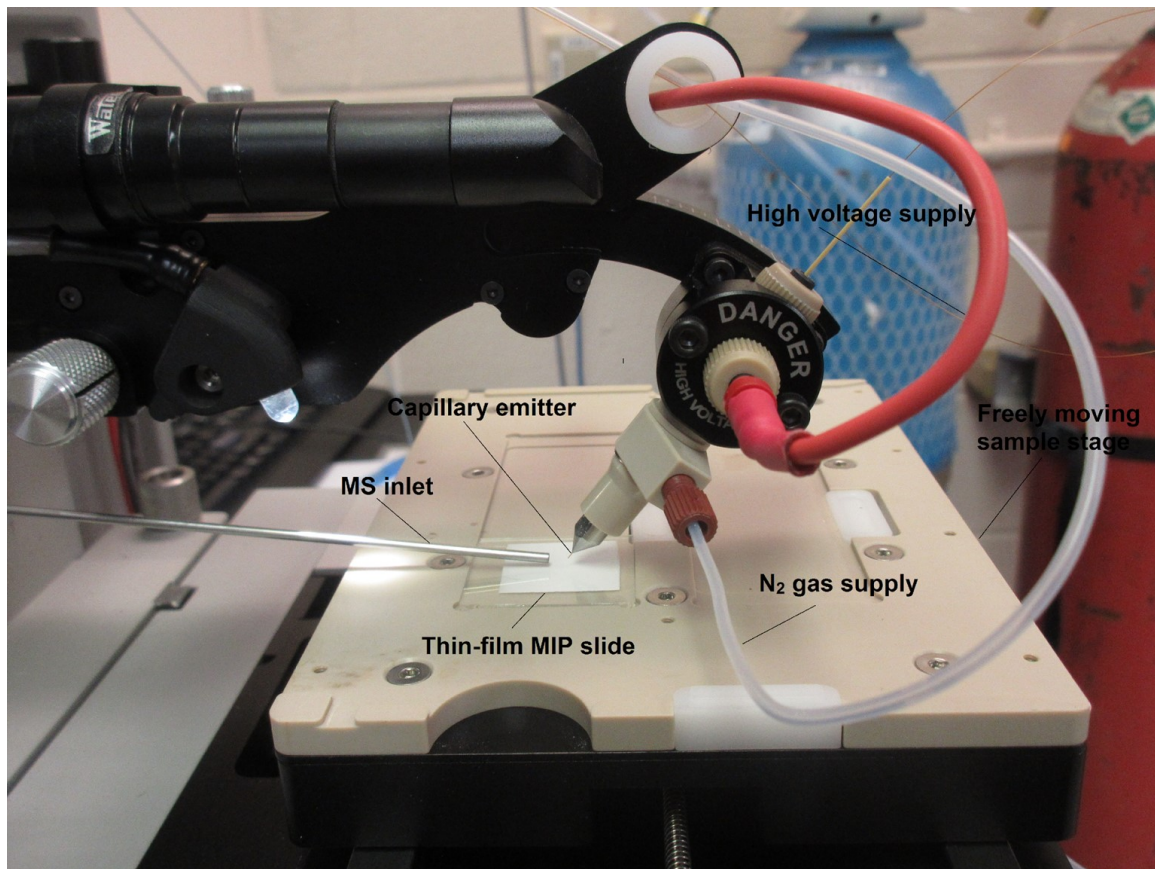


Figure 4.1. DESI source with MIP slide.

4.3.7. Analysis of water and seawater samples by MIP DESI-MS

Seawater samples were collected from St. John's Harbour (NL) in 4-L pre-cleaned amber glass bottles. No preservation method was used in the sampling process. The bottles were filled to the top to eliminate headspace, stoppered with screw caps and sealed with Parafilm then labeled and stored in a cold place until use.

Oxidation of thiophene compounds to sulfones (Figure 4.2) was carried out prior to analysis with MIP slides. 50 mL beakers containing 10 mL of seawater sample spiked with a mixture thiophene compounds at various concentrations 0.0, 0.1, 0.5, 1.0, 5.0 and 10.0 $\mu\text{g L}^{-1}$ with 0.4 mL of hydrogen peroxide and formic acid were placed in an oil bath with magnetic stirring at 65 °C. After 2 h, the beakers were removed and cooled to room temperature in an ice bath. The pH of each solution mixture was adjusted to 6.0 with a sodium hydroxide solution (40% w/v). MIP slide was placed in each beaker for uploading with stirring for 10 min. The slides were removed, rinsed with DI water and dried at room temperature. Finally, each slide was mounted on the sample stage of DESI source and analyzed, starting with slides exposed to the lowest concentrations. The MIP slides uploaded in non-spiked seawater samples which was treated with the same oxidation procedure were used as blank slides. DESI mass spectra were taken by scanning five different spots randomly on the surface of MIP thin-film and averaging the results for all spots. Typically, the area of each spot was approximately 1 mm² and the sampling time for each spot was 15 s. The lowest concentration of the analyte that gave a signal of intensity three times higher than of the blank was considered as the limit of detection (LOD). All analyses were conducted in triplicate.

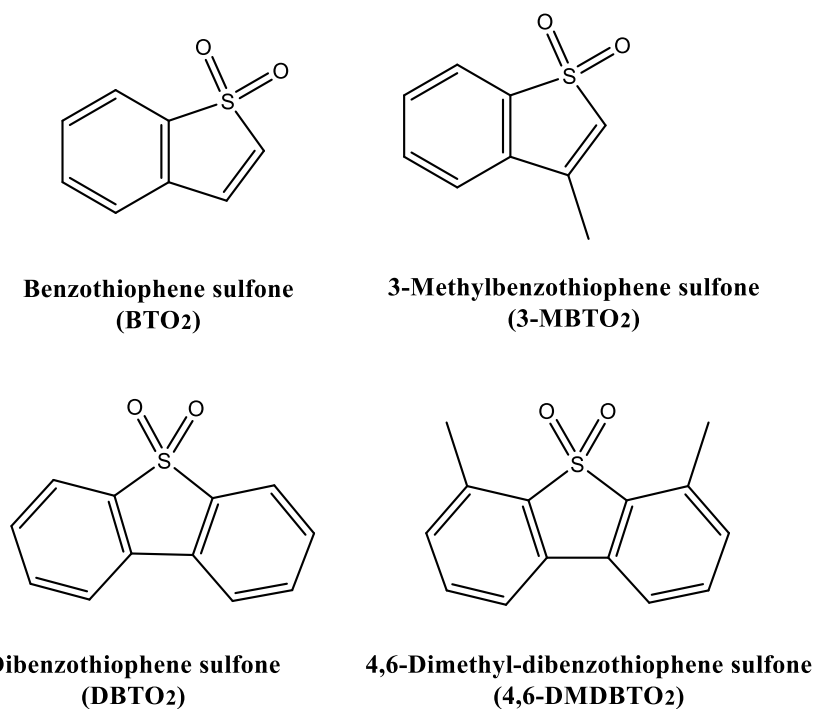


Figure 4.2. Chemical structures of sulfone compounds produced from oxidation reactions of targeted thiophene compounds in water.

4.4. Results and discussion

4.4.1. Preparation of MIP thin-films

Optimization and characterization of MIP thin-films were carried out in Chapter 2. In the preparation, a pseudo-template, 2-thiophenecarboxaldehyde is used instead of the target analyte to avoid the issue of template bleeding which significantly elevates the sample background and restricts the application of MIPs for analytical applications [16–18]. The pseudo-template used in the preparation of MIP also does not interfere with the signals of sulfones in DESI-MS analysis. Advantages, such as thickness, planarity of the surface and small dimension of the MIP films make them very suitable for DESI-MS

analysis. In addition, the porous structure of these films (see Chapter 2) exploits the extraction and desorption mechanism of DESI analysis. The low cost of preparation makes the reuse of MIP slides unnecessary, which may be viewed as a drawback of the fiber in solid-phase micro-extraction (SPME) where solvent-based washing steps are necessary after analysis to remove analyte carryover.

4.4.2. Oxidation of thiophene compounds in water

Direct analysis of thiophene compounds in this research by DESI-MS produce low or undetectable signals. This may be attributed to the low proton affinity and high ionization energy (Table 1.1) of these neutral compounds [19]. Indirect analysis is achieved by converting thiophene compounds to more detectable compounds in DESI. Acid catalyzed oxidation of targeted thiophene compounds by hydrogen peroxide in water is studied to determine the optimum oxidation reaction conditions. Maximum conversions are achieved by adding excess reagents to ensure that only sulfones will be formed alone and not in a mixture with sulfoxides. Quantitative oxidation of thiophene compounds is crucial for a good method of analysis. Figure 4.3 shows that the total thiophene compounds undergo oxidation to sulfones with approximately 99% conversion at 65 °C after 2 h, while the conversion at 40 °C was much slower.

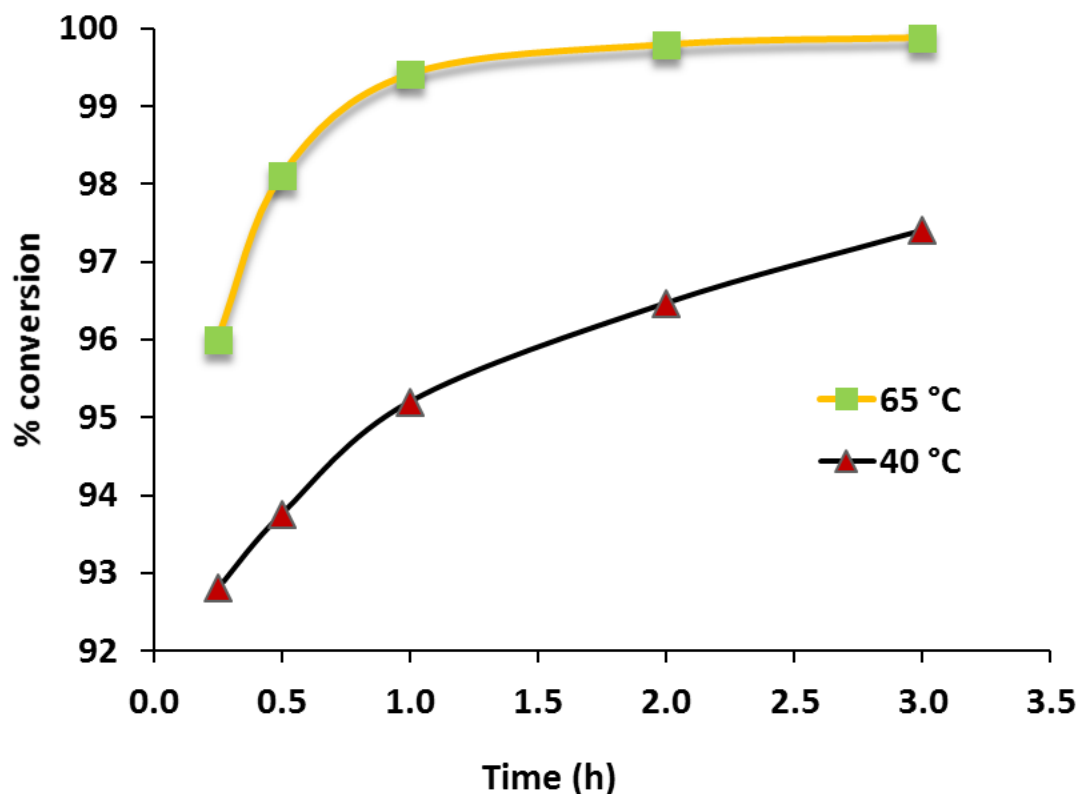


Figure 4.3. Graph of % conversion for the oxidation of total thiophene compounds as a function of time at 45°C and 65°C.

These results are supported by the SIM chromatograms of thiophene compounds before and after the oxidation by hydrogen peroxide and formic acid at 65 °C (Figure 4.4). The relative abundance of all thiophene compounds in Figure 4.4 decreased with increasing reaction time. The conversion of all thiophene compounds is achieved within 2 h; this time is used as the optimal time for the oxidation reactions in all experiments. Fluorene was used as an internal standard to track the conversion and to calculate the percent of conversions of thiophene compounds. The non-polar GC column which is used in this study was not suitable for analysis of sulfone compounds due to the high polarity of these

compounds. Although the percent recovery values of the sulfone compounds from the oxidation reactions were not determined, the calibration curve of $[\text{DBT-O}_2 + \text{Na}]^+$, which is obtained from the DESI-MS analysis, showed a linear increase in the signal intensities with the increasing of the concentrations in water as will be seen later.

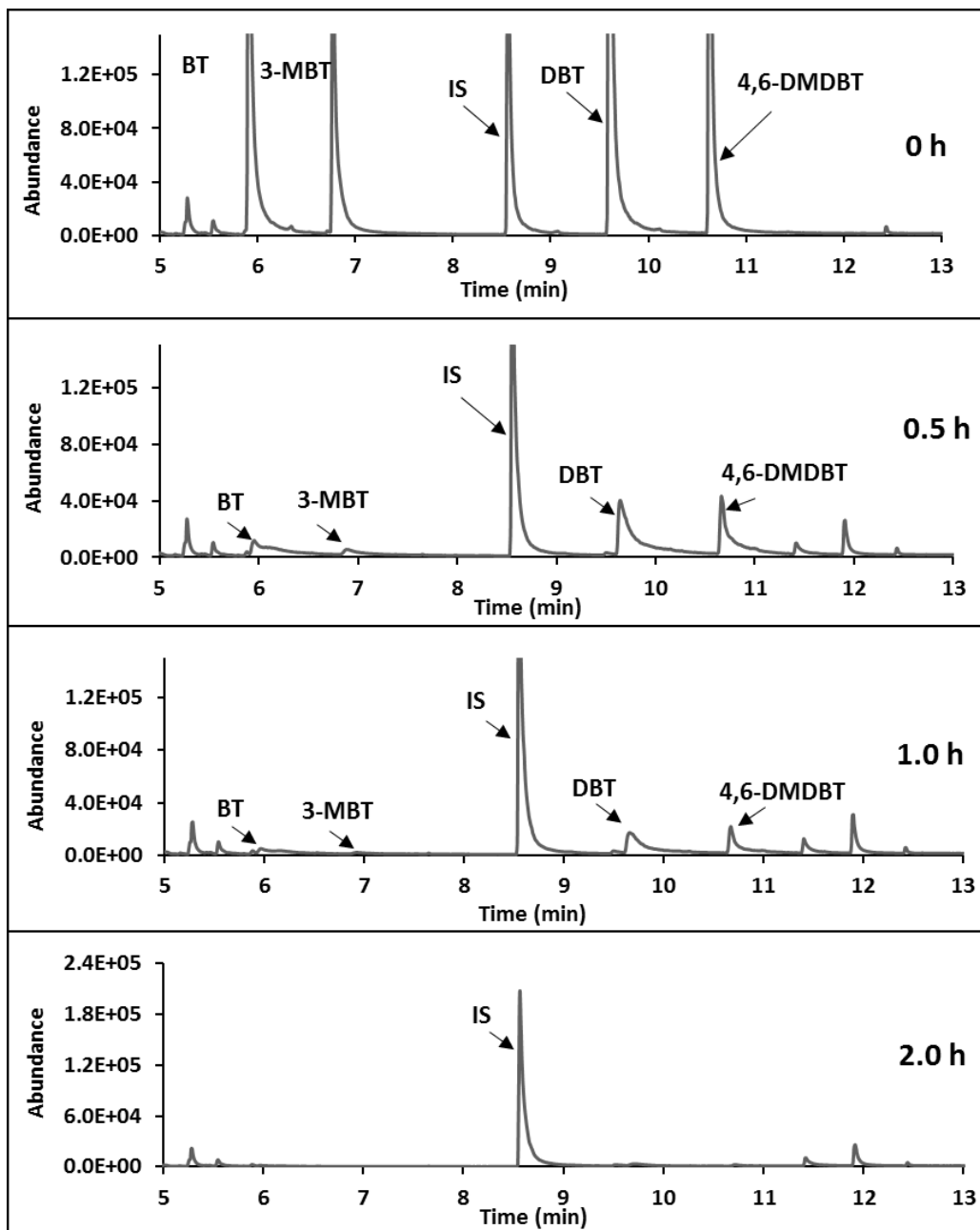


Figure 4.4. GC-MS (SIM) chromatograms of targeted thiophene compounds for different oxidation reaction time at 65 °C. IS: Fluorene.

4.4.3. DESI-MS analysis

Optimization of DESI-MS parameters for sulfone compounds were carried out directly on the MIP slides. This was done to avoid any variation in the optimization results which may be obtained from the optimization of those analytes when they are deposited onto different substrates such as polytetrafluoroethylene (PTFE). The Xevo™ triple quadrupole mass spectrometer (Xevo™ TQ-S) was operated in positive mode and used in all experiments. The identity of DBTO₂ was confirmed using tandem MS (MS/MS) experiments. The optimized parameters for DESI-MS conditions are summarized in Table 4.1.

Table 4.1. Optimal parameters and conditions for the DESI-MS analysis of dibenzothiophene sulfone compound.

Parameter	Setting
Electrospray voltage	3.0 kV
Cone voltage	40 V
Electrospray flow rate	2 $\mu\text{L min}^{-1}$
Nitrogen gas pressure	150 psi
Tip to surface distance	2 mm
Tip to inlet distance	4 mm
Surface to MS inlet distance	1 mm
MS inlet temperature	100 °C
Incident angle (α)	55°
Ions collection angle (β)	10°
Sampling spot size	$\sim 1 \text{ mm}^2$
Single spot sampling time	15 s

Unfortunately, the protonated ion peaks of BTO₂ (m/z 167) and 3-MBTO₂ (m/z 181) were not detectable or very weak. For 4,6-DMDBTO₂ (m/z 245) the signal was detectable, but weak. Only dibenzothiophene sulfone (DBTO₂) gave signals with good intensities in DESI-MS spectra. This may be due to the affinity of this compound to form a stable protonated molecule [DBTO₂ + H]⁺ and sodium adduct [DBTO₂ + Na]⁺ in the DESI-MS analysis (Figure 4.5) unlike the BTO₂ and 3-MBTO₂, where very weak or non-detectable peaks signals were observed. In the case of 4,6-DMDBTO₂, it is possible that the two methyl substituents on the aromatic rings produce a steric effect that prevents the Na⁺ ion from binding and forming of an adduct ions easily. Nevertheless, sulfones compounds that are not amenable to DESI can be analyzed by other techniques such as GC-MS.

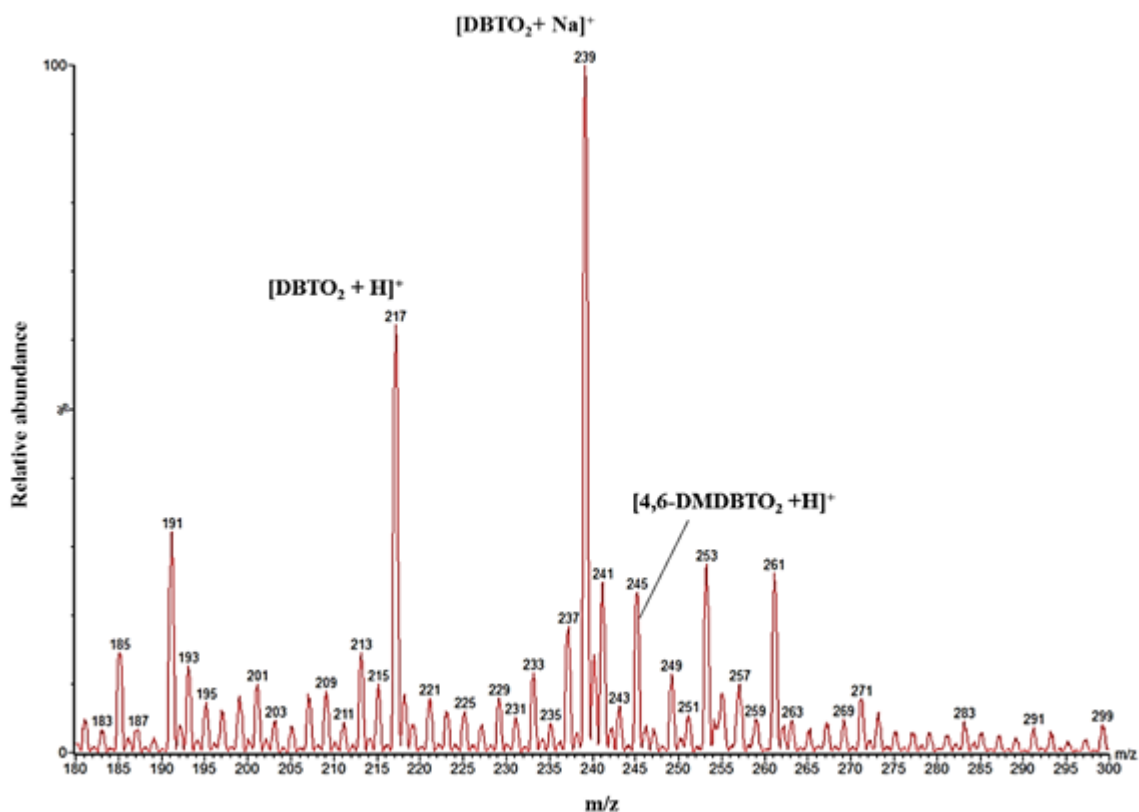


Figure 4.5. DESI-MS full scan of an MIP thin-film used for the extraction of the oxidation products of thiophene compounds in seawater sample. Protonated molecule and sodium adduct were detected.

Geometrical parameters including the tip to surface, tip to MS inlet and surface to MS inlet distances were varied until the highest and stable signal intensity for $[\text{DBTO}_2 + \text{Na}]^+$ m/z 239 was obtained. The nebulizing gas (nitrogen) pressure which was required to produce a spray with proper droplet size was tested from 50 to 150 psi. The optimal nebulizing gas pressure which was found to give signals with satisfactory intensity was 100 psi. The MS inlet temperature was also optimized and it was found that at 100 °C the highest signal intensities for protonated molecule and sodium adducts of DBTO_2 are achieved. The signal intensities dropped at 150 °C and this possibly results from low stability of the

DBTO₂ protonated ion and sodium adduct. The flow rate of the spray solvent was varied from 0.5 to 4 $\mu\text{L min}^{-1}$ and it was observed that at high flow rates above 2 $\mu\text{L min}^{-1}$ the signals intensity of the protonated DBTO₂ and sodium adduct decreased, while the background noise increased. Stable and reproducible intensities were observed at a flow rate of 2 $\mu\text{L min}^{-1}$.

Since sodium ions can come from any source, the [DBTO₂ + Na]⁺ adduct was observed in the DESI spectra even in the case of using spray solvents without adding sodium chloride. The [DBTO₂ + Na]⁺ adduct was used as the quantitation ion in the analysis of the thiophene compound in water since quantitation using sodium adducts instead of protonated ions when signals with stable intensities are required especially when tandem mass spectrometry are used [20]. Sodium chloride was added in excess to methanol/water mixture to produce a stable and constant signal intensity for the [DBTO₂ + Na]⁺ adduct during DSEI-MS analysis. The water was added in a small portion to the spray solvent mixture at a ratio of 95:5 methanol:H₂O to enhance the stability of spray, where using pure organic solvents usually lead to spray instability due to the limited electric conductivities of these solvents. The amount of water was also examined and it was found that poor signal stability was obtained when high proportions of water in the mixture were used. The optimum concentration of sodium chloride was found to be $5 \times 10^{-4} \text{ mol L}^{-1}$. Although the sodium adduct was selected for the quantitative analysis, the identity of DBTO₂ in the sample was confirmed by doing MS/MS scans (Figure 4.6) for the protonated ion and not the sodium adduct where it is usually difficult to interpret the sodium adduct fragmentation pattern in the ESI-MS/MS and leads to limited information [21,22]. Product ions of the

fragmentation of the protonated DBTO₂ are m/z 169, 153, which were due to the loss of SO and SO₂ respectively (Figure 4.6).

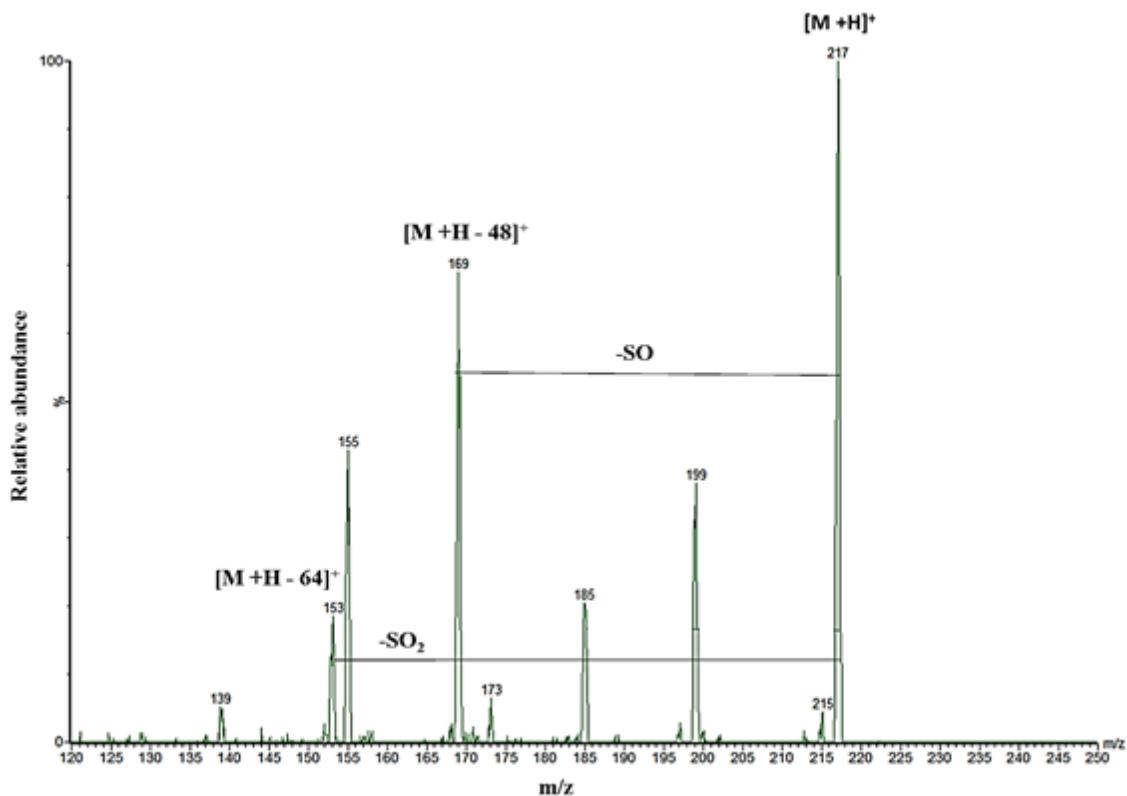


Figure 4.6. DESI-MS/MS confirmation scan of dibenzothiophene sulfone (DBTO₂) in MIP thin-film. Collision energy is 15 eV.

4.4.4. Analysis of seawater

DESI-MS analysis of MIP thin-films was carried out using [DBTO₂ + Na]⁺ ion instead of protonated ion due to its high intensity in mass spectra. The measured signal intensity of DBTO₂ extracted by MIP thin-films was related to the concentrations of spiked DBT in the seawater samples. It was observed that the adsorption of DBTO₂ from samples

by MIP at the pH of 1.5 was very low, so the pH was adjusted to 6.0 prior to the analysis with MIP. The calibration curve obtained from DESI-MS scans of MIP slides which used to extract the oxidation product of DBT at various concentrations ($0.1\text{-}10\ \mu\text{g L}^{-1}$) showed a linear relationship ($R^2 = 0.9756$) between the signal responses of $[\text{DBTO}_2 + \text{Na}]^+$ (m/z 239) and the concentrations in seawater sample (Figure 4.7). The inset calibration curve also showed a good linearity ($R^2 = 0.961$) at very low concentrations ($0.1\text{-}1.0\ \mu\text{g L}^{-1}$).

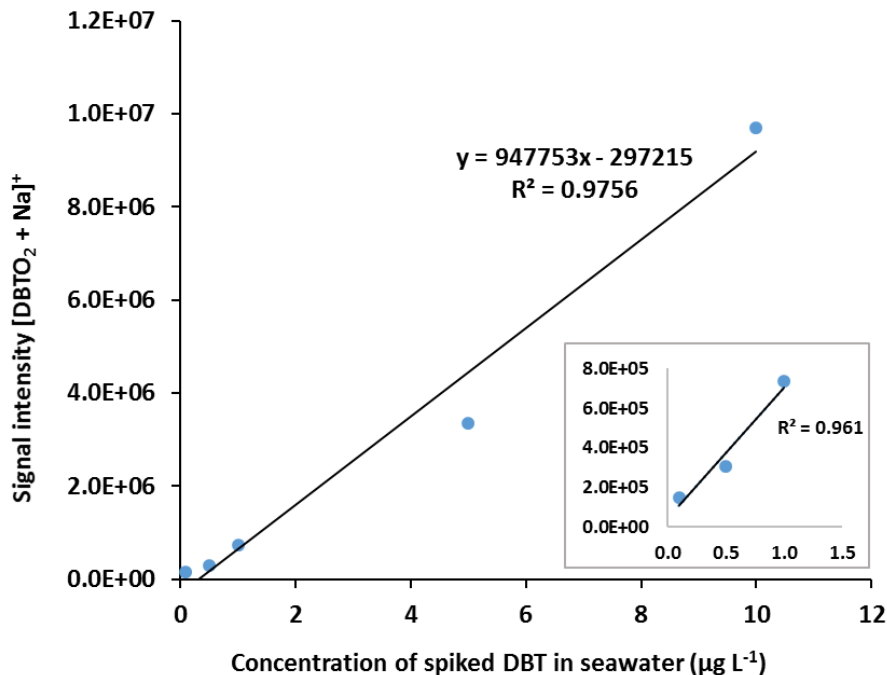


Figure 4.7. Calibration curves of the oxidized form of DBT at various spiked concentrations in seawater samples.

The LOD was very low for DBT in seawater at $3\ \text{ng L}^{-1}$. A relatively small volume of seawater samples was required for each analysis (10 mL) and the time of uploading was

very short (10 min). This method showed good reproducibility with acceptable relative standard deviations ($RSD_s \leq 8.0\%$).

4.5. Conclusions

Analysis of DBT in water samples by the oxidation to DBTO₂ with H₂O₂/formic acid followed by MIP-DESI-MS analysis was demonstrated. Among all sulfones, only DBTO₂ produce signals with high intensity in the DESI spectra. Protonated ions and sodium adducts were observed. Quantitative analysis of DBT was carried out using [DBTO₂ + Na]⁺ adduct. Stability and reproducibility of the sodium adduct signal was achieved by adding a small amount of sodium chloride to the spray solvent mixture (MeOH/H₂O). Tandem MS (MS/MS) scan was used to confirm the identity of DBTO₂. Advantages of coupling MIP thin-films with DESI-MS include simplicity, rapid analysis, low LOD value (sub-ng L⁻¹) and acceptable RSD_s ($\leq 8.0\%$). Small volumes of seawater sample were required and analysis of samples were carried out without pre-treatment. The obtained figures of merit make this method ideal for the analysis of DBT as well as DBTO₂ in environmental water samples.

4.6. References

- [1] Speight, J. G. *Handbook of Petroleum Product Analysis*. New Jersey: John Wiley and Sons; **2002**.
- [2] Kropp, K. G.; Fedorak, P. M. A Review of the Occurrence, Toxicity, and Biodegradation of Condensed Thiophenes Found in Petroleum. *Can. J. Microbiol.* **1998**, *44* (7), 605–622.
- [3] Avino, P.; Notardonato, I.; Cinelli, G.; Russo, M. Aromatic Sulfur Compounds Enrichment from Seawater in Crude Oil Contamination by Solid Phase Extraction. *Curr. Anal. Chem.* **2009**, *5* (4), 339–346.
- [4] Yu, C.; Yao, Z.; Hu, B. Preparation of Polydimethylsiloxane/ β -Cyclodextrin/divinylbenzene Coated “dumbbell-Shaped” stir Bar and Its Application to the Analysis of Polycyclic Aromatic Hydrocarbons and Polycyclic Aromatic Sulfur Heterocycles Compounds in Lake Water and Soil by Hig. *Anal. Chim. Acta* **2009**, *641* (1–2), 75–82.
- [5] Haupt, K.; Mosbach, K. Molecularly Imprinted Polymers and Their Use in Biomimetic Sensors. *Chem. Rev.* **2000**, *100* (7), 2495–2504.
- [6] Yan, H.; Row, K. H. Characteristic and Synthetic Approach of Molecularly Imprinted Polymer. *Int. J. Mol. Sci.* **2006**, *7* (5), 155–178.
- [7] Vasapollo, G.; Sole, R. Del; Mergola, L.; Lazzoi, M. R.; Scardino, A.; Scorrano, S.; Mele, G. Molecularly Imprinted Polymers: Present and Future Prospective. *Int. J. Mol. Sci.* **2011**, *12* (9), 5908–5945.

- [8] Mayes, A. G.; Whitcombe, M. J. Synthetic Strategies for the Generation of Molecularly Imprinted Organic Polymers. *Advanced Drug Delivery Reviews*. **2005**, pp 1742–1778.
- [9] Van Biesen, G.; Wiseman, J. M.; Li, J.; Bottaro, C. S. Desorption Electrospray Ionization-Mass Spectrometry for the Detection of Analytes Extracted by Thin-Film Molecularly Imprinted Polymers. *Analyst* **2010**, *135* (9), 2237–2240.
- [10] Takáts, Z.; Wiseman, J. M.; Gologan, B.; Cooks, R. G. Mass Spectrometry Sampling under Ambient Conditions with Desorption Electrospray Ionization. *Science (80-.)*. **2004**, *306* (5695), 471–473.
- [11] Cotte-Rodríguez, I.; Takáts, Z.; Talaty, N.; Chen, H.; Cooks, R. G. Desorption Electrospray Ionization of Explosives on Surfaces: Sensitivity and Selectivity Enhancement by Reactive Desorption Electrospray Ionization. *Anal. Chem.* **2005**, *77* (21), 6755–6764.
- [12] Yang, S.; Han, J.; Huan, Y.; Cui, Y.; Zhang, X.; Chen, H.; Gu, H. Desorption Electrospray Ionization Tandem Mass Spectrometry for Detection of 24 Carcinogenic Aromatic Amines in Textiles. *Anal. Chem.* **2009**, *81* (15), 6070–6079.
- [13] Dehkordi, A. M.; Kiaei, Z.; Sobati, M. A. Oxidative Desulfurization of Simulated Light Fuel Oil and Untreated Kerosene. *Fuel Process. Technol.* **2009**, *90* (3), 435–445.
- [14] Te, M.; Fairbridge, C.; Ring, Z. Oxidation Reactivities of Dibenzothiophenes in polyoxometalate/H₂O₂ and Formic acid/H₂O₂ Systems. *Appl. Catal. A Gen.*

2001, 219, 267–280.

- [15] De Filippis, P.; Scarsella, M.; Verdone, N. Oxidative Desulfurization I: Peroxyformic Acid Oxidation of Benzothiophene and Dibenzothiophene. *Ind. Eng. Chem. Res.* **2010**, 49 (10), 4594–4600.
- [16] Andersson, L. I.; Paprica, A.; Arvidsson, T. A Highly Selective Solid Phase Extraction Sorbent for Pre- Concentration of Sameridine Made by Molecular Imprinting. *Chromatographia* **1997**, 46 (1), 57–62.
- [17] Matsui, J.; Fujiwara, K.; Takeuchi, T. Atrazine-Selective Polymers Prepared by Molecular Imprinting of Trialkylmelamines as Dummy Template Species of Atrazine. *Anal. Chem.* **2000**, 72 (8), 1810–1813.
- [18] Liu, X.; Liu, J.; Huang, Y.; Zhao, R.; Liu, G.; Chen, Y. Determination of Methotrexate in Human Serum by High-Performance Liquid Chromatography Combined with Pseudo Template Molecularly Imprinted Polymer. *J. Chromatogr. A* **2009**, 1216, 7533–7538.
- [19] Gross, J. H. Chapter 2: Principles of Ionization and Ion Dissociation. In *Mass Spectrometry: A textbook. 2nd edition.*; Springer Berlin Heidelberg: Berlin, Heidelberg, **2011**; pp 21–66.
- [20] Manicke, N. E.; Wiseman, J. M.; Ifa, D. R.; Cooks, R. G. Desorption Electrospray Ionization (DESI) Mass Spectrometry and Tandem Mass Spectrometry (MS/MS) of Phospholipids and Sphingolipids: Ionization, Adduct Formation, and Fragmentation. *J. Am. Soc. Mass Spectrom.* **2008**, 19 (4), 531–543.

- [21] Chen, R.; Yu, X.; Li, L. Characterization of Poly(ethylene Glycol) Esters Using Low Energy Collision-Induced Dissociation in Electrospray Ionization Mass Spectrometry. *J. Am. Soc. Mass Spectrom.* **2002**, *13* (7), 888–897.
- [22] Godzien, J.; Ciborowski, M.; Martínez-Alcázar, M. P.; Samczuk, P.; Kretowski, A.; Barbas, C. Rapid and Reliable Identification of Phospholipids for Untargeted Metabolomics with LC–ESI–QTOF–MS/MS. *J. Proteome Res.* **2015**, *14* (8), 3204–3216.

Chapter 5: Conclusions and future work

The low cost, good selectivity and stability of MIPs make them ideal for chemical analysis. Several detection systems can be coupled with the MIPs for online and offline analysis. The type of coupling depends on the MIP format. Preparation of MIP in thin-film format makes their coupling with various detection systems easier. HS-SCD and DESI-MS are good examples of these detection systems as seen in this work. However, to obtain MIP with high analytical performance, the MIP components must be optimized. This is performed through the appropriate selection of MIP ingredients and by varying their amounts relative to each other in a systematic manner.

In this work, the MIP thin-films are prepared on glass slides and coupled with the GC-MS, HS-GC-SCD and DESI-MS. Extraction of the analytes (thiophene compounds) from the film by a solvent was necessary in the case of GC-MS analysis, while in the case of HS and DESI this step was not required where a direct desorption from the film was achieved directly.

In Chapter 2, the preparation of the MIP as a thin-film on a derivatized glass slide as a selective sorbent for thiophene compounds from a water sample is described in detail. The highest adsorption and imprinting factors for thiophene compounds was achieved by using the MIP film which was prepared using 1-vinylimidazole as a monomer and bisphenol A dimethacrylate as a cross-linker. The best ratio for the template:monomer:cross-linker was 1:4:8. An interpenetrating polymers networks (IPN) principle was adapted by adding the linear polymer-polyethylene glycol (PEG, MW 20,000) to the pre-polymerization mixture prior to the fabrication process. The optimal PEG percentage in the polymer was found to be 25 % w/w. It was found that the use of

PEG improves the shape and porosity of the film. This was confirmed by the study of the effect of mass and thickness on the adsorption of thiophene compounds by MIP in this work. This study revealed that the adsorption process occurred in the whole film (bulk adsorption) and not only at the surface as reported previously in another study [2]. The SEM images showed that the MIP film exhibited more porous structure with a uniform thickness ($\sim 13.5 \mu\text{m}$) compared to the NIP; this is due to the use of the template in the imprinting process.

The optimal stirring speed for the analysis of thiophene compounds by MIP film in water was 500 rpm. Below this speed, inconsistent binding capacity values were observed while above this speed no changes were noticed. The adsorption kinetic study showed that the adsorbed amounts of all thiophene compounds by MIP thin-film increased rapidly in the first 8 h then reached equilibrium at ~ 15 h, and finally leveled off. This makes the prepared film suitable for short and long-term analysis especially for environmental monitoring. Saturation of the MIP film was not observed at higher volumes, which makes it suitable for the analysis of a wide range of sample volumes.

In the binding isotherm study, the Freundlich isotherm is used to describe the binding equilibrium behaviour of MIP since the MIP is considered a heterogeneous material. The parameters including the heterogeneity index (m), fitting parameter (a) and correlation factor (R^2), which were obtained from the Freundlich isotherm curves of thiophene compounds, showed that the MIP film exhibited a more homogeneous surface and more fitting to the model compared to the NIP. The results obtained from Freundlich model agreed with the results obtained from adsorption binding experiments.

Excellent reproducibility was achieved for the extraction of thiophene compounds in spiked seawater samples ($RSD_s \leq 6.0\%$, $n = 3$). Calibration curves of spiked seawater samples were linear at a range of $0.5\text{-}100 \mu\text{g L}^{-1}$ and LOD values were in the range of $0.029\text{-}0.166$. The MIP thin-film showed higher selectivity toward all thiophene compounds compared to other interferents (p-cresol and indole), except in the case of 4,6-DMDBT, which showed equivalent adsorption selectivity compared to indole. The hydrophobic interaction is not the predominant type of interactions between the MIP and thiophene compounds. The results of this chapter show that the MIP thin-film can be used as a selective adsorbent for the extraction of thiophene compounds from water samples.

In Chapter 3, a novel method is developed for the analysis of thiophene compounds by coupling thiophenes-MIP film with the headspace gas chromatography sulfur chemiluminescence detector (MIP HS-GC-SCD). Advantages of this coupling include simplicity, rapidity and high selectivity with low LOD values range ($0.19 - 0.51 \mu\text{g L}^{-1}$). The targeted thiophene compounds were extracted from water samples without any sample pre-treatment. The template bleeding issue was resolved by using a pseudo-template instead of the original template. The observed peak of the pseudo-template did not overlap with the other peaks in the chromatogram (Figure 5.1). The optimal HS conditions (HS oven temperature and equilibration time) gave the highest area responses in the analysis of MIP films are $250 \text{ }^\circ\text{C}$ and 10 min respectively. The addition of a small amount of acetonitrile ($5 \mu\text{L}$) to each sample vial before HS analysis enhances the desorption of thiophene compounds from film and improve the reproducibility of the results. The matrix effect study showed a slight decrease in the adsorption recoveries of the thiophene

compounds was observed in the analysis of spiked seawater samples compared to the spiked DI water samples, except in the case of 4,6-DMDBT where the effect was more observed.

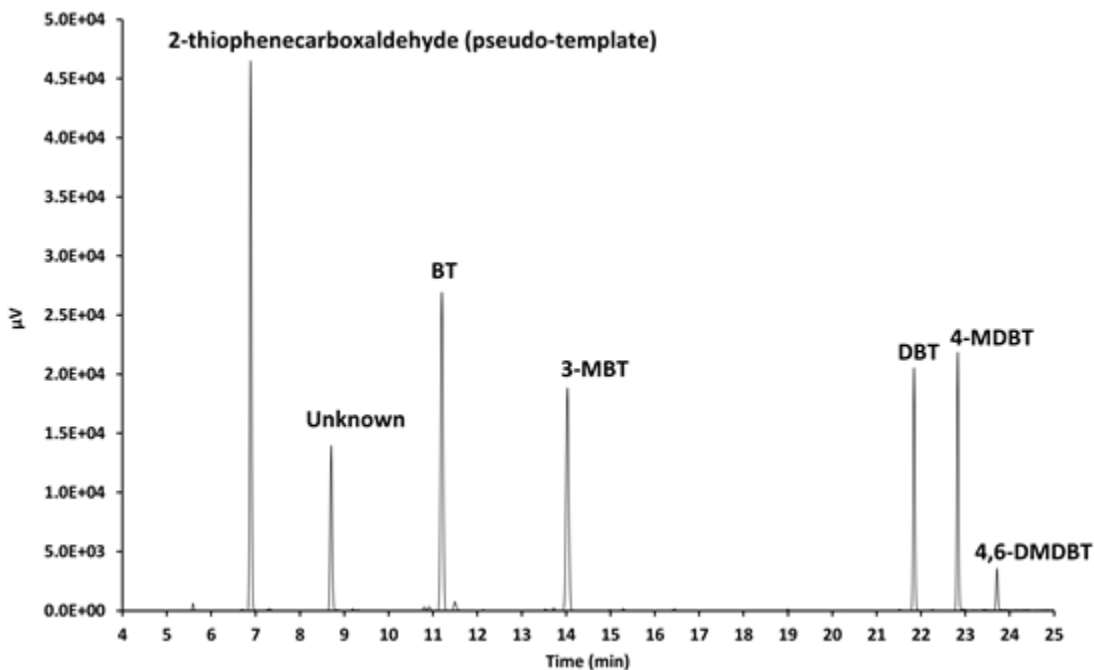


Figure 5.1. MIP HS-GC-SCD chromatogram obtained from the analysis of 50 mL seawater sample spiked with a mixture of thiophene compounds at a concentration of $50 \mu\text{g L}^{-1}$.

In Chapter 4, An MIP thin-film was coupled with desorption electrospray ionization mass spectrometry (DESI-MS) for indirect quantitative analysis of DBT compound in water. Conversion of thiophene compounds to sulfones in water was achieved by the oxidation with the H_2O_2 and formic acid. To get reproducible results for the analysis of thiophene compounds by the DESI-MS, the optimization of the oxidation reactions was

carried out. This optimization was very important to ensure a complete conversion of all thiophene compounds in water. The highest conversion was achieved at 65 °C after 2 h.

The optimal spray solvent for DESI analysis was MeOH/H₂O (95:5 v/v) contains 5 x 10⁻⁴ mol L⁻¹ NaCl. Dibenzothiophene sulfone (DBTO₂) was the only analyte that produce remarkable intensity signals in the positive ion mode. Signal intensity of [DBTO₂ + Na]⁺ adduct was used to construct a calibration curve for the determination of DBT concentrations in seawater sample. The DESI-MS response was linear ($R^2 = 0.9756$) over the range 0.1-100 µg L⁻¹. The limit of detection for this method was 3 ng L⁻¹ and relative standard deviations (RSDs ≤ 8.0%). The results illustrated that the method is ideal for indirect qualitative and quantitative analysis of DBT as well as DBTO₂ compound in water samples.

Finally, the outcomes of this research might be open the door for more applications of MIP thin-films. The preparation of MIP films in this work can be applied to any analyte of interest and is not limited to thiophene compounds. Because of the improved morphological properties and analytical performance of the MIP thin-films in this work, these films can be prepared and used in other application in the future. For example, these films can be prepared as recognition elements for chemical sensors [3-5]. The potential application of our work in the future may include the preparation of the MIP thin-film for thiophene compounds or other analytes on a quartz substrate of a transducer for optical measurements (e.g. fluorescence or IR measurements) or on a QCM and surface acoustic wave (SAW) sensors for mass-sensitive measurements [3]. Other applications will include integration of these films with surface enhanced Raman spectroscopic (SERS) detection

[6,7] or matrix-assisted laser desorption/ionization (MALDI) technique [8,9] for various environmental detections.

5.1. References

- [1] Farrington, J. W.; Mcdowell, J. E. Mixing Oil and Water. *Science* (80-.). **2002**, *43* (June), 2156–2157.
- [2] Egli, S. N.; Butler, E. D.; Bottaro, C. S. Selective Extraction of Light Polycyclic Aromatic Hydrocarbons in Environmental Water Samples with Pseudo-Template Thin-Film Molecularly Imprinted Polymers. *Anal. Methods* **2015**, *7*, 2028–2035.
- [3] Dickert, F. L.; Tortschanoff, M.; Bulst, W. E.; Fischerauer, G. Molecularly Imprinted Sensor Layers for the Detection of Polycyclic Aromatic Hydrocarbons in Water. *Anal. Chem.* **1999**, *71* (20), 4559–4563.
- [4] Tiu, B. D. B.; Krupadam, R. J.; Advincula, R. C. Pyrene-Imprinted Polythiophene Sensors for Detection of Polycyclic Aromatic Hydrocarbons. *Sensors Actuators, B Chem.* **2016**, *228*, 693–701.
- [5] Shoji, R.; Takeuchi, T.; Kubo, I. Atrazine Sensor Based on Molecularly Imprinted Polymer-Modified Gold Electrode. **2003**, *75* (18), 4882–4886.
- [6] Kostrewa, S.; Emgenbroich, M.; Klockow, D.; Wulff, G. Surface-Enhanced Raman Scattering on Molecularly Imprinted Polymers in Water. *Macromol. Chem. Phys.* **2003**, *204* (3), 481–487.
- [7] Li, D.; Li, D.-W.; Fossey, J. S.; Long, Y.-T. Portable Surface-Enhanced Raman Scattering Sensor for Rapid Detection of Aniline and Phenol Derivatives by On-Site Electrostatic Preconcentration. *Anal. Chem.* **2010**, *82* (22), 9299–9305.
- [8] Chen, C.; Chen, Y. Molecularly Imprinted TiO₂ -Matrix-Assisted Laser Desorption / Ionization Mass Spectrometry for Selectively Detecting R -Cyclodextrin. **2004**, *76*

(5), 2683–2687.

- [9] Taguchi, H.; Sunayama, H.; Takano, E.; Kitayama, Y.; Takeuchi, T. Preparation of Molecularly Imprinted Polymers for the Recognition of Proteins via the Generation of Peptide-Fragment Binding Sites by Semi-Covalent Imprinting and Enzymatic Digestion. *Analyst* **2015**, *140* (5), 1448–1452.